THE ROLE OF NITROGEN ASSIMILATION IN CELL CYCLE CONTROL OF *CAULOBACTER CRESCENTUS*

By

Hunter North

A DISSERTATION

Submitted to
Michigan State University
in partial fulfillment of the requirements
for the degree of

Microbiology and Molecular Genetics – Doctor of Philosophy

2025

ABSTRACT

Bacteria rely on complex regulatory networks to coordinate growth, development, and environmental adaptation. In *Caulobacter crescentus*, cell cycle progression is tightly controlled by the essential CckA-ChpT-CtrA two-component signaling phosphorelay. CckA, a bifunctional sensor histidine kinase (SHK), regulates the phosphorylation state of CtrA, a master response regulator (RR) that directs the transcription of over 90 genes involved in cell cycle progression, cell division, and polar morphogenesis. The activity of CckA is influenced by intracellular signals such as cyclic-di-GMP and ADP, as well as environmental stress cues that enhance its phosphatase activity. Altogether, regulation of CckA kinase/phosphatase activity leads to the properly timed oscillation of CtrA inactivation and degradation during each cell cycle, as well as a block in cell division under stress. Despite the essential nature of CckA and CtrA, genetic studies have identified alternative pathways that can bypass the requirement for CckA function, highlighting the flexibility of the *C. crescentus* regulatory network.

In this dissertation, I demonstrate that the bacterial enhancer binding protein (bEBP) NtrC, and its cognate SHK, NtrB, play critical but previously unrecognized roles in coordinating nitrogen metabolism with cell cycle progression and development in *C. crescentus*. NtrC is an unconventional bEBP that lacks the conserved GAFTGA motif required for σ^{54}-RNA polymerase activation. I show that deletion of *ntrC* slows growth in complex medium and that *ntrB* and *ntrC* are essential when ammonium is the sole nitrogen source due to their requirement for *glnA* expression. Interestingly, spontaneous insertion of an IS3-family mobile genetic element frequently restored the growth defect of *ntrC* mutants by reactivating transcription of the *glnBA* operon, suggesting that IS3 transposition may play a role in evolutionary adaptation of *C. crescentus* to nutrient limitation.

Genome-wide binding studies within this work identified numerous NtrC binding sites near genes involved in polysaccharide biosynthesis and cell cycle regulation, often overlapping

with binding sites for the essential nucleoid-associated protein GapR and the cell cycle regulator MucR1. Loss of NtrC function resulted in elongated polar stalks and increased synthesis of cell envelope polysaccharides, implicating NtrC in the direct regulation of cell morphogenesis and development. Furthermore, genetic suppression of a temperature-sensitive *cckA* mutant revealed that mutant forms of NtrC can bypass the essential CckA-ChpT-CtrA phosphorelay through two mechanisms: 1) increased levels of the alarmone ppGpp due to intracellular glutamine limitation, which sustain CtrA protein levels, and 2) activation of transcription at select σ^{54}-dependent promoters despite the absence of the GAFTGA motif.

My results presented in this dissertation provide evidence that NtrC can function as a central integrator of nitrogen status and cell cycle progression in *Caulobacter*, linking nutrient availability with core developmental processes. My discovery of *ntrC* mutants that rescue *cckA* loss-of-function highlights the remarkable plasticity of bacterial regulatory networks and underscores the complex interplay between nitrogen metabolism, nucleotide signaling, and cell cycle control. This work establishes NtrC as a key regulator of cell cycle progression and developmental plasticity in *C. crescentus*, revealing new insights into the adaptive potential of bacterial signaling pathways.

TABLE OF CONTENTS

Chapter 1: Introduction

Cell differentiation: A strategy used by bacteria to adapt to environmental stress

Bacteria typically reproduce clonally, which results in genotypically and phenotypically identical progeny. While this ensures faithful inheritance of genetic information, it provides limited potential for genetic variation that may enhance survival across diverse environments, aside from changes introduced by spontaneous mutation or horizontal gene transfer (reviewed in [1]). This can be limiting for bacteria, especially in fluctuating environmental conditions. To generate phenotypic diversity within a genetically identical population, bacteria have evolved mechanisms of cell differentiation. Differentiation can be “induced” (i.e., occurs upon detection of a stimulus) or “obligate” (i.e., hard-wired into the cell cycle). Differentiation ensures stable passage of genetic material, while also allowing for 1) environmental adaptation, 2) division of labor, and 3) bet-hedging (reviewed in [1]). Most species that undergo cell differentiation do so in an induced manner. For example, in *Bacillus subtilis*, a molecular signaling network senses stressful environmental conditions (e.g., starvation) and, subsequently, stimulates the formation of resistant biofilms or spores [2, 3]. In the soil-dwelling *Myxococcus xanthus*, a molecular signaling network stimulates a multicellular developmental program, resulting in the formation of cell aggregates that form fruiting bodies containing tens of thousands of spores [4, 5]. Additionally, cell differentiation programs can be induced in the context of pathogenesis. For example, upon host invasion, uropathogenic *Escherichia coli* can differentiate into coccoid and filamentous cells to increase host evasion [6, 7]. Altogether, induced cell differentiation allows bacteria to acclimate to their environmental conditions in real time.

In contrast, the dimorphic, oligotrophic Alphaproteobacterium *Caulobacter crescentus* follows an obligate differentiation program that is hard-wired into its cell cycle (reviewed in [1]). At cell division, *Caulobacter crescentus* will produce two genetically identical, yet developmentally and morphologically distinct daughter cells: 1) a replication-competent, sessile

stalked cell and 2) a non-replicative, flagellated swarmer cell (**Figure 1.1A**). Briefly, a swarmer cell must differentiate and "develop" into a replication-competent stalked cell to proceed with DNA replication and subsequent cell division (**Figure 1.1A**). At cell division, a motile swarmer cell disperses, which enables it to seek a more hospitable environment, while the sessile stalked cell remains in place to maintain the integrity of the established community and support proliferation and biofilm formation (reviewed in [1]). This obligate differentiation system provides *Caulobacter crescentus* with division-of-labor and bet-hedging strategies to thrive in its native environments. Although differentiation in *Caulobacter crescentus* is hard-wired, environmental signals, such as surface contact and starvation, can modulate the timing and coordination of cell differentiation and cell cycle (reviewed in [1]). This makes *Caulobacter crescentus* an excellent model for studying bacterial development and cell biology.

A history lesson: *Caulobacter crescentus* becomes a model system

Caulobacter crescentus belongs to the bacterial family Caulobacteraceae within the Caulobacterales order. The first evidence of this order was reported by Mabel Jones in 1905 when she isolated bacteria from city and sewage water in Chicago and described "comma-shaped cells" with a long, single polar "flagellum" (later identified as a stalk) that formed into rosettes or "clusters of cells" mediated through the tips of the "flagella" [8]. In 1914, Vasily Omeliansky reported a similar bacterium isolated from river water with similar vibrioid morphology and rosette formation mediated by "flagella" [9]. In 1935, Arthur Henrici and Delia Johnson isolated multiple similar bacterial species that adhered to microscope slides that were submerged in a freshwater lake [10]. It was then that Henrici and Delia identified these "flagella" as, in fact, stalks and officially recognized the bacterial order Caulobacterales. Using electron microscopy, Houwink and van Iterson [11] and Bowers [12] reported the presence of a single polar flagellum that forms at the free end of the opposite pole of the stalk preceding cell division. They observed that the motile, flagellated daughter cell breaks away from the sessile stalked

daughter cell at cell division and, after a certain amount of time [12] or upon adherence to another surface [11], will form a stalk that replaces the flagellum at that originally flagellated pole. These studies were the initial evidence of the now established dimorphic life cycle of Caulobacteraceae species. Years later, Jeanne Poindexter established a protocol for the cultivation of several species belonging to Caulobacteraceae that were isolated from freshwater [13], including the lab strain used for decades to come, *Caulobacter crescentus* (hereafter, *Caulobacter*) [14].

These initial observational studies investigating this dimorphic life cycle and establishing cultivation protocols set the foundation for researchers, such as Lucy Shapiro, Bert Ely, and Austin Newton [15] (reviewed in [16]), to use *Caulobacter* as a model bacterium for interrogating bacterial development and cell biology. As mentioned previously, the faithful, obligate morphological development during its cell cycle set *Caulobacter* apart from previously established bacterial models (reviewed in [1]). Moreover, researchers were tempted by the ability to synchronize a *Caulobacter* population according to cell cycle phase [15]. One method of synchronization is mediated through the oscillating presence of the cell cycle regulated exopolysaccharide (EPS) capsule [17]. In normal growth conditions, the replicative stalked cells produce EPS capsule, while the non-replicative swarmer cells lack EPS capsule [17]. The presence of capsule on stalked cells increases cellular buoyancy relative to uncapsulated swarmer cells. Consequentially, cell types can be separated through density gradient centrifugation [14, 18, 19]. Additionally, synchronization can be mediated through the oscillating presence of the cell cycle regulated polar appendage, the stalk, which is an extension and continuation of the cell envelope that harbors the adhesive holdfast at its tip [20]. When incubated on a glass petri plate with gentle agitation, adhesive stalked cells from a liquid culture will adhere to the glass plate, while the non-sticky swarmer cells will remain in the liquid phase [21]. Consequentially, for both of these synchronization methods, non-replicative swarmer cells can be isolated from other cell types within a culture to create a homogenous population

regarding both cell cycle phase and cellular morphology. The ability to synchronize a *Caulobacter* population according to cell cycle phase through the utilization of coordinated developmental morphologies and polar appendages provides a powerful tool for interrogating cell cycle processes and developmental regulation.

Following the development of synchronization protocols, researchers established genetic and biochemical tools to study *Caulobacter* as a model organism (reviewed in [16]). The isolation of *Caulobacter*-specific phages (i.e., caulophages), which infect *Caulobacter* at specific cell cycle stages based on oscillating developmental morphologies and appendages (e.g., pili, flagellum, capsule), provided a valuable tool for tracking cell cycle progression in synchronized populations. This enabled researchers to precisely characterize the timing of key cell cycle transitions [22]. Tools and methods were optimized for genetic manipulation, including a conjugation system, phase-based generalized transduction, electroporation, chromosomal gene inactivation, and transposon mutagenesis (reviewed in [16]). The *Caulobacter* genome map was constructed [23, 24] and, eventually, the *Caulobacter* genome was published in 2001 [25], allowing for targeted genetic manipulation to probe questions regarding cell cycle control and cellular development (reviewed in [16]).

Caulobacter crescentus: A dimorphic life cycle optimized for its environments

As mentioned previously, *Caulobacter* belongs to the Caulobacterales order. This order is part of the bacterial class Alphaproteobacteria within the Proteobacteria phylum [26]. The Alphaproteobacteria class is composed of Gram-negative, environmentally-abundant, and metabolically-diverse species, including plant symbionts/nitrogen-fixers, obligate and facultative intracellular pathogens, and oligotrophs that can survive in nutrient-limited environments such as freshwater [26, 27]. Due to the history of its isolation (described above), *Caulobacter* was thought to mostly reside in aquatic, oligotrophic environments [13], but more recent work has found *Caulobacter* species to be abundant in nutrient-replete environments, such as compost

and decomposing wood [28], suggesting roles in the decomposition of plant material. Moreover, *Caulobacter* species have been isolated from the rhizosphere [29] and found to have plant growth promoting effects [30]. This aligns with the fact that *Caulobacter* harbors regulatory, transport, and enzymatic proteins for the metabolism of plant-derived materials [31, 32] and, moreover, utilizes plant-derived carbon sources, such as xylose and vanillate in laboratory settings [13, 33]. The dimorphic life cycle of *Caulobacter*—producing a replication-competent, sessile stalked cell and a non-replicative, motile swarmer cell at each cell division—supports its ability to thrive in diverse and nutrient-variable environments. The polar appendages of these distinct cell types may serve as a "bet-hedging" strategy [34]. The flagellated, motile swarmer cell allows *Caulobacter* to explore its local environment for more abundant resources before committing to cell division. Simultaneously, the dispersal of the swarmer daughter cell after cell division removes competition from the sessile stalked at that environmental location. The stalked cell may become a part of the local biofilm community, protecting the cell from predation and environmental stresses [35]. This balance between attachment and planktonic lifestyles allows *Caulobacter* to thrive in oligotrophic and nutrient-variable environments. This dimorphic life cycle is described further, below.

Importantly, and unlike most bacteria, *Caulobacter* initiates chromosome replication only once per cell division [36], resulting in distinguishable developmental phases throughout its cell cycle as seen in eukaryotic cells (i.e., G1, S, G2) (**Figure 1.1A**). During the *Caulobacter* cell cycle, the swarmer cell resides in a growth-arrested state (G1-phase). After a set period of time or upon surface contact and subsequent irreversible attachment [20], a swarmer cell will differentiate into a stalked cell, which undergoes DNA synthesis (S-phase) and, ultimately, cell division. This G1-to-S transition is characterized by the shedding of the polar flagellum and retraction of the type IV tight adherence (tad) pili [37] from the cell pole (**Figure 1.1A**). These events coincide with the secretion of the adhesive holdfast from that site, which eventually tips the stalk that extends from that same cell pole [20]. This morphological transition from

“swarmer-to-stalk” is therefore tightly coupled to the developmental G1-to-S transition under standard cultivation conditions; therefore, the “G1-to-S” transition terminology can be used synonymously with the “swarmer-to-stalk” transition terminology. After the G1-to-S/swarmer-to-stalk transition, the replicative (S) stalked cell will proceed with DNA replication and morph into a predivisional cell (G2-phase), in which the newly formed daughter cell compartment will produce a polar flagellum at the opposite pole of the division plane (**Figure 1.1A**). Upon cell division, the swarmer daughter cell will disperse and form type IV pili at the flagellated cell pole [38]. This piliated, flagellated swarmer daughter cell will eventually differentiate into the stalked cell, while the stalked daughter cell can immediately proceed with DNA replication and subsequent cell division (**Figure 1.1A**). All these critical events coincide with global intracellular molecular rewiring, which is required for the faithful coordination of cell cycle and cellular development of *Caulobacter*.

The essential cell cycle CckA-ChpT-CtrA TCS phosphorelay

The asymmetric cell division of *Caulobacter* relies on tight molecular regulation to achieve faithful coordination of cell cycle and cellular development. In *Caulobacter*, this regulation is mediated by the temporally and spatially oscillating global master regulators GcrA [39], DnaA [40], CcrM [41], and CtrA (reviewed in [16, 42-45]). Altogether, these proteins regulate over 200 genes required for timely, coordinated progression through *Caulobacter* cell cycle. In this work, I will focus on the master cell cycle regulator CtrA.

Cells use sophisticated molecular mechanisms to monitor both their internal state and the external environment, ensuring the maintenance of homeostasis. In bacteria, a common mechanism of environmental monitoring involves sensor histidine kinase (SHK) proteins, which detect physical and chemical cues and regulate adaptive physiological responses through phosphoryl transfer to their partner response regulator (RR) proteins [46]. SHKs and RRs together form two-component signaling systems (TCSs), one of the most widely conserved

gene regulatory mechanisms in bacteria [47]. TCSs were initially thought to regulate gene expression and behavioral responses only under specific environmental conditions [48, 49]. However, studies in the years following their discovery uncovered TCSs and multi-component TCS phosphorelays [50] that regulate core cellular processes, including cell envelope biogenesis, cell cycle progression, and cell division. The TCS genes that regulate such core processes are often essential for cell viability under standard cultivation conditions [51-54]. In *Caulobacter*, one such TCS phosphorelay essential for cell cycle progression and cellular development is the CckA-ChpT-CtrA TCS phosphorelay (**Figure 1.1B**).

Cell cycle progression and coordinated cellular development in *Caulobacter* is governed by the activation and inactivation of the essential DNA-binding RR CtrA, which is under precise spatiotemporal control [55]. Specifically, CtrA is activated by phosphorylation via a multiprotein phosphorelay initiated by the essential SHK CckA (**Figure 1.1B**) [56-58]. Once activated, CtrA directly regulates the transcription of over 90 genes involved in cell cycle progression, cell division, and polar morphogenesis [59] (**Figure 1.1B**). However, CckA is a bifunctional SHK, capable of switching between kinase and phosphatase states [60]. In its phosphatase mode, CckA dephosphorylates both CtrA and the single-domain RR CpdR (**Figure 1.1B**). Once dephosphorylated, CpdR serves as a proteolytic adapter, directing similarly dephosphorylated CtrA for degradation by the ClpXP protease, thereby supporting precise regulation of CtrA protein levels during the cell cycle [60-62] (**Figure 1.1A**). The switch in CckA activity from kinase to phosphatase is regulated by changes in levels of cyclic-di-GMP [63] and ADP [64], and its spatial localization within the membrane [65, 66]. In addition to these regulatory inputs, CckA function is influenced by environmental stress cues that are proposed to enhance its phosphatase activity, leading to CtrA degradation and a consequent block in cell division under stress conditions [67]. Additional essential TCS proteins further refine the spatial and temporal control of CckA activity within developmentally distinct *Caulobacter* cell compartments [68]. The

regulation of CtrA activity by 1) transcription, 2) phosphorylation, 3) localization, and 4) proteolysis renders CtrA present and active at precise times during the cell cycle (**Figure 1.1**). Moreover, CtrA differentially regulates promoters in the G1 swarmer cell versus the S stalked cell due to the oscillating presence of transcriptional regulators that have opposing regulation at CtrA target promoters [17]. Altogether, this regulation of CtrA activity is critical for timely coordination of *Caulobacter* cell cycle and developmental events. CtrA activity at precise *Caulobacter* cell cycle and developmental events is discussed further, below.

CtrA oscillation governs coordination of cell cycle and cellular development

The spatiotemporal control of CtrA activity during the *Caulobacter* cell cycle is critical for proper cell cycle progression and tight coordination of cellular development. In the G1 swarmer cell, CtrA is phosphorylated by CckA through the phosphotransferase ChpT [56-58] (**Figure 1.1B**). Notably, CckA harbors kinase activity in the G1 swarmer cell due to low levels of c-di-GMP and its polar localization to the flagellated pole, which are events controlled by a series of additional essential TCS proteins (reviewed in [16, 43, 56]). Phosphorylated CtrA (CtrA~P) binds a conserved sequence at five sites on the *Caulobacter* origin of replication (i.e., *Cori*) [69]. This binding inhibits DNA replication (**Figure 1.1B**) by preventing assembly of DnaA-ATP at *Cori* and, thereby, prevents formation of the replisome and subsequent DNA replication in the G1 swarmer cell [69]. Additionally, in the G1 swarmer cell, CtrA~P activates transcription of G1-specific genes due to the presence of the small CtrA inhibitory protein, SciP, which apparently binds and represses non-G1 CtrA target promoters [70, 71]. G1-specific promoters activated by CtrA~P include P_{sciP}, itself, to ensure repression of non-G1 promoters [70, 71], as well as the major pilin subunit, *pilA* [72] and the negative regulator of capsulation, *hvyA* [17]. Consequentially, the G1 swarmer cell maintains the type IV pili filaments and is non-capsulated. CtrA~P can also act as a repressor in the G1 swarmer cell, repressing transcription of *gcrA*, a cell cycle regulator that oscillates spatially and temporally out-of-phase with CtrA [39], as well as

cell division gene *ftsZ* and polar development gene *podJ* [73]. CtrA-mediated silencing of *Cori* and repression of cell division and polar development genes maintain the swarmer cell in a non-replicative (G1) state.

Under permissible growth conditions, a spike in c-di-GMP levels induced by a series of cell cycle regulated TCS proteins stimulates the G1-to-S and swarmer-to-stalk transitions, synchronously (reviewed in [16, 43, 56]). Increased c-di-GMP and TCS regulators facilitate the degradation of flagellar structural components, as well as the subsequent synthesis of the stalk, thereby promoting the swarmer-to-stalk transition [74-76]. Simultaneously, these signals stimulate the delocalization of CckA and its subsequent phosphatase activity. Consequentially, CtrA and CpdR are dephosphorylated by CckA. Dephosphorylated CpdR, along with other accessory proteolytic factors, recruit the ubiquitous ATP-dependent ClpXP protease and dephosphorylated CtrA to the swarmer cell pole where CtrA is subsequently degraded [61, 62, 77, 78] (**Figure 1.1**). Importantly, SciP is degraded and cleared through action of the Lon protease during the G1-to-S/swarmer-to-stalk transition [79]. The proteolytic clearance of CtrA during the G1-to-S/swarmer-to-stalk transition allows for DnaA, the conserved DNA replication initiator protein (Reviewed in [80]), to bind *Cori* and initiate replisome formation, thereby stimulating DNA replication. Additionally, clearance of CtrA allows for de-repression of its repressive target, *gcrA* [39]. In addition to its role in activation of DNA replication, DnaA functions as a transcriptional activator, promoting the expression of genes involved in nucleotide synthesis and DNA replication [81]. It also activates *gcrA* transcription, contributing to the rise in GcrA levels during the G1-to-S/swarmer-to-stalk transition [82]. GcrA activates transcription of genes involved in cell cycle processes that promote progression of the stalked cell into S-phase. The GcrA direct regulon includes genes involved in nucleotide synthesis, DNA repair, chromosome organization and segregation, and cell division [83, 84]. Importantly, transcriptional regulation by GcrA occurs at methylated sites on promoters [83, 84]. Altogether, these molecular events allow for differentiation to a stalked cell which commits to DNA replication (S-

phase).

During the S-phase of the stalked cell, DNA replication is actively underway. As the replication fork advances, newly synthesized chromosomes become hemimethylated (reviewed in [85]), introducing an additional layer of cell cycle regulation [39, 41]. Specifically, as the replication fork passes through *dnaA*, the P_{dnaA} promoter becomes hemimethylated and inactivated [41]. Since DnaA is subject to proteolytic regulation in *Caulobacter* [86], the inactivation of P_{dnaA} reduces DnaA levels. Lower DnaA levels prevent reinitiation of chromosome replication, reinforcing the "once per cell cycle" DNA replication pattern in *Caulobacter*. At the same time, hemimethylation of one of the *ctrA* promoters (i.e., *ctrA* P1) enables GcrA-dependent activation of *ctrA* [39]. As a result, CtrA begins to reaccumulate during S-phase (**Figure 1.1A**). The resynthesis of CtrA during S-phase further blocks chromosome reinitiation by binding to and inhibiting *Cori* (**Figure 1.1B**). Additionally, GcrA activates transcription of genes involved in polar development and localization. For example, *podJ* [87] and *pleC* [88], genes involved in eventual pilus formation and proper polar assembly at the new pole of the swarmer cell compartment of the predivisional cell, are transcriptionally activated by GcrA [39]. In late S-phase, CtrA accumulates and becomes phosphorylated and activated by CckA, which regains kinase activity through regulation by associated TCSs and its proper localization [68]. CtrA~P auto-activates one of its own strong promoters (i.e., *ctrA* P2), resulting in a burst of CtrA production [89]. In turn, increased CtrA~P represses P_{gcrA}, resulting in decreased GcrA levels. Notably, in S-phase, CtrA~P activates transcription of S-specific genes due to 1) the absence of SciP, which would typically repress S-specific promoters [79], and 2) the activity of MucR1 and MucR2 proteins that repress G1-specific promoters that are typically activated in the G1 swarmer cell (e.g., *sciP*, *hvyA*, *pilA*) [17]. Altogether, in S-phase, CtrA~P activates transcription of over 50 genes required for completing cell cycle progression, including the DNA methyltransferase *ccrM* and the chemoreceptor *mcpA* [73, 90, 91]. CtrA-dependent activation of S-phase genes is required for proper polar assembly of the flagellum, pili, and chemotaxis

apparatus at the new cell pole of the future swarmer daughter cell.

In the predivisional (G2) cell, CcrM has accumulated due to CtrA-dependent transcriptional activation and fully methylates daughter chromosomes [40]. Notably, fully methylated P_{dnaA} allows for transcriptional activation of *dnaA*, allowing for re-accumulation of DnaA (reviewed in [85]). Prior to cell separation, the division plane establishes two cellular compartments (i.e., the stalked and swarmer daughter cell compartments) [92]. Reaccumulated CtrA is proteolyzed and cleared in the stalked daughter cell compartment while maintained and activated in the swarmer daughter cell compartment (**Figure 1.1A**) due to the differential regulation of CckA activity by the differential polar localization of TCS regulatory proteins [92, 93]. Additionally, just prior to cell division, CcrM is cleared via degradation by the Lon protease [94]. Upon cell division, daughter cells are released with fully methylated chromosomes. The absence of CtrA in the stalked daughter cell allows immediate reentry into S-phase, in which re-accumulated DnaA will stimulate DNA replication. The dispersed swarmer daughter cell will reside in the non-replicative (G1) state due to CtrA~P binding and blocking *Cori* from DnaA-ATP binding. Also, CtrA~P has re-activated *sciP* and, consequentially, increased SciP levels, together with loss of MucR1/2 activity [17], allows for the transcriptional switch to the CtrA-dependent activation of G1-specific promoters, including *pilA*, which results in proper assembly of the pilus filaments in the swarmer cell upon cell division [72]. If conditions permit, the swarmer daughter cell remain in the non-replicative (G1) state for a set period of time before differentiating into a replicative stalked cell to reinitiate DNA replication and subsequent cell division.

In summary, unlike many other bacteria, *Caulobacter* exhibits tightly coordinated cellular development during its cell cycle. This coordination is driven by oscillating master regulators that are controlled at multiple levels, including transcriptional, post-transcriptional, allosteric, and proteolytic regulation. A key master regulator is CtrA, a RR whose DNA-binding and transcriptional activity is stimulated by phosphorylation. This phosphorylation is carried out by its

cognate SHK, CckA, which switches between kinase and phosphatase activity in a cell cycle-dependent manner [60] (**Figure 1.1**). CtrA~P differentially activates G1- and S-specific genes throughout the cell cycle, guided by the activity of inhibitory proteins (i.e., SciP, MucR1/2) at CtrA-regulated promoters [17]. Altogether, these integrated regulatory networks and molecular checkpoints are critical for the coordination of cell cycle and cellular development, as well as timely progression through *Caulobacter* cell cycle.

As mentioned previously, *Caulobacter* progresses through its cell cycle in a highly predictable manner under optimal laboratory conditions, almost as if governed by an "internal clock" [43]. For example, *Caulobacter* typically spends about one-third of its life cycle in the non-replicative (G1) swarmer cell stage before differentiating into the replicative (S) stalked cell. However, standard laboratory conditions rarely reflect the oligotrophic environments where *Caulobacter* naturally resides, nor do they mimic the natural fluctuations typical of such environments [95]. Indeed, under unfavorable growth conditions that simulate these natural settings—such as nutrient starvation—*Caulobacter* experiences disruptions in the timing of cell cycle transitions and the coordination between cell cycle progression and cellular development (reviewed in [96]). These perturbations can be detected phenotypically through shifts in population dynamics (e.g., changes in the relative abundance of G1 swarmer vs. S stalked cells) and through molecular analysis (e.g., altered protein levels of cell cycle regulators and changes in DNA content) (reviewed in [96]). These stress-induced disruptions are largely mediated by the stringent response, a conserved stress signaling pathway discussed below.

Stringent response: Ubiquitous stress signaling system in bacteria

Bacteria possess a wide range of regulatory mechanisms that enable them to rapidly sense and adapt to constantly changing environments. One such mechanism is the ubiquitous stress signaling system known as the stringent response. The stringent response is typically activated in response to nutrient deprivation, such as amino acid starvation, fatty acid limitation, and

nitrogen starvation (reviewed in [97, 98]). It also plays a key role in virulence, biofilm formation, and antibiotic tolerance in some bacterial pathogens (reviewed in [99-101]). Under stressful environmental conditions, the stringent response enables bacteria to shift from a "growth" state to a "survival" state by modulating core cellular processes such as transcription, translation, DNA replication, and lipid synthesis (reviewed in [102]).

The stringent response is mediated by the signaling nucleotides guanosine tetra- and pentaphosphate (collectively, (p)ppGpp or alarmone). These signaling nucleotides were discovered over 50 years ago by chance when Cashel & Gallant were characterizing changes in previously identified phosphorylated metabolites in *E. coli* starved for amino acids [103]. By cultivating cells in media containing radiolabeled phosphate and subsequent thin layer chromatography, Cashel & Gallant saw two novel phosphorylated molecular species, which they termed “magic spots (MS) I & II” [103]. Notably, these magic spots only appeared in the amino acid starved condition and coincided with inhibition of other phosphorylated nucleotides, such as tRNA and rRNA. Cashel and Gallant postulated that these “magic spots” could be products of an uncharacterized enzyme at the time whose deletion was associated with a “relaxed phenotype” under starvation conditions (i.e., deletion of the enzyme restored stable RNA synthesis under amino acid starvation) [104, 105]. This enzyme, originally termed “RC” [106], is now known as RelA (named after the “relaxed” phenotype), the major *E. coli* (p)ppGpp synthetase. Although the terminology “stringent response” was originally coined specifically regarding the “stringency of amino acid control on RNA synthesis” [106], this terminology now broadly encompasses (p)ppGpp-mediated changes in physiology under a range of stressful conditions (reviewed in [102]).

The RelA/SpoT homologue (RSH) enzyme superfamily is responsible for the synthesis and hydrolysis of (p)ppGpp signaling molecules. Specifically, these enzymes mediate the synthesis of ppGpp and pppGpp through transfer of a pyrophosphate from ATP to GDP and GTP, respectively (reviewed in [102]). Conversely, these enzymes mediate hydrolysis by removal of a

pyrophosphate from ppGpp and pppGpp to produce GDP and GTP, respectively. RSH enzymes are divided into three classes: 1) long RSH enzymes, 2) small alarmone synthetase (SAS) proteins, and 3) small alarmone hydrolase (SAH) proteins. SAS and SAH proteins always have monofunctional synthetase and hydrolase (p)ppGpp activity, respectively. Long RSH enzymes are more complex in nature, possessing N-terminal enzymatic and C-terminal regulatory regions. The N-terminal region is comprised of synthetase and hydrolase (active or inactive) domains, while the C-terminal region possesses regulatory domains comprised of TGS (ThrRS, GTPase, and SpoT), a zinc-finger domain or conserved cysteine domain, an alpha-helical domain, and an ACT domain (aspartate kinase, chorismite, and TyrA) or a RNA recognition motif domain (reviewed in [102]). The bifunctional long RSH protein, Rel, is deemed the "ancestral" long RSH and is the most vastly distributed RSH, possessing both (p)ppGpp synthetase and hydrolase activity.

Broadly, in the Beta- and Gammaproteobacteria classes of the Proteobacteria phylum, the *rel* gene was duplicated, producing the paralogs that are now called *relA* and *spoT* [107, 108]. RelA is a monofunctional synthetase that harbors a catalytically-inactive or "pseudo" hydrolase domain [109, 110]. SpoT in these bacteria is bifunctional, although it possesses weak synthetase activity and strong hydrolase activity [111-114]. Because high levels of (p)ppGpp can bring bacterial replication to a halt (reviewed in [97]), SpoT is essential in these species to prevent toxic accumulation of (p)ppGpp by RelA synthetase activity [115]. Unlike Beta- and Gammaproteobacteria, most other bacteria possess the sole ancestral bifunctional long RSH Rel and, in addition, may possess one or two SAS proteins [107, 116]. Amongst these Rel-possessing bacteria is the Alphaproteobacteria class. Generally, Alphaproteobacteria solely possess the ancestral bifunctional Rel [107], which was confusingly termed SpoT at the time of its identification due to its similar bifunctional nature as seen by *E. coli* SpoT. Like other Alphaproteobacteria, *Caulobacter* solely possesses ancestral Rel, which will be referred to as SpoT moving forward due to its previous naming in the literature [117, 118].

PTS^{Ntr} regulates nitrogen-stimulated (p)ppGpp synthesis in *Caulobacter*

Because (p)ppGpp has massive effects on physiology and core metabolism, activity of RSH enzymes is highly regulated and these enzymes respond to varying stress signals. In bacteria that harbor duplicated Rel proteins (i.e., RelA and SpoT), these proteins' activities are regulated by differing signals. For example, in *E. coli*, RelA synthetase activity is stimulated by amino acid starvation, while *E. coli* SpoT activity is regulated by carbon [119, 120], nitrogen, and fatty acid [121-124] starvation. The molecular mechanisms by which these signals stimulate activity of RelA and SpoT paralogs differ across Beta- and Gammaproteobacteria. As an example, the molecular mechanism by which amino acid starvation stimulates RelA activity in *E. coli* has been established. Briefly, upon amino acid starvation, deacylated (i.e., uncharged) tRNAs will accumulate and, in complex with RelA, will enter into the A-site of stalled ribosomes, stimulating RelA synthetase activity through suppression of the C-terminal inhibitory activity of RelA (reviewed in [96]). Unlike *E. coli* and other copiotrophs, members of Alphaproteobacteria that possess the sole ancestral long RSH, SpoT (i.e., Rel), do not typically produce (p)ppGpp under amino acid starvation. For example, *Rhodobacter sphaeroides* and *Sinorhizobium meliloti* strain 41 do not accumulate (p)ppGpp in response to amino acid starvation [125, 126]. Instead, the photosynthetic bacterium *R. sphaeroides* produces (p)ppGpp in response to decreased light [125], whereas the nitrogen-fixing plant symbiont *S. meliloti* produces (p)ppGpp in response to carbon and ammonium starvation [126]. Although (p)ppGpp-mediated signaling is ubiquitous across bacteria, signals that regulate RSH activity and, therefore, (p)ppGpp synthesis differ across species.

As seen in other Alphaproteobacteria, *Caulobacter* SpoT (i.e., Rel) synthesizes (p)ppGpp under carbon and nitrogen starvation conditions [86, 117, 118, 127, 128], as well as fatty acid depletion [129]. Although the mechanism by which *Caulobacter* SpoT synthesizes (p)ppGpp in response to carbon starvation remains elusive, it has been characterized that nitrogen starvation regulates SpoT activity and, consequentially, (p)ppGpp synthesis through the

nitrogen-related phosphoenolpyruvate (PEP) phosphotransferase system (PTS^{Ntr}) [128, 130]. In bacteria, canonical PTS catalyzes the uptake and phosphorylation of sugars and sugar derivatives but, additionally, can have regulatory roles in carbon, nitrogen, and phosphate metabolism [131]. Regulation by PTS is characterized by its utilization of PEP as an energy source and phosphoryl donor to initiate a phosphorylation cascade through PTS proteins [131]. This phosphorylation cascade ultimately leads to the phosphorylation of carbohydrates or regulation by phosphorylated PTS proteins (including but not limited to protein-protein interactions, transcriptional activity, or phosphorylation of non-PTS proteins to modulate activity) [131]. In the case of *Caulobacter* PTS^{Ntr}, nitrogen starvation in the form of decreased intracellular glutamine activates the phosphorylation cascade [128]. Under nitrogen starvation and, therefore, decreased intracellular glutamine levels, the first enzyme of the PTS^{Ntr} (i.e., EI) autophosphorylates, which is followed by a series of phosphoryltransfers to PTS^{Ntr} proteins HPr and EIIA. HPr~P indirectly stimulates SpoT synthetase activity through some unknown mechanism, while EIIA~P directly interacts with SpoT to inhibit hydrolase activity, altogether resulting in increased (p)ppGpp synthesis by SpoT [128]. Conversely, in the presence of sufficient nitrogen, intracellular glutamine will be at levels to bind to and inhibit autophosphorylation by EI and prevent subsequent phosphoryltransfer [128, 132], thereby preventing nitrogen-dependent activation of SpoT by PTS^{Ntr} [128] and subsequent stringent response. As seen in *Caulobacter*, PTS^{Ntr}-mediated activation of SpoT under nitrogen starvation has also been established in other Alphaproteobacteria, such as the plant-associated *S. meliloti* [132], suggesting conservation of PTS^{Ntr}-mediated regulation of SpoT across the diverse Alphaproteobacteria class.

In summary, while the stringent response is a conserved stress signaling system in bacteria, the regulation of RSH enzyme activity varies regarding the type of environmental stress signal(s) and the molecular mechanisms that stimulate (p)ppGpp synthesis. This variability regarding the activation of stringent response across diverse bacteria may be reflective of

evolutionary adaptation, in which stringent response has been “optimized” according to bacterial lifestyle and environmental niche. For example, copiotrophs such as *E. coli* will activate stringent response under the starvation of “rich” biomolecules such as amino acids, while oligotrophs such as *Caulobacter* will not activate stringent response under amino acid starvation, alone [118]. In aquatic, oligotrophic environments, amino acids are not freely abundant, and this environment would not sustain growth of a copiotroph such as *E. coli*, while *Caulobacter* will continue to slowly grow and divide under these conditions. Therefore, evolutionary adaptation of stringent response has ensured growth of a bacterium in their environmental niche. Additionally, there is variability across bacteria in how activation of stringent response and (p)ppGpp modulates physiology to acclimate to environmental stressors. Below, I discuss the different ways in which (p)ppGpp modulates bacterial physiology.

(p)ppGpp in *Caulobacter*: Modulator of cell cycle & cellular development

As mentioned previously, (p)ppGpp modulates bacterial physiology and central metabolism, allowing bacteria to acclimate to their local environment. To begin, (p)ppGpp is famously known for its role in tuning the global transcriptional profile due to its direct interaction with RNA polymerase (RNAP) in Proteobacteria. In *E. coli*, (p)ppGpp directly binds two sites on RNAP: 1) a site between the β’ and ω subunits and 2) a site at the interface of the β’ subunit and the transcription factor DksA (reviewed in [133]). (p)ppGpp binding to RNAP modulates activity both positively and negatively, altering transcription of genes depending on the nature of their promoters [134]. For example, genes encoding rRNA and genes involved in DNA and phospholipid synthesis are repressed, while genes for amino acid biosynthesis and genes encoding nutrient transporters are activated (reviewed in [102, 133]. In *E. coli*, ectopic expression of *relA* altered expression of 757 genes after 5 minutes of induction, which, notably, was direct due to dependence on (p)ppGpp binding to RNAP [135]. In addition, (p)ppGpp has effects on ribosome maturation and function through its inhibition of key enzymes, such as

initiation factor IF2 [136, 137] and GTPases [138, 139] (reviewed in [102]). Outside of transcription and translation, (p)ppGpp also has direct and indirect impacts on DNA replication (reviewed in [96]). For example, in *B. subtilis* and *E. coli*, (p)ppGpp directly binds and inhibits DNA primase (DnaG), thereby directly inhibiting DNA replication [140, 141]. Additionally, in *E. coli*, increased (p)ppGpp induced by amino acid starvation blocks DNA replication in part by apparent decreased *dnaA* transcription [142], but, also, by modulation of chromosome topology at the origin of replication (i.e., decreased negative supercoiling) that prevents DnaA binding and subsequent replisome recruitment [143]. In addition, (p)ppGpp modulates bacterial cellular development. For example, starvation-induced (p)ppGpp accumulation in *M. xanthus* stimulates signals to induce fruiting body formation (reviewed in [98]); (p)ppGpp is necessary [144] and sufficient [145] for fruiting body formation in *M. xanthus*. Altogether, (p)ppGpp has a wide range of effects on bacterial physiology, including transcription, translation, DNA replication, and developmental programs.

Similar to other bacteria, (p)ppGpp influences *Caulobacter* physiology. As noted earlier, *Caulobacter* populations exhibit phenotypic heterogeneity due to the presence of distinct morphotypes (e.g., swarmer and stalked cells), which are typically associated with different cell cycle phases (e.g., G1 and S, respectively). As mentioned, these morphotypes can be separated and synchronized through methods such as density centrifugation and adhesion assays. Moreover, morphotypes in a population can be quantified through flow cytometry, taking advantage of DNA content; that is, G1 swarmer cells harbor a single chromosome, while S stalked cells and G2 predivisional cells harbor two chromosomes. Under optimal growth conditions, the swarmer-to-stalk transition is tightly coupled to the G1-to-S transition; that is, when a swarmer cell differentiates into a stalked cell, DNA replication will simultaneously commence, resulting in the cell cycle G1-to-S transition in which the stalked cell is actively undergoing DNA replication. As seen with *M. xanthus*, (p)ppGpp impedes on developmental programs and cellular differentiation in *Caulobacter*. Indeed, increased (p)ppGpp levels either

through 1) nitrogen or carbon starvation [86], 2) entry into stationary phase [86, 130], or 3) artificial induction [146] leads to modulation of the *Caulobacter* G1-to-S/swarmer-to-stalk transition. Specifically, (p)ppGpp delays this transition, resulting in perturbation of the previously mentioned “internal clock” that *Caulobacter* typically harbors in optimal growth conditions. Delays in the G1-to-S/swarmer-to-stalked transition increase the time *Caulobacter* spends in the G1 swarmer phase, leading to a higher proportion of G1 swarmer cells within a population. This relative increase in G1 swarmer cells can be detected using experimental methods, which are described later in detail. But what are the molecular mechanisms by which (p)ppGpp inhibits the G1-to-S/swarmer-to-stalk transition? While the exact mechanism remains unclear, growing evidence suggests that (p)ppGpp inhibits this transition by modulating CtrA stability and activity, as discussed below.

It was initially observed that when *Caulobacter* is grown in conditions that activate stringent response (i.e., nitrogen and carbon starvation, entry into stationary phase), DnaA is strongly downregulated and CtrA is stabilized [86, 117, 147, 148], which are molecular events that could explain a block in DNA replication initiation and morphological differentiation. Notably, under nutrient starvation, DnaA is actively cleared while its synthesis is still occurring [86], suggesting nutrient starvation modulates DnaA post-transcriptionally. Indeed, it was established that under nitrogen and carbon starvation, inhibition of DnaA translation in combination with Lon-mediated proteolysis results in decreased DnaA protein levels [147-149]. Interestingly, it was also recently established that decreased DnaA in these nutrient starved conditions occurs independent of (p)ppGpp accumulation [147], suggesting other signal(s) regulate DnaA synthesis under nutrient starvation. Furthermore, reduced DnaA levels, alone, do not account for the starvation-induced inhibition of the G1-to-S/swarmer-to-stalk transition, since artificially increasing DnaA levels does not rescue the associated cell cycle and developmental defects under starvation conditions [149].

Interestingly, inhibition of the G1-to-S/swarmer-to-stalk transition under carbon and nitrogen

limitation depends on the presence of *spoT*, indicating that this process is (p)ppGpp-dependent. As noted earlier, CtrA stability increases under starvation conditions, suggesting that (p)ppGpp modulates cell cycle progression and morphological differentiation by influencing the molecular pathways that regulate CtrA activity and stability. Supporting this idea, artificially increasing (p)ppGpp levels in non-starved *Caulobacter* similarly enhances CtrA stability and delays the G1-to-S/swarmer-to-stalk transition [146]. In summary, while the exact mechanisms by which (p)ppGpp delays the G1-to-S/swarmer-to-stalk transition remain unclear, the regulation of CtrA by (p)ppGpp represents a promising avenue for future investigation. Altogether, these findings highlight the complexity of starvation-induced signaling under different nutrient limitations and underscore the need to further explore how (p)ppGpp influences cell cycle progression and development, potentially through its effects on master regulators like CtrA.

Nitrogen stress and stringent response are coupled in Proteobacteria

As mentioned, it is established that nitrogen starvation is a major signal for the activation of stringent response in bacteria. In *Caulobacter*, decreased intracellular levels of the amino acid glutamine serve as the signal or "readout" for nitrogen status of the cell [128]. This readout is mediated through regulation of the PTS^{Ntr} and, ultimately, nitrogen-dependent SpoT activity [128]. Given the critical role of glutamine in nitrogen-dependent SpoT regulation, the intracellular regulatory and metabolic networks monitoring nitrogen availability and, consequentially, governing glutamine synthesis are critical in the nitrogen-dependent activation of SpoT and subsequent stringent response. The molecular mechanisms governing core nitrogen metabolism are further discussed, below.

From an evolutionary standpoint, glutamine has several molecular properties that make it well-suited as a "readout" for nitrogen status. To begin, glutamine is one of the 20 amino acids used in protein synthesis and, additionally, serves as a starting substrate for the biosynthesis of many essential nitrogen-containing compounds of the cell (reviewed in [150, 151]). Importantly,

glutamine is the primary product of intracellular ammonium (NH_4^+) assimilation and incorporation. The preferred inorganic nitrogen source for many bacteria is NH_4^+ [152]. This NH_4^+ can be derived from both organic and inorganic nitrogen sources in the environment. The assimilation of NH_4^+, either directly from the environment or through the catabolism of complex nitrogen sources, results in the production of metabolites which can serve as signals for nitrogen status. In bacteria, the most efficient reaction to initially assimilate NH_4^+ into organic biosynthetic molecules is through ATP-dependent glutamine synthetase (GlnA), which incorporates NH_4^+ into glutamate to generate glutamine (reviewed in [151]). In this way, glutamine serves as a nitrogen metabolite that directly reflects the abundance of available nitrogen (i.e., NH_4^+) inside and outside of the cell. Given the role of glutamine as a central metabolite for nitrogen sensing, GlnA activity is highly regulated in response to nitrogen availability. In bacteria, the regulation of GlnA is often mediated through the highly conserved PII superfamily of nitrogen sensor proteins.

Nitrogen exists in a multitude of forms in the environment. Bacteria have evolved different molecular mechanisms to monitor intracellular nitrogen status and assimilate this essential element, accordingly. A major conserved mechanism of nitrogen regulation in bacteria is through the PII superfamily of nitrogen sensor proteins (reviewed in [153]). PII proteins sense “low” and “high” intracellular nitrogen through the presence/absence of nitrogen signaling metabolites that serve as proxy for the nitrogen status of the cell. Accordingly, these PII proteins go on to alter activity of targets mostly through protein-protein interactions. Targets include regulatory enzymes, metabolic enzymes, and nutrient transporters. In Proteobacteria, glutamine is the molecular nitrogen signal that is sensed by PII proteins (reviewed in [151]). Importantly, the presence/absence of glutamine elicits a PII-mediated feedback response that affects both 1) GlnA enzymatic activity and 2) *glnA* transcription. Moving forward, I will discuss the method of signaling mediated by PII proteins in response to glutamine in the model Proteobacterium *E.*

coli. The mechanistic details of PII-mediated signaling that are described below have been incorporated from concepts reviewed extensively in [150, 151, 153, 154].

In *E. coli*, the paralogous GlnB and GlnK PII proteins are modified in response to glutamine (i.e., the output of NH_4^+ assimilation) through the primary nitrogen sensor GlnD. GlnD is a bifunctional uridylyltransferase/uridylyl-removing (UTase/UR) enzyme that reversibly catalyzes the transfer of uridine monophosphate (UMP) groups to PII proteins. When intracellular glutamine is low (reflecting low NH_4^+ and, therefore, nitrogen deplete conditions), GlnD uridylylates PII proteins GlnB and GlnK [155]. Consequentially, GlnB~UMP stimulates deadenylylation of GlnA through the bifunctional adenylyltransferase (ATase) GlnE. Deadenylylation of GlnA removes inhibition of its activity and allows for the ATP-dependent synthesis of glutamine from NH_4^+ and glutamate. When intracellular glutamine is high (reflecting high NH_4^+ and, therefore, nitrogen replete conditions), there is negative feedback on this pathway. Glutamine will bind GlnD and stimulate UR activity on GlnB and GlnK [155]. Consequentially, deuridylylated GlnB allows for GlnE to adenylylate GlnA, inhibiting the synthetase activity of GlnA. Although GlnB and GlnK have overlapping redundant functions and undergo the same modifications in this pathway under certain conditions (reviewed in [153]), GlnK also serves independent functions. In nitrogen replete conditions, deuridylylated GlnK will bind and inhibit AmtB, an NH_4^+ uptake transporter, to prevent further unnecessary uptake of NH_4^+. Conversely, in low nitrogen, GlnK~UMP no longer inhibits AmtB, allowing for uptake of NH_4^+. Thus far, regulation of GlnA synthetase activity by the PII signaling pathway has been discussed. As previously mentioned, PII proteins also regulate *glnA* transcription in response to nitrogen signaling metabolites, specifically glutamine. This regulation of *glnA* by PII proteins is mediated through the NtrB-NtrC TCS. The conserved NtrB-NtrC TCS canonically regulates transcription of nitrogen assimilation genes in bacteria, including *glnA*, *amtB*, etc. In high nitrogen (i.e., high glutamine), deuridylylated GlnB binds NtrB, the bifunctional SHK, and promotes NtrB phosphatase activity. Consequentially, NtrB dephosphorylates and inactivates its

cognate RR, NtrC, as a transcriptional activator of its targets, including *glnA*, to prevent further nitrogen assimilation under replete conditions. Conversely, in low nitrogen (i.e., low glutamine), GlnB~UMP does not interact with NtrB, promoting NtrB kinase activity. Phosphorylated NtrC (NtrC~P) will activate transcription of its targets, including *glnA*, to promote assimilation of nitrogen and glutamine synthesis. Altogether, glutamine serves as a nitrogen signaling molecule that modulates central nitrogen metabolism due to its reflection of nitrogen status of the cell. PII-mediated glutamine sensing and response allows cells to coordinate central nitrogen metabolism with environmental nitrogen conditions.

Given 1) the role of glutamine as the primary product of inorganic nitrogen (i.e., NH_4^+) incorporation and 2) the role of glutamine as the signaling molecule for nitrogen status in Proteobacteria, one would predict that loss of PII sensor proteins, as well as interacting regulatory and metabolic proteins, would have detrimental effects on central nitrogen metabolism, and, consequentially, affect bacterial physiology and cell growth, perhaps through stringent response. Indeed, in *E. coli* mutants harboring deletions in PII and PII-related proteins have defects in sensing nitrogen status and are auxotrophic for glutamine. For example, deletion of *E. coli glnD*, the primary nitrogen sensor, results in decreased GlnA levels, decreased GlnA activity, and glutamine auxotrophy [156]. This absence of UTase activity by GlnD results in deuridylylated GlnB, which 1) stimulates phosphatase activity by NtrB, thereby dephosphorylating and inactivating NtrC-dependent transcription of *glnA* and 2) stimulates adenylylation of GlnA by GlnE, inhibiting GlnA synthetase activity.

In *Caulobacter*, PII and PII-related proteins have been investigated regarding their role in activation of the PTS^{Ntr} due to dysregulation of glutamine synthesis. As mentioned previously, the obligate dimorphic life cycle of *Caulobacter* (i.e., G1 swarmer cells vs S stalked cells), allows for straightforward morphological and developmental detection of perturbations in cell cycle progression, specifically perturbations mediated through stringent response. Nitrogen-induced stringent response classically slows the G1-to-S/swarmer-to-stalk *Caulobacter* transition,

resulting in increased time spent in the G1 swarmer phase (reviewed in [96]). This extended time in G1 swarmer phase will result in an increased relative number of G1 swarmer cells in a *Caulobacter* population and can be quantified using the following methods: 1) motility assays, 2) density centrifugation, and 3) chromosome quantification using flow cytometry. Respectively, increased G1 swarmer cells in a population will result in 1) a larger motility halo, 2) a smaller buoyant population, and 3) a higher relative number of 1N (i.e., single chromosome) cells. Indeed, deletion of *glnD*, *glnA*, *glnB*, and *ntrC* all result in these G1 swarmer extension phenotypes in *Caulobacter*, importantly, even when grown in the complex medium peptone yeast extract (PYE) [128], suggesting that these strains “feel” glutamine starved and activate stringent response in PYE complex medium. Apparently, PYE possesses low levels of glutamine, making up ≤0.02% of total amino acid content [128]. Low glutamine levels in PYE in combination with loss of intracellular glutamine synthesis result in low intracellular glutamine in these nitrogen metabolism mutants and, thereby, activate PTS^{Ntr}, resulting in G1 extension phenotypes. Indeed, glutamine supplementation to the PYE medium complements the G1 extension phenotypes of these nitrogen metabolism mutants [128].

In summary, as seen in other Proteobacteria, the PII and PII-related proteins of central nitrogen metabolism play critical roles in intracellular glutamine synthesis in *Caulobacter*. Modulation and dysregulation of central nitrogen metabolism has downstream effects on PTS^{Ntr} due to the inability of nitrogen metabolism mutants to synthesize glutamine from the catabolism of other abundant nitrogen sources in the complex PYE medium. Altogether, the literature suggests central nitrogen metabolism and stringent response are indirectly coupled through PTS^{Ntr}, which detects intracellular glutamine levels.

Although this coupling seems to be mediated through glutamine levels and activation of PTS^{Ntr} in *Caulobacter*, components of central nitrogen metabolism have been shown to directly regulate stringent response. One such protein is NtrC. As mentioned previously, phosphorylation of NtrC by its cognate SHK, NtrB, under nitrogen starvation results in

transcriptional activity by NtrC (reviewed in [153]). Specifically, in *E. coli*, phosphorylation of NtrC stimulates its σ^{54}-dependent transcription, thereby allowing transcriptional activation of its targets, including genes encoding regulatory, metabolic, and transporter proteins involved in nitrogen assimilation [157]. It has been established that NtrC activates transcription of *nac*, which encodes a LysR-like transcriptional regulator that activates transcription of σ^{70}-dependent genes in nitrogen starved conditions [157, 158]. In this way, Nac serves as an adapter between NtrC and σ^{70}-dependent gene targets during nitrogen starvation and, thereby, amplifies the response to nitrogen starvation. More recently, it has been established in *E. coli* that NtrC directly activates expression of *relA,* itself, in a σ^{54}-dependent manner [159]. It was previously thought that *relA* only had two promoters, P1 and P2, which are σ^{70}-dependent. These σ^{70}-dependent promoters are constitutively active and induced in stationary phase, respectively [112, 160]. Brown et al found that *E. coli relA* additionally harbors two σ^{54}-dependent promoters, P3 and P4, which are activated by NtrC under nitrogen starvation [159]. These σ^{54} promoter elements of *relA* seem to be conserved in Enterobacteriaceae, a bacterial family belonging to the class Gammaproteobacteria, suggesting a conserved mechanism of NtrC-dependent activation of σ^{54} *relA* promoters within this bacterial family [159]. Notably, there is no evidence of direct binding or regulation by *E. coli* NtrC to the promoter of the paralogous *spoT*, although, RNAP binding to P_{spoT} seems to be inhibited under nitrogen starvation in *E. coli* [159]. Given SpoT is the sole RSH that possesses (p)ppGpp hydrolase activity in Enterobacteriaceae, it is predicted this inhibition of *spoT* transcription induced under nitrogen starvation amplifies (p)ppGpp levels under these conditions. Altogether, NtrC couples nitrogen metabolism and stringent response in Enterobacteriaceae.

The conserved RR NtrC serves critical roles in bacteria, including its roles in 1) central nitrogen metabolism and homeostasis and 2) the of coupling nitrogen metabolism and stringent

response. NtrC belongs to a dynamic class of proteins called bacterial enhancer binding proteins (bEBPs), which canonically regulate σ^{54}-dependent transcription.

σ^{54}-dependent transcription versus σ^{70}-dependent transcription

Transcription of genetic information is an essential biological process. Canonically, transcription is the process by which genetic information in the form of DNA is synthesized into messenger RNA (mRNA) that relays the information necessary for protein synthesis. The initiation of transcription requires 1) sequence-specific recognition at promoters and 2) melting of double-stranded DNA to provide template for RNA synthesis by RNAP. Sequence-specific recognition is performed by sigma (σ) factors that bind and recruit RNAP to target promoters. In certain instances, σ factors are also critical for DNA melting, also known as “open complex formation” (reviewed in [161]). There are two families of σ factors that recognize promoter sequences and recruit RNAP: 1) the σ^{70} family and 2) the “alternate” σ^{54} family. The σ^{70} family are often termed as “housekeeping” due to its primary member, σ^{70}, characteristically activating the transcription of essential genes required to maintain basic cellular functions and genes required for exponential growth [161, 162]. These "housekeeping" genes include those involved in DNA replication, central metabolism, and cell division. Beyond the essential primary housekeeping σ^{70}, the σ^{70} family includes a diverse group of σ^{70}-like σ factors [162, 163], such as σ^{32}, the σ factor involved in heat shock response [164]. Alternatively, the σ^{54} family is composed of a single member, σ^{54}, which is canonically used for signal transduction pathways stimulated under particular environmental conditions. Notably, σ^{54} is best known for its role in nitrogen metabolism and is also called σ^{N} for this reason [165]. Although both families of σ factors bind the same core RNAP, the σ^{54}-RNAP and σ^{70}-RNAP holoenzymes possess vastly different properties, discussed below.

Both σ^{54}- and σ^{70}-RNAP holoenzymes bind their target promoters forming a closed, nonproductive complex with DNA [166], although, differences in sequence recognition and

binding by these holoenzymes alters their ability to promote open complex formation to initiate transcription (reviewed in [167]). σ^{70}-RNAP binds the consensus -10 (TATAAT) and -35 (TTGACA) sequences (i.e., -10 and -35 reflect distance relative to the transcription start site). Binding of σ^{70}-RNAP at these sites results in the formation of an energetically-unfavorable closed complex that is coupled to thermally-driven melting of the -10 element, exposing the nontemplate strand to interact with the σ^{70}-RNAP holoenzyme [168]. These events result in spontaneous isomerization to form open complex that allows for transcription initiation (reviewed in [167]). Alternatively, σ^{54}-RNAP recognizes and binds the conserved -12 (TGC) and -24 (GG) promoter elements, forming a stable closed complex (reviewed in [167]). Interaction of σ^{54} at the -12/-11 position prevents interaction between the holoenzyme and the nontemplate strand, thereby preventing open complex formation [161, 166]. Therefore, σ^{54}-dependent transcription is distinct from σ^{70}-dependent transcription in that the σ^{54} holoenzyme requires the presence of an activator protein that hydrolyzes ATP to provide the mechanical energy needed to remove the inhibitory interaction at the −12/−11 position, allowing for open complex formation and subsequent transcription initiation [166, 169, 170]. These activator proteins belong to a broad class of universal proteins called AAA+ (ATPases associated with various cellular activities) proteins that canonically hydrolyze ATP, converting the chemical energy from ATP hydrolysis into mechanical energy for various cellular processes (reviewed in [171-173]). Specifically, these σ^{54}- activating AAA+ proteins bind to upstream activator sequences (UASs) or enhancer sites located 80 to 150 base pairs upstream of the promoter—similar to the binding pattern of eukaryotic enhancer-binding proteins (EBPs) [174]. Consequently, these σ^{54}-activating AAA+ proteins are referred to as bacterial enhancer binding proteins (bEBPs). To promote open complex formation and initiate σ^{54}-dependent transcription, bEBPs must directly contact the closed nucleoprotein complex through interaction with σ^{54}. This interaction supplies the mechanical energy generated from ATP hydrolysis, which drives the transition from closed to

open complex. Because bEBPs bind distant UAS enhancer sites relatively far upstream of the transcription start site, DNA looping must occur to bring the bEBP into proximity of the σ^{54}-RNAP holoenzyme. This DNA looping can be mediated by DNA-bending proteins, such integration host factor (IHF) or HU proteins, which bind between UAS enhancer sites and promoters to bend DNA and to bring bEBPs into direct contact with σ^{54}-RNAP [175, 176]. Next, I will discuss the canonical molecular features of bEBP, as well as their canonical activity.

Defining the canonical structural features of bEBPs

bEBPs typically consist of three domains: 1) N-terminal regulatory domain (REC), 2) central AAA+ domain (AAA), and 3) C-terminal DNA-binding/helix-turn-helix domain (HTH) domain. The REC domain perceives intra- and extracellular signals. Signal perception by REC is transduced to the AAA catalytic domain to modulate bEBP activity. The AAA domain is responsible for ATP binding and hydrolysis, oligomerization, and direct interaction with σ^{54} of the σ^{54}-RNAP holoenzyme; therefore, the AAA domain is indispensable for σ^{54}-dependent transcription (reviewed in [167]). Given the critical role of AAA in bEBP activity, this domain is the most conserved across bEBPs. The AAA domain contains seven conserved regions (i.e., C1 to C7) [177, 178], which are broadly conserved among the AAA+ protein family. However, the AAA domain of bEBPs is distinct from other AAA+ proteins due to unique insertions that form surface-exposed loops. Loop 1 extends from region C3, while Loop 2 is positioned between C5 and C6. Several key conserved residues are located within these regions, including the Walker A motif, "switch" asparagine, GAFTGA motif, Walker B motif, sensor I, arginine fingers, and sensor II (reviewed in [167]). These key residues and their functions are discussed in detail, below.

The Walker A and B motifs are involved in ATP binding and hydrolysis, respectively. Walker A forms a structurally conserved P loop with the consensus sequence GxxxxGK(T/S), where X is any amino acid. The conserved lysine (K) serves to stabilize the interaction with the

negatively charged γ phosphate of ATP, while the threonine/serine (T/S) residues contribute to coordination of Mg^{2+}. Notably, the conserved lysine (K) residue is essential for subsequent ATP hydrolysis. Altogether, this P loop coordinates ATP for subsequent hydrolysis (reviewed in [179]). Walker B has the conserved consensus sequence hhhhDE, where h is any hydrophobic amino acid. The conserved aspartate (D) is required for ATP hydrolysis, in which this residue coordinates Mg^{2+} through bridging a water molecule [180, 181]. Sensor I and II motifs reside in C6 and C7, respectively. A conserved threonine residue of sensor I interacts with residues of the Walker B motif and apparently plays a role in the coupling of ATP hydrolysis and conformational changes of the exposed loops [182]. Conserved residues of sensor II have similarly been implicated in ATP binding and hydrolysis [178, 183]. Arg fingers are also important for ATP hydrolysis and have been implicated in intermolecular catalysis, where these residues transmit the chemical energy from ATP hydrolysis to induce conformational changes in neighboring subunits of the bEBP oligomer [172]. The “switch” Asn has been implicated in interaction with the conserved glutamate (E) of the Walker B motif and, moreover, implicated in ATP hydrolysis, DNA melting, and overall organization of the active site [184] (reviewed in [167, 185]). The AAA motif known as GAFTGA resides in the exposed surface loop, Loop 1, of the C3 region and is uniquely conserved in the bEBP class of AAA+ proteins (reviewed in [177]). This motif is essential for ATP hydrolysis-dependent direct interaction with σ^{54} [186] and subsequent open complex formation (reviewed in [183]).

Finally, the C-terminal HTH domain is primarily responsible for binding to DNA upstream of σ^{54}-dependent target promoters. The HTH domain specifically recognizes and binds to UAS enhancer sequences located about 80–150 base pairs upstream of the target promoter. In a HTH-dependent manner, bEBPs typically bind at tandem sites within UAS enhancer elements sites as inactive dimers. This binding allows for specificity and proper bEBP-mediated activation at select σ^{54} promoters upon response to specific intra- and extracellular stimuli, which are

mediated through upstream REC and AAA activity. Altogether, activities of the REC, AAA, and HTH domains ultimately result in ATPase-active oligomers on DNA that remodel σ^{54}-RNAP at promoters, allowing for open complex formation and subsequent transcription initiation.

The mechanism of bEBP regulation and subsequent activity described above is the "canonical model". However, as noted earlier, bEBPs are a dynamic class of proteins that regulate various cellular processes in response to various intra- and extracellular stimuli. Well-studied examples include phage shock protein F (PspF) from *E. coli*, which regulates transcription of the *psp* operon in response to filamentous phage infection, heat shock, osmotic stress, and ethanol treatment [187, 188]. Another well-studied example is the C4-dicarboxylate transport transcriptional regulatory protein (DctD) from *S. meliloti* and *Rhizobium leguminosarum*, which activates the transcription of a transporter gene that enables the utilization of four-carbon dicarboxylic acids for free-living growth or nitrogen fixation during plant symbiosis [189]. Tyrosine regulatory protein (TyrR) from *E. coli* responds to aromatic amino acids and regulates transcription for their biosynthesis, accordingly [190, 191]. In other words, the intra- and extracellular signals that stimulate bEBP activity and the corresponding transcriptional regulons of bEBPs can vary greatly. Reflectively, the molecular mechanisms by which different signals stimulate bEBP activity and subsequent transcriptional regulation vary across bEBPs. Due to the diversity within this protein class, bEBPs have been categorized into five groups (Group I–V) based on their molecular features, including domain architecture (reviewed in [167]). The molecular characteristics of these groups are discussed below.

Structural and molecular diversity within the bEBP class

To begin, not all bEBPs possess a REC domain (Group IV). For example, PspF lacks a REC domain and, instead, forms a repressive complex with a protein that inhibits its bEBP activity (reviewed in [192]). For bEBPs that possess a REC domain, this domain can sense intra- and extracellular stimuli through a variety of molecular routes, including phosphorylation,

ligand binding, and protein-protein interactions (reviewed in [167]). Moreover, bEBPs possess conserved domains and residues within the REC region according to their method of signal perception (reviewed in [192]). bEBPs stimulated by phosphorylation of their REC domains are often part of TCSs (described previously). bEBPs such as NtrC, DctD, and FlgR have RR-like domains in the N-terminal REC region that harbor a conserved aspartyl residue for phosphorylation (Group I) (reviewed in [167]). Phosphorylation of the aspartyl residue is required for bEBP activity and consequential σ^{54}-dependent transcription of target genes. In other cases, bEBPs possess REC regions that contain ligand-binding domains, such as Per, ARNT, and Sim (PAS) (Group II) [193, 194], cyclic GMP [cGMP]-specific and -stimulated phosphodiesterases (GAF) (Group III) [195], and aspartokinase, chorismate mutase, and TyrA (ACT) domains (reviewed in [167]). These domains typically bind and sense small effector molecules to stimulate bEBP activity. Lastly, bEBP activity can be regulated through protein-protein interactions mediated through the REC domain. Typically, these regulatory proteins bind and inhibit their target bEBP, acting as “antiactivators” and, upon certain signals, will dissociate from the bEBP, allowing for downstream transcriptional activity (reviewed in [167]). Importantly, although REC domains of bEBPs may sense a variety of signals, these signals are transduced to the catalytic AAA domain. Notably, signal perception by REC can exhibit both positive and negative control of the AAA activity [196]. Deletion of the REC domain is an experimental method that can be used to determine if the REC domain has repressing or activating control on AAA domain activity. One example of negative regulation by REC is seen with NtrC1 of the extreme thermophile *Aquifex aeolicus*. When the REC domain of NtrC1 is deleted, the AAA domain becomes an active heptamer, while the REC-possessing native NtrC1 forms inactive dimers. This is because phosphorylation of the REC rearranges this domain, exposing surfaces promoting heptamer formation and interaction with σ^{54} [197]. In other words, phosphorylation of REC domain of NtrC1 has derepressive function of its bEBP activity. In contrast, the AAA

domain of NtrC, the first characterized bEBP, is subject to positive regulation by REC [198, 199]. Specifically, deletion of the NtrC REC domain results in a constitutively inactive protein, highlighting the stimulatory function of the REC domain in its bEBP activity. These two NtrC-type bEBPs possess high sequence similarity (~60%), yet display different methods of regulation (reviewed in [167]). Additionally, the C-terminal HTH domain of bEBPs can have multiple roles in protein activity, including directing the protein to DNA target sequences and facilitating oligomer formation. Canonically, bEBPs bind specific UAS enhancer sequences upstream of promoter targets. Typically, these proteins will bind DNA at enhancer sites as inactive dimers. All HTH-possessing bEBPs possess at least one enhancer site, although it is not uncommon for there to be up to three enhancer sites upstream of their target promoter(s). Oligomerization, which is a method of regulation of bEBP activity, has been shown to be DNA-dependent for some bEBPs. Multiple enhancer binding sites upstream of their target promoter(s) allows for multiple dimers to bind. This increase in local concentration of bEBPs facilitates oligomerization. It is common for three enhancer binding sites to allow for the hexamerization of three dimers at these sites, although, it is known that some bEBPs will bind two enhancer sites and recruit a third dimer from solution to form a functional oligomer upon phosphorylation of REC, as seen with NtrC of *Salmonella typhimurium* [200]. Moreover, it has been shown that high concentrations of bEBPs can stimulate oligomerization independent of binding native enhancer sites. For example, bEBPs which were truncated of their HTH domains were able to stimulate σ^{54}-dependent transcription *in vivo* and *in vitro*, including PspF, NifA, DctD, and NtrC [201-205]. Moreover, some bEBPs naturally lack a HTH domain and activate σ^{54}-dependent transcription from solution (Group V) and, therefore, are enhancer binding-independent bEBPs (reviewed in [206]). In this type of instance, regulation and specificity of σ^{54}-dependent transcription is mediated through other routes. For example, bEBPs naturally lacking the HTH domain are, in some instances, the sole σ^{54}-activator in the bacterium [207, 208]. An

example of this is seen in *Helicobacter pylori* that possesses the sole bEBP, FlgR, which activates flagellar genes upon phosphorylation of its REC domain [209, 210]. Notably, FlgR levels are much higher in *H. pylori* [209] compared to levels of enhancer binding-dependent bEBPs in other bacteria, such as NtrC in *E. coli* [211]. Additionally, it is sometimes the case that promoter specificity is determined through σ^{54}, itself, as in the case of *R. sphaeroides*, which harbors the HTH-lacking bEBP, FleT, which specifically regulates transcription of flagellar genes [212]. Perhaps the most striking variability seen within the class of bEBPs is the ability of some bEBPs to activate σ^{70}-dependent transcription instead of σ^{54}. In these instances, these bEBPs lack the conserved GAFTGA motif, which, as mentioned previously, is essential for σ^{54}-dependent transcription. Examples of σ^{70}-activating bEBPs include *E. coli* TyrR, *R. capsulatus* NtrC, and *V. cholera* VspR [191, 213, 214].

In summary, σ^{54}-dependent transcription is tightly regulated due to the need for bEBP activators that provide energy for open complex formation of the σ^{54}-RNAP holoenzyme at promoters. Intra- and extracellular signals regulate activity of bEBPs, which results in specific and timely activation of σ^{54}-dependent transcription. Specifically, σ^{54}-dependent transcription typically occurs in response to stressor signals that regulate bEBP activity and consequentially, activate σ^{54}-dependent transcription. This mode of regulation may act as an energy-conserving strategy by bacteria to conserve resources unless stress-induced gene activation is absolutely required under niche environmental conditions. bEBPs represent a highly diverse class of AAA+ proteins that differ in domain composition, activation mechanisms, signal perception, and even the type of transcription they regulate (i.e., σ^{54}- vs. σ^{70}-dependent transcription). As research on bEBPs expands, an increasing number of proteins have emerged as “exceptions to the rule.” Key unanswered questions include: What selective pressures led to the loss of enhancer site binding? What drove the shift from σ^{54}- to σ^{70}-dependent transcriptional activation? Given that σ^{54}-dependent transcription is tightly regulated by environmental signals through bEBP activity,

broader questions remain, such as what physiological advantages are conferred by this transcriptional mechanism. Overall, the complexity and regulatory diversity of bEBPs and σ^{54}-dependent transcription make these proteins intriguing targets for further investigation.

The distribution of bEBPs across bacteria

The distribution of bEBPs and σ^{54} vary across bacteria. bEBPs and σ^{54} are widely distributed across Proteobacteria and their more closely related species, such as the Chlamydias and Spirochetes (reviewed in [215]). Some low-GC Gram-positive bacteria, including *B. subtilis* and *Clostridium difficile*, also encode σ^{54} and its activators, though *Streptococcus* and *Staphylococcus* species lack these genes (reviewed in [215]). In contrast, many high-GC Gram-positive bacteria, including *Mycobacterium tuberculosis*, do not encode σ^{54} or bEBPs in their genomes (reviewed in [192, 215]). The number of bEBPs encoded by a species also varies significantly. For example, *E. coli* K-12 encodes 12 known bEBPs [216], while the gastric pathogen *H. pylori* encodes only one bEBP, FlgR [210]. *Caulobacter* encodes σ^{54}, as well as four bEBPs within its genome: NtrC, NtrX, TacA, and FlbD (reviewed in [42]). TacA and FlbD have been studied extensively in *Caulobacter* regarding their roles in stalk biosynthesis and flagellar biosynthesis, respectively (reviewed in [42]). Similar to canonical bEBPs, TacA and FlbD activate σ^{54}-dependent transcription of target genes involved in stalk and flagellar biosynthesis upon activation. Notably, *rpoN* (encoding σ^{54}), *flbD*, and *tacA* are transcriptionally regulated by the master cell cycle regulator CtrA (reviewed in [217]). As a result, their activation is tightly linked to the cell cycle, playing a critical role in the timely synthesis of the stalk and flagellum that are coordinated with cell cycle. This cell cycle-dependent regulation is a unique feature of these bEBPs, since bEBPs and σ^{54} more commonly regulate metabolic pathways in response to niche environmental signals.

Although some initial studies have explored NtrX and NtrC function in *Caulobacter* [128, 218], their transcriptional mechanisms, regulons, and potential roles in cell cycle and

developmental control remain unclear. Given the established roles of σ^{54}, FlbD, and TacA in *Caulobacter* cell cycle regulation, it will be interesting to determine whether NtrX and NtrC exhibit similar regulatory patterns. In particular, since NtrC couples nitrogen stress with the stringent response in other bacteria, it presents an obvious target for exploring cell cycle regulation in *Caulobacter*. I describe my investigations of this topic in this dissertation.

Figures

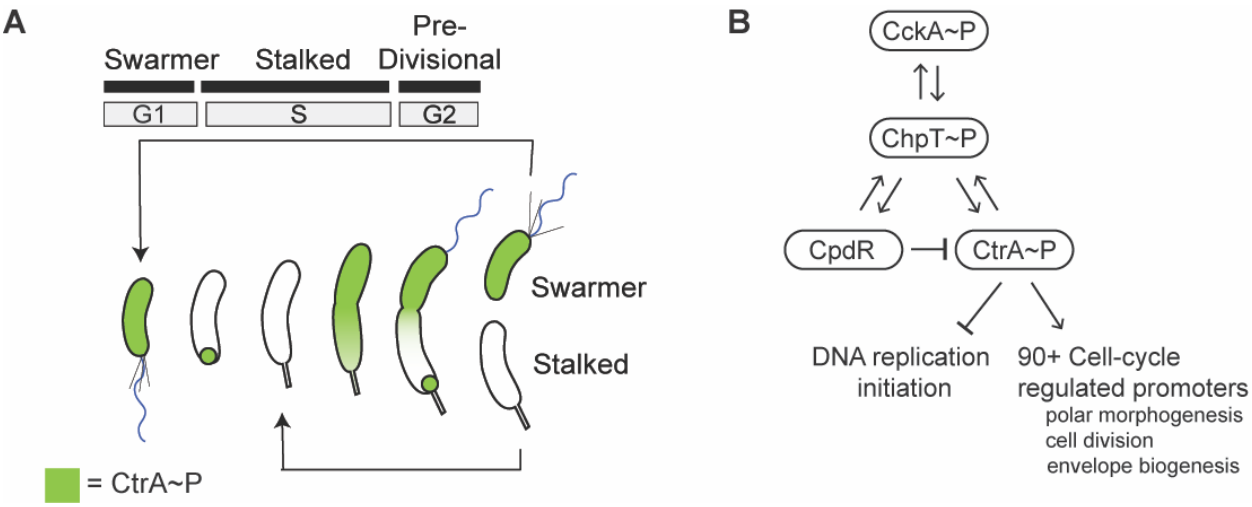

Figure 1.1. CckA-ChpT-CtrA phosphorelay dictates the dimorphic life cycle of *Caulobacter crescentus*. (A) *Caulobacter* harbors a developmental program within its cell cycle resulting in asymmetric cell division producing two morphologically and replicatively distinct cells—the G1 swarmer cell and the S stalked cell. CtrA is spatially and temporally regulated throughout the cell cycle. In the G1 swarmer cell, CtrA is phosphorylated by CckA and activates G1-specific cell cycle promoters and, additionally, binds and inhibits the origin of replication. During the G1-to-S/swarmer-to-stalk transition, CtrA is dephosphorylated and recruited to the swarmer cell pole where it is degraded. CtrA is resynthesized and phosphorylated by CckA in the S stalked cell, where it activates S-specific cell cycle promoters and is, again, able to bind and inhibit the origin of replication. Upon cell division, CtrA is dephosphorylated and degraded in the stalked cell and remains phosphorylated in the swarmer cell. The swarmer cell, again, must develop into the stalked cell to proceed with cell division, while the stalked cell can immediately proceed with another round of cell division. The presence of phosphorylated CtrA (CtrA~P) throughout the cell cycle is shown in green. This figure was adapted from Fiebig et al [219]. (B) Model of the essential *Caulobacter* cell cycle regulatory phosphorelay. CckA is a bifunctional sensor histidine kinase that regulates CtrA, the master cell cycle and class I flagellar regulator, and its proteolytic adapter CpdR through phosphorylation or dephosphorylation via the histidine phosphotransferase ChpT. When CckA acts as a kinase, it phosphorylates CtrA, enabling it to bind DNA, block chromosome replication initiation, and activate cell cycle-regulated promoters. When CckA acts as a phosphatase, it dephosphorylates CpdR, which then facilitates CtrA degradation. CckA, ChpT, and CtrA are all essential for viability.

Chapter 2: The *Caulobacter* NtrB-NtrC two-component system bridges nitrogen assimilation and cellular development

Preface

The content of this chapter was modified and adapted from its published form: North H, McLaughlin M, Fiebig A, Crosson, S. (2023) *J Bacteriol.* 205(10):e0018123.

Abstract

A suite of molecular sensory systems enables *Caulobacter crescentus* to control growth, development, and reproduction in response to levels of essential elements. The bacterial enhancer binding protein (bEBP) NtrC, and its cognate sensor histidine kinase NtrB, are key regulators of nitrogen assimilation in many bacteria, but their roles in *C. crescentus* are not well defined. Notably, *C. crescentus* NtrC is an unconventional bEBP that lacks the σ^{54}-interacting loop commonly known as the GAFTGA motif. Here we show that deletion of *C. crescentus ntrC* slows cell growth in complex medium, and that *ntrB* and *ntrC* are essential when ammonium is the sole nitrogen source due to their requirement for glutamine synthetase (*glnA*) expression. Random transposition of a conserved IS3-family mobile genetic element frequently rescued the growth defect of *ntrC* mutant strains by restoring transcription of the *glnBA* operon, revealing a possible role for IS3 transposition in shaping the evolution of *C. crescentus* populations during nutrient limitation. We further identified dozens of direct NtrC binding sites on the *C. crescentus* chromosome, with a large fraction located near genes involved in polysaccharide biosynthesis. The majority of binding sites align with those of the essential nucleoid associated protein, GapR, or the cell cycle regulator, MucR1. NtrC is therefore predicted to directly impact the regulation of cell cycle and cellular development. Indeed, loss of NtrC function led to elongated polar stalks and elevated synthesis of cell envelope polysaccharides. This study establishes regulatory connections between NtrC, nitrogen metabolism, polar morphogenesis, and envelope polysaccharide synthesis in *C. crescentus*.

Introduction

Nitrogen exists in a multitude of forms in the environment, and bacteria have a variety of molecular mechanisms to assimilate this essential element. Accordingly, bacterial cells commonly express sensory transduction proteins that detect environmental nitrogen and regulate the transcription of genes that function in nitrogen assimilation. The conserved NtrB-NtrC two-component system (TCS) is among the most highly studied of these regulatory systems. The NtrB-NtrC TCS has been broadly investigated, particularly in Enterobacteriaceae where it is well established that the NtrB sensor histidine kinase (SHK) controls phosphorylation state of the DNA-binding response regulator (RR), NtrC, in response to intracellular nitrogen and carbon status [220-223]. Phosphorylated NtrC (NtrC~P) activates transcription of multiple genes involved in inorganic nitrogen assimilation and adjacent physiologic processes.

The preferred inorganic nitrogen source for many bacteria is ammonium (NH_4^+) [152] and NtrC~P commonly activates transcription of glutamine synthetase (*glnA*) [153], which functions to directly assimilate NH_4^+ in the process of glutamine synthesis. In the freshwater- and soil-dwelling bacterium, *Caulobacter crescentus* (hereafter, *Caulobacter*) [28], glutamine levels *per se* are a key indicator of intracellular nitrogen status and impact cell differentiation and cell cycle progression via the nitrogen-related phosphotransferase (PTS^{Ntr}) system [128]. The deletion of *ntrC* results in a nitrogen deprivation response in *Caulobacter* [128], and it is expected that this is due, at least in part, to reduced *glnA* transcription. However, NtrC belongs to a broadly conserved class of transcriptional regulators known as bacterial enhancer binding proteins (bEBPs) that can function as global regulators of gene expression (reviewed in [167]), so NtrC is predicted to regulate expression of more than just *glnA* in *Caulobacter*. Indeed, ChIP-seq and transcriptomic studies in *Escherichia coli* demonstrated that NtrC binds dozens of sites on the chromosome [159, 224] and affects transcription of ≈2% of the genome [157]. Given the importance of cellular nitrogen status as a cell cycle and developmental regulatory cue in *Caulobacter*, we sought to

define the NtrC regulon and to assess the role of the NtrB-NtrC TCS in the regulation of cellular development and physiology.

We conducted a molecular genetic analysis of the *Caulobacter* NtrB-NtrC TCS. A main objective of this study was to determine the functional roles of *ntrB* and *ntrC* during growth in media containing inorganic and organic nitrogen sources. Using transcriptomic and ChIP-seq approaches, we defined the NtrC regulon, revealing its dual function as both an activator and a repressor. Our ChIP-seq analysis identified dozens of NtrC binding sites across the *Caulobacter* chromosome, many of which directly overlap with binding sites for the essential nucleoid-associated protein, GapR [225, 226], and the cell cycle regulator, MucR1 [227]. Deletion of *ntrC* led to slow growth in complex medium and an inability to grow when NH_4^+ was the sole nitrogen source, due to a lack of *glnBA* transcription. Random transposition of a conserved *Caulobacter* IS3-family mobile genetic element into the promoter of the *glnBA* operon was a frequent and facile route to rescue the growth defect of *ntrC* mutants; IS3 transposition effectively rescued *glnBA* transcription, enabling growth of the Δ*ntrC* strain. *Caulobacter* is a prosthecate bacterium that elaborates a thin stalk structure from its envelope at one cell pole, and we further discovered that loss of *ntrC* resulted in hyper-elongated stalks and a hyper-mucoid phenotype. These phenotypes were complemented by either glutamine supplementation to the medium or by ectopic *glnBA* expression. Our study provides a genome-scale view of transcriptional regulation by a NtrC protein with distinct structural features and defines a regulatory link between NtrC and nitrogen assimilation, polar morphogenesis, and envelope polysaccharide synthesis in *Caulobacter*.

Results

*Orthologous ntrC does not complement Caulobacter Δ*ntrC* nitrogen assimilation defect*

Given the well-established role for the NtrB-NtrC TCS in inorganic nitrogen assimilation [228], we predicted that a *Caulobacter* mutant harboring an in-frame deletion of *ntrC* (Δ*ntrC*) would exhibit growth defects in a defined medium with NH_4^+ as the sole nitrogen source (M2 minimal

salts with glucose; M2G). As expected, the Δ*ntrC* mutant failed to grow in M2G and this growth defect was genetically complemented by restoring *ntrC* at an ectopic locus (**Figure 2.1A**). The sole predicted route of NH_4^+ assimilation in *Caulobacter* is via glutamine synthetase (GlnA) [128], and we, therefore, predicted that replacement of NH_4^+ with glutamine as the nitrogen source would restore growth of Δ*ntrC* in M2G. As expected, replacement of NH_4^+ with molar-equivalent (9.3 mM) levels of glutamine restored Δ*ntrC* growth in M2G (**Figure 2.1A**). We conclude that *ntrC* is required for NH_4^+ assimilation in a defined medium.

The functional conservation of *ntrC* between phylogenetically proximal [229-231] and distal [232] species has been demonstrated by heterologous genetic complementation. *Caulobacter* NtrC shares 40% sequence identity with the highly studied *Escherichia coli* NtrC (See **Figure S2.1** in Appendix 1), but expression of *E. coli ntrC* from a xylose-inducible promoter did not restore growth of *Caulobacter* Δ*ntrC* in M2G (**Figure 2.1B**), even though *E. coli* NtrC was stably produced in *Caulobacter* (See **Figure S2.2A** in Appendix 1). Inspection of NtrC primary sequences revealed that the AAA+ domain from *Caulobacter* species lacks the conserved GAFTGA motif (See **Figure S2.1** in Appendix 1), which is important for the promoter remodeling activity of the AAA+ domain and for coupling promoter conformation information to σ^{54}-RNAP [233]. *Rhodobacter capsulatus*, like *Caulobacter*, is in the class Alphaproteobacteria. NtrC from this species and others in the order Rhodobacterales also harbor a deletion of the L1 loop containing the GAFTGA motif (See **Figure S2.1** in Appendix 1); *R. capsulatus* NtrC is reported to activate gene expression through σ^{70} rather than σ^{54} [213]. Expression of *R. capsulatus ntrC* from a xylose-inducible promoter also failed to restore growth of *Caulobacter* Δ*ntrC* in M2G (**Figure 2.1B),** though the protein was stably produced (See **Figure S2.2A** in Appendix 1). The L1 deletion surrounding the GAFTGA motif in *R. capsulatus* NtrC differs – and is larger than – the deletion in *Caulobacter* NtrC (See **Figure S2.1** in Appendix 1). These results provide evidence that *Caulobacter* NtrC has distinct structural and functional features, which merit further investigation.

Mutation of ntrB & ntrC has disparate effects on growth in defined vs complex medium

We demonstrated that *ntrC* is essential in M2G defined medium. Glutamine levels in peptone yeast extract (PYE) – a complex medium – are reported to be low [128], and we have confirmed a previous report by Ronneau and colleagues [128] that Δ*ntrC* has a growth defect in PYE that is complemented by expression of *ntrC* from an ectopic locus (**Figure 2.2A**) or by addition of glutamine to the medium (**Figure 2.2B**). We predicted that deletion of the gene encoding NtrB, the SHK that phosphorylates NtrC *in vitro* [234], would result in similar defects as deletion of *ntrC*. We created an in-frame deletion of *ntrB* (Δ*ntrB*) and observed no effect on growth rate in complex medium relative to wild type (WT) (**Figure 2.2A**).

Given this result, we explored the possibility that phosphorylation is not required for NtrC-dependent growth regulation in PYE complex medium. To assess the functional role of NtrC phosphorylation, we mutated the conserved aspartyl phosphorylation site in the receiver domain of NtrC to either alanine (*ntrC*(D56A)), which cannot be phosphorylated, or glutamic acid (*ntrC*(D56E)), which functions as a "phosphomimetic" mutation in some cases [235]. Like Δ*ntrB*, the growth rates of *ntrC*(D56A) and *ntrC*(D56E) strains were indistinguishable from WT in PYE complex medium, though *ntrC*(D56A) cultures had reduced terminal density (**Figure 2.2C**) that was complemented by glutamine supplementation to the medium (**Figure 2.2D**). Both NtrC point mutants were stably produced in *Caulobacter* as determined by Western blot (See **Figure S2.2B** in Appendix 1). In fact, steady-state levels of NtrC were elevated in Δ*ntrB* and *ntrC*(D56A) compared to WT and *ntrC*(D56E) (See **Figure S2.2B** in Appendix 1), indicating that these proteins are either more stable, more highly expressed, or both. We further investigated growth of these mutants in M2G defined medium. The Δ*ntrB* and *ntrC*(D56A) strains failed to grow in M2G, while *ntrC*(D56E) grew like WT (**Figure 2.2G**). Like Δ*ntrC*, the growth defect of Δ*ntrB* and *ntrC*(D56A) in M2G was rescued by replacing NH_4^+ with molar-equivalent (9.3 mM) glutamine (**Figure 2.2H**). We conclude that, while NtrC phosphorylation does not greatly impact growth in PYE complex medium, it is essential for growth when NH_4^+ is the sole nitrogen source.

To extend our structure-function analysis of *Caulobacter ntrC*, we engineered mutant strains harboring *ntrC* alleles in which either the receiver domain (*ntrC*(ΔREC); residues 17-125), the σ^{54}-activating/AAA ATPase domain (*ntrC*(ΔAAA); residues 159-363), or the DNA-binding/helix-turn-helix domain (*ntrC*(ΔHTH); residues 423-462) were removed. Growth of all three mutants (i.e., *ntrC*(ΔREC), *ntrC*(ΔAAA) and *ntrC*(ΔHTH)) was slower than WT in PYE complex medium, though the growth defects of *ntrC*(ΔREC) and *ntrC*(ΔAAA) were more extreme than *ntrC*(ΔHTH) and Δ*ntrC* (**Figure 2.2E**). The growth defects of all domain mutants in PYE were complemented by glutamine supplementation to the medium (**Figure 2.2F**). Each of these domain truncation alleles was stably expressed in *Caulobacter* (See **Figure S2.2C** in Appendix 1). Again, steady-state levels of NtrC(ΔHTH), NtrC(ΔREC), and NtrC(ΔAAA) were elevated, indicating that these mutant proteins are either more stable, more highly expressed, or both. All *ntrC* domain mutants failed to grow in M2G defined medium (**Figure 2.2G**). Replacement of NH_4^+ with molar-equivalent (9.3 mM) glutamine in M2G fully rescued the culture yield (i.e. terminal density) of *ntrC*(ΔHTH), although, yields of *ntrC*(ΔREC) and *ntrC*(ΔAAA) were only partially rescued (**Figure 2.2H).** Altogether, these results provide evidence that each of the NtrC domains is required for proper NH_4^+ assimilation, though the culture yield defects of NtrC(ΔREC) and NtrC(ΔAAA) are not solely linked to nitrogen availability.

Having shown that the AAA+ domain of NtrC is required for growth in defined medium, we next investigated the role of ATP binding and ATP hydrolysis by this domain in NH_4^+ assimilation. To probe the impact of ATP binding on NtrC function, we mutated the conserved lysine (K178) in the Walker A motif of AAA+, which is necessary for ATP binding in bEBPs [181] (See **Figure S2.1** in Appendix 1). To evaluate ATP hydrolysis, we mutated the conserved aspartate residue (D235) within the Walker B motif of AAA+ (See **Figure S2.1** in Appendix 1). This residue is vital for ATP hydrolysis but not for ATP binding [180, 181]. Strains solely expressing either the *ntrC*(K178A) or *ntrC*(D235A) alleles did not grow in M2G defined medium (See **Figure S2.3** in Appendix 1),

though these mutant proteins were stably expressed in *Caulobacter* (See **Figure S2.2D** in Appendix 1). As observed in other null NtrC mutants, steady state levels of NtrC(K178A) and NtrC(D235A) were increased, suggesting that these proteins are either more stable, more highly expressed, or both. These results provide evidence that conserved residues in the NtrC AAA+ domain known to impact ATP binding and ATP hydrolysis are required for NH_4^+ assimilation in defined medium.

IS3 rescue of glnBA transcription restores growth of ΔntrC

During our investigation of Δ*ntrC*, we noticed occasional instances of robust bacterial growth in M2G defined medium, indicating the possibility that spontaneous mutation(s) could bypass the growth defect of Δ*ntrC*. Indeed, in four independent cases in different *ntrC* mutant backgrounds, we isolated suppressor mutants that exhibited growth in M2G (**Figure 2.3A**; **Supplemental Table 1**). Whole genome sequencing revealed that in three of these strains, an IS3-family (IS511/ISCc3) insertion element had integrated into the promoter of the *glnBA* operon. In the Δ*ntrC* parent strain, an IS3-family insertion element inserted 8 bp upstream of *glnB* (Δ*ntrC* P_{glnBA}::IS3) (**Figure 2.3B**); this insertion was accompanied by a large deletion of sequence in the adjacent operon (*CCNA_02043-02045*). We also identified two independent IS3-family (IS511/ISCc3) insertions upstream of *glnBA* (16 bp and 51 bp upstream of *glnB*) that rescued the growth defect of *ntrC*(ΔHTH) mutants (**Supplemental Table 1**). In diverse bacteria, NtrC~P is known to activate transcription of *glnA* [153], which encodes glutamine synthetase. This enzyme directly assimilates NH_4^+ by synthesizing glutamine from NH_4^+ and glutamate. *glnB* encodes a conserved PII protein that regulates GlnA [153]. We observed a fourth growth rescue mutation in *ntrC*(D56A), where a non-synonymous intragenic transversion resulting in a N94Y mutation rescued growth of the non-phosphorylatable NtrC(D56A) mutant (**Supplemental Table 1**).

To determine the transcriptional consequences of IS3 insertion at P_{glnBA}, we assessed global transcript levels in WT, Δ*ntrC*, and the Δ*ntrC* P_{glnBA}::IS3 suppressor strain (i.e., sup 1 in **Supplemental Table 1**). As expected, the Δ*ntrC* strain had negligible *glnBA* transcripts compared

to WT (**Figure 2.3C**; **Supplemental Table 2**). However, *glnB* and *glnA* transcription was restored in Δ*ntrC* P_{glnBA}::IS3 (**Figure 2.3C**; **Supplemental Table 2**). Mapped reads demonstrated transcription originating from the IS3 element that extended into *glnBA* (**Figure 2.3D**). This provides evidence that sequences within the IS511-ISCc3 mobile element promote transcription of *glnBA* independent of NtrC, thereby enabling growth of the *Caulobacter* Δ*ntrC* mutant in M2G. To test if *glnBA* transcription alone is sufficient to restore Δ*ntrC* growth, we expressed *glnBA* from a xylose-inducible promoter (Δ*ntrC glnBA*$^{++}$). We observed similar growth restoration in M2G in this strain (**Figure 2.3A**). Altogether, these findings demonstrate that the inability of Δ*ntrC* to grow when NH_4^+ is the sole nitrogen source is due to the lack of *glnBA* transcription, and that this transcriptional (and growth) defect can be rescued by insertion of mobile DNA elements into the *glnBA* promoter.

Considering that strains with mutations affecting NtrC phosphorylation (e.g., Δ*ntrB*, *ntrC*(D56A)) do not grow in M2G (**Figure 2.2G**), we examined the effect of *ntrB* and *ntrC* mutations on *glnBA* expression using a fluorescent P_{glnBA} transcriptional reporter (P_{glnBA}-*mNeonGreen*). Reporter activity was significantly reduced in Δ*ntrB*, *ntrC*(D56A), and *ntrC*(D56E) when cultivated in PYE complex medium, although *ntrC*(D56E) had higher P_{glnBA}-*mNeonGreen* transcription than *ntrC*(D56A) (See **Figure S2.4** in Appendix 1). These results provide evidence that an intact phosphorylation site in the NtrC REC domain (D56) is important for the activation of *glnBA* transcription by NtrC. The lack of P_{glnBA} activity in Δ*ntrB* supports a model in which NtrB functions as the NtrC kinase *in vivo*.

Defining the Caulobacter NtrC regulon

NtrC belongs to a class of proteins known as bEBPs, which often function as global regulators of transcription in bacteria. We sought to comprehensively define the NtrC regulon in *Caulobacter*. To this end, we used RNA sequencing (RNA-seq) and chromatin immunoprecipitation sequencing (ChIP-seq) approaches. Deletion of *ntrC* significantly changed transcript levels for nearly one-quarter of genes in the *Caulobacter* genome relative to WT ($P <$

10^{-4}) when strains were cultivated in PYE complex medium (**Figure 2.4A**; **Supplemental Table 2**). To distinguish genes directly regulated by NtrC from indirectly regulated genes, we performed ChIP-seq using a 3xFLAG-tagged NtrC fusion. This experiment identified 51 significantly enriched peaks (**Figure 2.4D**; **Supplemental Table 3**), which represent direct NtrC binding sites. From these peaks, we identified a common DNA sequence motif (**Figure 2.5A**) that is significantly related to the multifunctional DNA-binding protein Fis of *E. coli*, and with the NtrC motif of *E. coli*, though there are features that clearly distinguish the *Caulobacter* NtrC motif from *E. coli* NtrC (See **Figure S2.5** in Appendix 1).

As expected, the data indicate that NtrC directly activates *glnBA*: a major NtrC peak was identified in the *glnBA* promoter region (**Figure 2.4D**; **Supplemental Table 3**). NtrC also directly binds the promoter region of the *glnK-CCNA_01399* operon (**Figure 2.4D**; **Supplemental Table 3**). *glnK* encodes a PII protein homologous to GlnB, which has been shown to similarly regulate GlnA in bacteria [153, 236], while *CCNA_01399* is an annotated as an AmtB-family NH_4^+ transporter. Transcript levels of *glnK* and *CCNA_01399* are decreased by 8- and 15-fold ($P < 10^{-61}$), respectively, in Δ*ntrC* relative to WT (**Figure 2.4A**; **Supplemental Table 2**); we conclude that NtrC directly activates transcription of these genes. We further observed a NtrC peak in the promoter regions of two genes in the nitrate assimilation locus, which is transcriptionally activated by nitrate [237] and functions to reduce nitrate to NH_4^+. Specifically, NtrC peaks are present at the 5' end of the nitrate RR NasT and in the promoter region of the MFS superfamily nitrate/nitrite transporter NarK (**Supplemental Table 3**). RNA-seq measurements were conducted in the absence of nitrate so, as expected, we did not observe differential transcription of this locus. Transcription of genes residing in the same operon as *ntrC*, including *ntrB* and a predicted tRNA-dihydrouridine synthase (*CCNA_01813*), are increased in Δ*ntrC* by approximately 20-fold (**Figure 2.4A**; **Supplemental Table 2**). NtrC directly binds the promoter of its operon (**Figure 2.4D**; **Supplemental Table 3**), providing evidence that it functions as an autorepressor. This is consistent with our Western blot data showing that *ntrB* and *ntrC* loss-of-function mutants (e.g.,

Δ*ntrB*, *ntrC*(D56A), *ntrC*(ΔREC), *ntrC*(ΔAAA), *ntrC*(ΔHTH), *ntrC*(K178A), *ntrC*(D235A)) have increased levels of NtrC protein (See **Figure S2.2B-D** in Appendix 1), indicating loss of autorepression at this genetic locus.

We have further identified genes in our datasets that are not known to be directly involved in nitrogen assimilation. In fact, 9 of the 51 NtrC binding sites are located within a mobile genetic element (MGE) (*CCNA_00460-00482*) that is known to spontaneously excise from the *Caulobacter* genome at low frequency [14]. This MGE is responsible for biosynthesis of a capsular polysaccharide [14] that is differentially regulated across the cell cycle and confers resistance to the caulophage fCr30 [17]. Select genes within this locus have enhanced transcription in Δ*ntrC* ($P < 10^{-5}$), including those encoding GDP-L-fucose synthase (*CCNA_00471*), GDP-mannose 4,6 dehydratase (*CCNA_00472*), and a P4-family DNA integrase (*CCNA_00480*) (**Supplemental Table 2**). Two NtrC binding sites also flank a second capsule biosynthesis and regulatory locus (*CCNA_00161-CCNA_00167*) outside of the MGE (**Supplemental Table 3**), and deletion of *ntrC* results in significantly enhanced expression of several genes within this locus, including the capsule restriction factor, *hvyA* [17] (3-fold) (**Supplemental Table 2**). In all cases, NtrC binding sites within the MGE directly overlap reported binding sites of the nucleoid associated protein, GapR [225, 226] and either overlap or are adjacent (within 200 bp) with binding sites for the cell cycle regulators MucR1/2 [227] (**Figure 2.5B; Supplemental Table 3**). Thirty-seven of the 51 total NtrC binding sites that we have identified directly overlap with one of the 599 reported GapR binding sites across the *Caulobacter* genome [226] (**Figure 2.5B**; **Supplemental Table 3**). *gapR* itself is significantly downregulated by 2-fold in the Δ*ntrC* mutant (**Supplemental Table 2**). These results suggest that NtrC has a chromosome structuring role in addition to its direct role in transcriptional regulation of nitrogen assimilation genes.

The promoter region of the cell cycle regulator, *sciP* (*CCNA_00948*) [70, 71], contains an NtrC binding site (**Supplemental Table 3**), and the transcription of *sciP* and adjacent flagellar genes, *flgE* and *flgD*, is significantly increased in Δ*ntrC* (**Supplemental Table 2**), indicating that

NtrC represses transcription from this site. NtrC also directly binds the promoter of *mucR1* (*CCNA_00982*) (**Supplemental Table 3**); this regulator, along with SciP, has been implicated in controlling the S-to-G1 cell cycle transition [227]. Like *sciP*, deletion of *ntrC* results in enhanced expression of *mucR1* (**Supplemental Table 2**), and we conclude that NtrC also represses transcription from this site. We assessed overlap of NtrC binding sites with SciP binding sites across the genome but observed no significant overlap (**Figure 2.5B**). We note occasional overlap between NtrC and binding sites for the essential cell cycle regulator, CtrA (**Figure 2.5B**), including sites within the promoters of *sciP* and *hvyA* (**Supplemental Table 3**). An additional cell cycle gene that is regulated by NtrC is *hdaA*, which is reported to inactivate DnaA after replication initiation [238]. NtrC binds the chromosome upstream of *hdaA* (**Supplemental Table 3**), and deletion of *ntrC* results in significantly diminished transcription of *hdaA* (**Supplemental Table 2**). Conversely, the region upstream of the DNA replication inhibitor toxin *socB* [239] (within the *socA* gene) is bound by NtrC (**Supplemental Table 3**), and deletion of *ntrC* results in significantly enhanced transcription of *socB* (2-fold) without corresponding induction of the *socA* antitoxin (**Supplemental Table 2**). Together, these results provide support for a model in which NtrC can function to modulate expression of key cell cycle/DNA replication regulators in *Caulobacter*.

Transcripts corresponding to the contact-dependent inhibition by glycine zipper proteins (*cdzCDI*) system [240] are highly elevated in Δ*ntrC* relative to WT (15- to 22-fold) (**Figure 2.4A**; **Supplemental Table 2**), although the nearest NtrC ChIP-seq peak resides downstream of the promoter of this operon, within *cdzI*, itself (**Figure 2.4D**; **Supplemental Table 3**). It is unclear whether expression of these genes is directly impacted by NtrC, but this NtrC binding site overlaps with a reported GapR binding site [226]. *CCNA_02727,* encoding an uncharacterized PhoH-family protein [241, 242], provides yet another example of gene with overlapping NtrC and GapR binding sites [226] in its promoter that exhibits strongly increased transcription in Δ*ntrC* relative to WT (10-fold) (**Figure 2.4A&D**; **Figure 2.7A-B**).

Glutamine and glnBA activation rescue the ΔntrC transcriptional defect

Glutamine supplementation rescued the growth defect of Δ*ntrC* in PYE complex medium (**Figure 2.2B**), which raised the question of whether glutamine supplementation would also restore the global transcriptional defect of Δ*ntrC* in PYE. Indeed, glutamine supplementation broadly restored transcription of genes dysregulated in the Δ*ntrC* mutant to WT levels (**Figure 2.4B**; **Supplemental Table 2**) (See **Figure S2.6** in Appendix 1). However, genes directly regulated by NtrC that are involved in nitrogen assimilation remained significantly dysregulated when glutamine was added to the medium (**Figure 2.4B**; **Supplemental Table 2**) (See **Figure S2.6** in Appendix 1). For example, *glnB* and *glnA* transcript levels remained 15- and 8-fold lower in Δ*ntrC* than in WT in the presence of 9.3 mM glutamine, while *glnK* and *CCNA_01399* remained 6- and 4-fold lower, respectively (**Figure 2.4B**; **Supplemental Table 2**). Transcripts from the *ntrC* locus, which is autorepressed, also remained significantly elevated in Δ*ntrC*, as did genes of the *cdz* locus (**Figure 2.4B**; **Supplemental Table 2**).

We further analyzed transcription in the suppressor mutant, Δ*ntrC* P_{glnBA}::IS3, which permitted us to assess the transcriptome in a strain that lacks *ntrC* but that expresses *glnBA* (**Figure 2.3C**). Restoration of *glnBA* expression in this background restored transcription to WT levels for a subset of the loci that were dysregulated in Δ*ntrC*, though transcription of many dysregulated genes was only partially rescued or remained unchanged (**Figure 2.4C**; **Supplemental Table 2**) (See **Figure S2.6** in Appendix 1). Again, NtrC-regulated genes directly involved in nitrogen assimilation (e.g., *glnK-CCNA_01399*) remained significantly dysregulated in this strain (**Figure 2.4C**; **Supplemental Table 2**). Furthermore, while *gapR* transcription is significantly reduced in Δ*ntrC*, its transcription is significantly increased (3-fold) above WT in Δ*ntrC* P_{glnBA}::IS3 to a level that is congruent to WT cultivated in the presence of 9.3 mM glutamine (**Supplemental Table 2**). This same effect is observed for the iron-dependent Fur regulon [243] (e.g., *CCNA_00027*, *CCNA_00028*) (**Supplemental Table 2**). Thus, for a subset of genes, IS3 insertion at P_{glnBA} results in a transcriptional effect that mimics media supplementation with 9.3

mM glutamine.

Loss of the ntrB-ntrC system results in stalk elongation

Caulobacter has a dimorphic life cycle wherein each cell division produces two morphologically and developmentally distinct cells including 1) a flagellated, motile swarmer cell and 2) a sessile stalked cell (**Figure 1.1A**). The *Caulobacter* stalk is a thin extension of the cell envelope and its length is known to be impacted by phosphate limitation [244] and sugar-phosphate metabolism imbalances [245]. We observed that Δ*ntrC* mutant cells develop elongated stalks when cultivated in PYE complex medium (**Figure 2.6A-B**). Δ*ntrB* and *ntrC*(D56A) mutants displayed an intermediate stalk elongation phenotype, while stalks of *ntrC*(D56E) mutants did not differ from WT (**Figure 2.6B**). We conclude that loss of *ntrC* function results in development of elongated stalks in complex medium.

Our transcriptomic data showed no evidence of a phosphate limitation response upon *ntrC* deletion, nor did we observe changes in *manA* or *spoT/rsh* expression (**Supplemental Table 2**), which have been implicated in stalk elongation [245]. We did observe that expression of the *phoH*-like gene, *CCNA_02727*, was elevated 10-fold in Δ*ntrC* compared to WT (**Figure 2.7A**). This gene has an NtrC peak in its promoter (**Figure 2.7B**), suggesting it is directly repressed by NtrC. PhoH proteins have been implicated in phosphate starvation responses in other bacteria [246, 247], so we tested whether de-repression of this gene in Δ*ntrC* impacted stalk development, which is known to be stimulated by phosphate starvation in *Caulobacter* [244]. Overexpression of *CCNA_02727* from a xylose-inducible promoter in WT resulted in significantly longer stalks compared to WT (**Figure 2.7C**). However, deletion of *CCNA_02727* in the Δ*ntrC* strain did not ablate stalk elongation (**Figure 2.7C**). We conclude that elevated expression of *CCNA_02727* is sufficient to promote stalk elongation, but that enhanced expression of *CCNA_02727* in Δ*ntrC* does not solely explain the long stalk phenotype.

Supplementation of PYE with 9.3 mM glutamine fully complemented the stalk length phenotype of Δ*ntrC* (**Figure 2.6A-B**), and restoration of *glnBA* expression, either in the suppressor

(Δ*ntrC* P_{glnBA}::IS3) or in the *glnBA* overexpression strain (Δ*ntrC glnBA*$^{++}$), restored Δ*ntrC* stalk length to WT levels (**Figure 2.6B**). Similarly, glutamine supplementation complemented stalk length defects of Δ*ntrB* and *ntrC*(D56A) (**Figure 2.6B**). Altogether, these results indicate that the stalk elongation phenotype of *ntrB* and *ntrC* mutants grown in PYE results from an explicit lack of usable nitrogen or a nutrient imbalance due to the reduced availability of usable nitrogen. We note that expression of *CCNA_02727* in Δ*ntrC* is restored to WT levels when PYE is supplemented with glutamine (**Figure 2.7A**). This result indicates that regulation of *CCNA_02727* by NtrC is not via a simple, direct repressive mechanism.

ΔntrC is hyper-mucoid

The *Caulobacter* swarmer and stalked cell types differ not only in cellular morphology, but also in their capsulation state [17]. The swarmer cell is non-capsulated, while the stalked cell elaborates an exopolysaccharide (EPS) capsule composed of a repeating tetrasaccharide [248]. Capsulation results in enhanced buoyancy, which is apparent during centrifugation [17]. When centrifuged, Δ*ntrC* cells cultivated in PYE displayed a “soft” or “fluffy” pellet compared to WT (**Figure 2.8A**), which suggested that Δ*ntrC* had altered EPS. Over-production of EPS results in colonies that appear mucoid (i.e., glossy) on solid medium containing abundant sugar [14, 17], and Δ*ntrC* displayed a mucoid phenotype on PYE solid medium supplemented with 3% sucrose (**Figure 2.8B**), a condition that has been shown to enhance *Caulobacter* mucoid growth [14]. We conclude that loss of *ntrC* impacts the production or composition of envelope polysaccharides.

We again tested whether glutamine supplementation could restore a phenotype of Δ*ntrC* to that of WT. Centrifugation of Δ*ntrC* cultures grown in PYE supplemented with 9.3 mM glutamine resulted in a compact pellet like WT (**Figure 2.8A**). Furthermore, Δ*ntrC* cultivated on PYE solid medium supplemented with 3% sucrose and 9.3 mM glutamine had a WT appearance (**Figure 2.8B**). Ectopic expression of *glnBA* in Δ*ntrC* grown in PYE similarly complemented Δ*ntrC* mucoid phenotypes (**Figure 2.8A-B**). These results support a model in which genetic or chemical restoration of intracellular glutamine levels complements the mucoid phenotype of Δ*ntrC*.

The ΔntrC hyper-mucoid phenotype requires the MGE

The mucoid appearance of Δ*ntrC* aligns with transcriptomic and ChIP-seq data that show NtrC-dependent repression of EPS synthesis genes, including those located within the *Caulobacter* MGE (e.g., *CCNA_00471*, *CCNA_00472*) (**Supplemental Table 2**; **Supplemental Table 3**). Considering the numerous NtrC binding sites within the MGE and its role in capsular polysaccharide biosynthesis [14], we tested whether the mucoid phenotype of Δ*ntrC* required the MGE. Specifically, we deleted *ntrC* from a *Caulobacter crescentus* NA1000 strain that had spontaneously lost the MGE [14], resulting in a *Caulobacter* ΔMGE Δ*ntrC* mutant. When cultivated in PYE, the NA1000 ΔMGE Δ*ntrC* strain did not display a "fluffy" pellet or exhibit a mucoid phenotype on PYE solid medium (See **Figure S2.7A** in Appendix 1). We further deleted *ntrC* in *C. crescentus* CB15 strain (CB15 Δ*ntrC*), which similarly lacks the MGE [14]. CB15 Δ*ntrC* had a WT phenotype in pellet and plate growth assays (See **Figure S2.7B** in Appendix 1). These results provide evidence that the mucoid phenotype of Δ*ntrC* is dependent on the EPS synthesis genes of the MGE. We conclude that transcriptional dysregulation due to loss of NtrC impacts cell envelope polysaccharide production via the MGE and, perhaps, through other genes involved in EPS biosynthesis (**Supplemental Table 2**; **Supplemental Table 3**).

Conclusion

Environmental nitrogen is an important cell cycle and developmental regulatory cue in *Caulobacter* [128], which motivated us to explore the function of the NtrB-NtrC TCS, a broadly conserved regulator of nitrogen metabolism. In this work, we have confirmed the role of *Caulobacter* NtrC as a regulator of nitrogen assimilation. Through genetic analysis, we have established that NtrC is required for utilization of NH_4^+ and, moreover, established that this is due to the direct role of NtrC in transcriptional activation of *glnA*, the sole route of NH_4^+ assimilation in *Caulobacter* [128]. Slow growth of Δ*ntrC* in complex medium highlights the role of NtrC in intracellular glutamine synthesis, given glutamine starved mutants display slow growth in

complex medium [128]. The *Caulobacter* Δ*ntrC* mutant feeling nitrogen starved even in complex medium that contains an abundance of various nitrogen sources further highlights the central role of intracellular glutamine as a readout for nitrogen status of the cell [128]. In addition to slow growth, there are other glutamine starvation phenotypes of the *Caulobacter* Δ*ntrC* mutant when grown in complex medium; that is, Δ*ntrC* displays phenotypes that can be complemented with glutamine supplementation. Specifically, deletion of *ntrC* results in long stalks and hyper-mucoid growth. Notably, stalk biosynthesis and capsulation are regulated in a cell cycle-dependent manner in *Caulobacter*, suggesting NtrC has implications in cell cycle and cellular development in *Caulobacter*.

Additionally, we have characterized the direct transcriptional regulon of NtrC in *Caulobacter*. As mentioned previously, NtrC belongs to a broad class of AAA+ proteins called bEBPs that canonically regulate σ^{54}-dependent transcription (reviewed in [171-173]). According to transcriptomic and ChIP-seq datasets, *Caulobacter* NtrC regulates transcription of σ^{70}-dependent genes. This is a perhaps expected result due to the absence of the GAFTGA motif within its AAA domain. As predicted, included in its regulon are nitrogen assimilation genes, such as *glnBA*, genes encoding NH_4^+ transporters, and itself (i.e., autoregulation). Unexpectedly, *Caulobacter* NtrC regulates transcription of genes outside of canonical nitrogen assimilation, including genes involved DNA replication control (i.e., *hdaA*), capsulation (e.g., *hvyA*), and cell cycle control (e.g., *sciP*). Moreover, NtrC binding sites across the chromosome tend to overlap with previously published binding sites of cell cycle regulators MucR1 and GapR, suggesting functional interactions of NtrC with these regulators and potential cell cycle and cellular development consequences.

Through genetic routes, we have interrogated the molecular features of NtrC. As shown in other NtrC-type bEBPs, the conserved aspartyl residue in the REC domain of *Caulobacter* NtrC is critical for activity. Mutation of this aspartyl residue to a non-phosphorylatable residue

results in loss-of-function phenotypes. Moreover, deletion of the predicted cognate SHK, *ntrB*, similarly results in loss-of-function phenotypes emphasizing both 1) the role of NtrB as the major SHK for NtrC *in vivo* and 2) the role of the conserved phosphorylatable aspartyl residue in NtrC activity. Altogether, these data suggest a critical role for phosphorylation of NtrC by NtrB for protein activity. In addition, we interrogated the roles of each domain of NtrC through genetic routes. Interestingly, the REC, AAA, and HTH domains are required for NtrC activity; that is, deletion of any of the three domains resulted in loss-of-function phenotypes, despite these mutant peptides being stably produced. Although *Caulobacter* NtrC is regulating σ^{70}-dependent transcription instead of σ^{54}, this result suggests the AAA domain, conserved for σ^{54}-RNAP activation, has some functional role in the transcriptional activity of NtrC. Moreover, conserved residues for ATP binding (i.e., K178) and ATP hydrolysis (i.e., D235) within the AAA domain are required for NtrC activity *in vivo*, suggesting ATP binding and hydrolysis have roles in NtrC activity.

In summary, these results support a model, in which *Caulobacter* NtrC has predicted molecular features of canonical NtrC-like bEBPs but displays non-canonical molecular features that deem it unique from its paralogs. More broadly, these results confirm the predicted, canonical role of *Caulobacter* NtrC in the transcriptional regulation of nitrogen assimilation, although, *Caulobacter* NtrC provides a novelty compared to its paralogs, in which it displays transcriptional regulation of cell cycle and cellular development genes. In support of this, upon deletion of *ntrC*, *Caulobacter* displays cell cycle- and cellular development-related perturbations. Altogether, this study establishes regulatory connections between NtrC, nitrogen metabolism, polar morphogenesis, and envelope polysaccharide synthesis in *Caulobacter*.

Materials & Methods

Growth conditions

E. coli strains were cultivated in Lysogeny Broth (LB) [10 g tryptone, 5 g yeast extract, 10

g NaCl per L] or LB solidified with 1.5% (w/v) agar at 37˚C. LB was supplemented with appropriate antibiotics when necessary. Antibiotic concentrations for selection of *E. coli* were as follows: kanamycin 50 μg/ml, chloramphenicol 20 μg/ml, carbenicillin 100 μg/ml. *Caulobacter* strains were cultivated in peptone yeast extract (PYE) [2 g/L peptone, 1 g/L yeast extract, 1 mM $MgSO_4$, 0.5 mM $CaCl_2$] complex medium or PYE solidified with 1.5% (w/v) agar at 30˚C or 37˚C. Antibiotic concentrations for selection of *Caulobacter* were as follows: kanamycin 25 μg/ml (in solid medium), 5 μg/ml (in liquid medium), chloramphenicol 1.5 μg/ml. Nalidixic acid (20 μg/ml) was added to counterselect *E. coli* after conjugations. For glutamine supplementation experiments in PYE, 9.3 mM (final concentration) glutamine was added. For experiments in defined medium, *Caulobacter* strains were grown in M2 minimal salts medium with glucose (M2G) [6.1 mM Na_2HPO_4, 3.9 mM KH_2PO_4, 9.3 mM NH_4Cl, 0.25 mM $CaCl_2$, 0.5 mM $MgSO_4$, 10 μM ferrous sulfate chelated with EDTA (Sigma), and 0.15% glucose]. For glutamine supplementation experiments in M2G, NH_4^+ was replaced with molar-equivalent (9.3 mM) glutamine.

Strains and plasmids

Strains, plasmids, and primers used in this study are presented in **Supplemental Table 4**. To generate plasmid constructs for in-frame deletions and other allele replacements, homologous upstream and downstream fragments (~500 bp/each) were PCR-amplified and joined via overlap extension PCR [249]. PCR products were cloned into plasmid pNPTS138 by restriction enzyme digestion and ligation. Similarly, to create genetic complementation constructs, target genes were amplified and fused to their upstream promoters (~500 bp fragment immediately upstream of the start of the annotated operon) via overlap extension PCR and these fused PCR products were purified and cloned into pXGFPC-2 (pMT585) [33], a plasmid that integrates into the *xylX* locus in *Caulobacter*. For complementation, the genes with their native promoters were cloned in the opposite orientation of the P_{xylX} promoter in this plasmid. For xylose-inducible expression, target genes were PCR-amplified and ligated into pMT585 in the same orientation as (i.e., downstream of) the P_{xylX} promoter. To create the *glnBA* transcriptional reporter

construct, the target promoter (~500 bp fragment upstream of the start of the *glnBA* operon) was PCR-amplified and cloned into pPTM056 [250], which resulted in the fusion of P_{glnBA} to *mNeonGreen*. All ligations were transformed into *E. coli* TOP10. All plasmids were sequence confirmed.

Plasmids were transformed into *Caulobacter* via electroporation or triparental mating from TOP10 using FC3 as a helper strain [251]. In-frame deletion and allele replacement strains were generated via two-step recombination using *sacB* counterselection using an approach similar to that described by Hmelo et al [252]. Briefly, primary recombinants bearing pNPTS138-derived allele-replacement plasmids were selected on solidified PYE containing kanamycin. Single colonies were then grown in PYE broth without selection for 6-18 hours (h) before secondary recombinants were selected on PYE containing 3% sucrose. The resulting clones were screened to confirm kanamycin sensitivity. Then allele replacement was confirmed by PCR for in-frame deletion alleles or PCR amplification and Sanger sequencing for point mutation alleles.

Measurement of growth in PYE complex medium

Starter cultures were grown overnight in PYE or PYE plus 9.3 mM glutamine shaken at 30˚C. Overnight cultures were diluted to OD_{660} 0.1 in the same media and incubated shaking for 2 h at 30˚C to bring cultures to a similar (logarithmic) phase of growth. Cultures were then diluted to OD_{660} 0.025 in the same media and shaken at 30˚C. Optical density at 660 nm was measured at the timepoints indicated.

Measurement of growth in M2G defined medium

Starter cultures were shaken overnight in PYE at 30˚C. Starter cultures were pelleted and washed three times with M2G or M2G in which NH_4^+ was replaced with molar-equivalent (9.3 mM) glutamine before dilution to OD_{660} 0.025 in the respective medium. These cultures were incubated at 30 ˚C with shaking for 24 h and culture density was measured optically (OD_{660}).

Selection of ΔntrC, ntrC(ΔHTH), and ntrC(D56A) suppressors

When Δ*ntrC*, *ntrC*(ΔHTH), or *ntrC*(D56A) cultures incubated in M2G overnight at 30˚C

exhibited visible turbidity, cultures were spread on PYE to isolate individual colonies bearing suppressing mutations. These putative suppressor strains were re-inoculated into M2G to confirm growth in the absence of a functional *ntrC* allele. Strains that grew rapidly - similar to WT - were saved and genomic DNA was purified and sequenced. Briefly, genomic DNA was extracted from 1 ml of saturated PYE culture using guanidinium thiocyanate [253]. Genomic DNA was sequenced (150 bp paired-end reads) at SeqCenter (Pittsburgh, PA) using an Illumina NextSeq 2000. DNA sequencing reads were mapped to the *Caulobacter* NA1000 genome (Genbank accession CP001340) [14] and polymorphisms were identified using breseq [254].

RNA extraction, sequencing, and analysis

Starter cultures were grown for 18 h at 30˚C in PYE or PYE plus 9.3 mM (final concentration) glutamine. Cultures were then diluted to OD_{660} 0.1 in their respective medium and grown for 2 h to get the cultures in similar (logarithmic) phase of growth. Once again, cultures were diluted to OD_{660} 0.1 in their respective medium and grown another 3.25 h (OD_{660} < 0.4) to capture mRNA in a similar log phase of the growth curve. 6 ml of each culture were pelleted via centrifugation (1 min at 17,000 x g). Pellets were immediately resuspended in 1ml TRIzol and stored at -80˚C until RNA extraction. To extract RNA, thawed samples were incubated at 65˚C for 10 min. After addition of 200 µl of chloroform, samples were vortexed for 20 s and incubated at room temperature (RT) for 5 min. Phases were separated by centrifugation (10 min at 17,000 x g). The aqueous phase was transferred to a fresh tube and an equal volume of isopropanol was added to precipitate the nucleic acid. Samples were stored at 80˚C (1 h to overnight), then thawed and centrifuged at 17,000 x g for 30 min at 4˚C to pellet the nucleic acid. Pellets were washed with ice-cold 70% ethanol then centrifuged for at 17,000 x g for 5 min at 4˚C. After discarding the supernatant, pellets were air-dried at RT, resuspended in 100 µl RNAse-free water, and incubated at 60˚C for 10 min. Samples were treated with TURBO DNAse (Invitrogen) following manufactures protocol for 30 min at RT and then column purified using RNeasy Mini Kit (Qiagen). RNA samples were sequenced at SeqCenter (Pittsburgh, PA). Briefly, sequencing libraries were prepared using

Illumina's Stranded Total RNA Prep Ligation with Ribo-Zero Plus kit and custom rRNA depletion probes. 50 bp paired end reads were generated using the Illumina NextSeq 2000 platform (Illumina). RNA sequencing reads are available in the NCBI GEO database under series accession GSE234097. RNA sequencing reads were mapped to the *Caulobacter* NA1000 genome [14] using default mapping parameters in CLC Genomics Workbench 20 (Qiagen). To identify genes regulated by NtrC, the following criteria were use: fold change > 1.5, FDR P < 0.000001 and maximum group mean RPKM > 10. Gene expression data were hierarchically clustered in Cluster 3.0 [255] using an uncentered correlation metric with average linkage. The gene expression heatmap was generated using Java TreeView [256].

Chromatin immunoprecipitation with sequencing (ChIP-seq)

Caulobacter ntrC was PCR-amplified and inserted into pPTM057-3xFLAG expression vector via restriction digestion and ligation to generate a 3xFLAG-NtrC fusion expressed from a cumate-inducible promoter. This suicide plasmid was propagated in *E. coli* TOP10 and conjugated into *Caulobacter* Δ*ntrC* to integrate at the xylose locus. For ChIP-seq experiments, the Δ*ntrC xylX*::pPTM057-3xFLAG-*ntrC* strain was grown overnight in PYE at 30˚C. The overnight culture was diluted to OD_{660} 0.1 in PYE and outgrown for 2 h at 30˚C. This culture was back-diluted to OD_{660} 0.1 in PYE supplemented with 50 μM cumate and grown for 3.25 h at 37˚C to induce 3xFLAG-*ntrC* during log phase growth. To crosslink 3xFLAG-NtrC to DNA, formaldehyde was added to 125 ml of culture to a final concentration of 1% (w/v) and shaken at 37˚C for 10 min. The crosslinking was quenched using a final concentration of 125 mM glycine and shaken at 37˚C for 5 min. Cells were pelleted by centrifugation at 7,196 x g for 5 min at 4˚C. Supernatant was removed and the pellet was washed 4 times with ice-cold PBS pH 7.5. To lyse the cells, the washed pellet was resuspended in 1 ml lysis buffer [10 mM Tris pH 8, 1 mM EDTA, protease inhibitor tablet (Roche), 1 mg/ml lysozyme]. After a 30 min incubation at 37˚C for 0.1% (w/v) sodium dodecyl sulfate (SDS) was added. To shear the genomic DNA to 300-500 bp fragments, the lysate was sonicated on ice for 10 cycles (20% magnitude for 20 sec on/off pulses using a

Branson Sonicator). Cell debris was cleared by centrifugation (15,000 x g for 10 min at 4°C). Supernatant was transferred to a clean tube and Triton X-100 was added to a final concentration of 1% (v/v). The sample was pre-cleared via incubation with 30 µl of SureBeads Protein A magnetic agarose beads (BioRad) for 30 min at RT. The supernatant was transferred to a clean tube and 5% of the total lysate was saved as the input DNA reference sample. Pulldown was performed as previously described [250]. Briefly, 100 µl magnetic agarose anti-FLAG beads (Pierce / Thermo) were pre-equilibrated in binding buffer [10 mM Tris pH 8 at 4°C, 1 mM EDTA, 0.1% (w/v) SDS, 1% (v/v) Triton X-100] supplemented with 1% (w/v) bovine serum albumin (BSA) overnight at 4˚C, washed with binding buffer and incubated in the lysate for 3 h at RT. Beads were cleared from the lysate with a magnet, and washed with a low-salt buffer [50 mM HEPES pH 7.5, 1% (v/v) Triton X-100, 150 mM NaCl], followed by a high-salt buffer [50 mM HEPES pH 7.5, 1% (v/v) Triton X-100, 500 mM NaCl], and then LiCl buffer [10 mM Tris pH 8 at 4°C, 1 mM EDTA, 1% (w/v) Triton X-100, 0.5% (v/v) IGEPAL CA-630, 150 mM LiCl]. Finally, beads were incubated with 100 µl elution buffer [10 mM Tris pH 8 at 4°C, 1 mM EDTA, 1% (w/v) SDS, 100 ng/µl 3xFLAG peptide] for 30 min at RT. After pulldown, the input sample was brought to equal volume as the output/pulldown sample using elution buffer [10 mM Tris pH 8, 1 mM EDTA pH 8, 1% SDS, 100 ng/µl 3xFLAG peptide]. Input and output samples were supplemented with 300 mM NaCl and 100 µg/ml RNAse A and incubated at 37°C for 30 min. Proteinase K was added to samples at a final concentration of 200 µg/ml and samples were incubated overnight at 65°C to reverse crosslinks. Samples were purified using the Zymo ChIP DNA Clean & Concentrator kit. ChIP DNA was sequenced at SeqCenter (Pittsburgh, PA). Briefly, sequencing libraries were prepared using the Illumina DNA prep kit and sequenced (150 bp paired end reads) on an Illumina Nextseq 2000. ChIP-seq sequence data have been deposited in the NCBI GEO database under series accession GSE234097.

ChIP-seq analysis

Paired-end reads were mapped to the *C. crescentus* NA1000 reference genome

(GenBank accession number CP001340) with CLC Genomics Workbench 20 (Qiagen). Peak calling was performed with the Genrich tool (https://github.com/jsh58/Genrich) on Galaxy; peaks are presented in **Supplemental Table 3**. Briefly, PCR duplicates were removed from mapped reads, replicates were pooled, input reads were used as the control dataset, and peak were called using the default peak calling option [Maximum q-value: 0.05, Minimum area under the curve (AUC): 20, Minimum peak length: 0, Maximum distance between significant sites: 100].

To identify promoters that contained NtrC peaks, promoters were designated as 300 bp upstream and 100 bp downstream of the transcription start sites (TSS) annotated for each operon [257, 258]. For genes/operons that did not have an annotated TSS, the +1 nucleotide of the first gene in the operon was designated as the TSS. Promoters were defined as containing an NtrC peak if there was any overlap between the NtrC ChIP-seq peak and the indicated promoter. To compare the relative location of NtrC binding sites with various cell cycle regulators, ChIPpeakAnno [259] was used to determine distance from the summit of the NtrC peaks to the nearest CtrA, SciP, MucR1, and GapR peak summit. To compare the relative location of NtrC binding sites with various cell cycle regulators, ChIPpeakAnno [259] was used to determine distance from the summit of the NtrC peaks to the nearest CtrA, SciP, MucR1, and GapR peak summit. ChIP-seq peaks (50 bp windows) for CtrA, SciP, and MucR1 were derived from [227] and the summits were considered the center of the 50 bp window. ChIP-seq summits for GapR were derived from [226]. For motif discovery, sequences of the ChIP-seq peaks were submitted to MEME suite [260]. Sequences were scanned for enriched motifs between 6 and 30 bp in length that had any number of occurrences per sequence.

NtrC protein purification

Caulobacter ntrC was PCR-amplified and inserted into a pET23b-His6-SUMO expression vector using classical restriction digestion and ligation, such that ntrC was inserted 3' of the T7 promoter and the His6-SUMO coding sequence. After sequence confirmation, pET23b-His6-SUMO-*ntrC* was transformed into chemically competent *E. coli* BL21 Rosetta (DE3) / pLysS. This

strain was grown in 1 L of LB at 37˚C. When the culture density reached approximately OD_{600} ≈ 0.4, expression was induced with 0.5 mM isopropyl β-D-1-thiogalactopyranoside (IPTG) overnight at 16˚C. Cells were harvested by centrifugation (10,000 x g for 10 min) and resuspended in 20 ml lysis buffer [20 mM Tris pH 8, 125 mM NaCl, 10 mM imidazole] and stored at -80˚C until purification.

For protein purification, resuspended cell pellets were thawed at RT. 1 mM phenylmethylsulfonyl fluoride (PMSF) was added to inhibit protease activity and DNase I (5 µg/ml) was added to degrade DNA after cell lysis. Cells incubated on ice were lysed by sonication (Branson Instruments) at 20% magnitude for 20 sec on/off pulses until the suspension was clear. The lysate was cleared of cell debris by centrifugation (30,000 x g for 20 min) at 4˚C. The cleared lysate was applied to an affinity chromatography column containing Ni-nitrilotriacetic acid (NTA) superflow resin (Qiagen) pre-equilibrated in lysis buffer. Beads were washed with wash buffer [20 mM Tris pH 8, 125 mM NaCl, 30 mM imidazole]. Protein was eluted with elution buffer [20 mM Tris pH 8, 125 mM NaCl, 300 mM imidazole]. The elution fractions containing His6-SUMO-NtrC were pooled and dialyzed in 2 L dialysis buffer [20 mM Tris pH8, 150 mM NaCl] for 4 h at 4˚C to dilute the imidazole. Purified ubiquitin-like-specific protease 1 (Ulp1) was added to the eluted His6-SUMO-NtrC containing solution which was then dialyzed overnight at 4˚C in 2 L fresh dialysis buffer to cleave the His6-SUMO tag. Digested protein was mixed with 3 ml of NTA superflow resin (Qiagen) that had been pre-equilibrated in wash buffer. After incubation for 30 min at 4˚C, the solution was placed onto a gravity drip column at 4˚C. Flowthrough containing cleaved NtrC was collected and used to generate α-NtrC polyclonal antibodies (Pacific Immunology).

Western blotting

To prepare cells for analysis, overnight PYE cultures of *Caulobacter* strains presented in **Figure S2.2B** and **Figure S2.2C** in Appendix 1 were diluted in fresh PYE to OD_{660} 0.1 and grown 2 h at 30˚C. These outgrown cultures were then re-diluted in fresh PYE to OD_{660} 0.1 and grown

for 3.25 h at 30˚C to capture exponential growth phase. Cells from 1 ml of each culture were collected by centrifugation (12,000 x g for 1 min). After discarding the supernatant, cell pellets were stored at -20˚C until western blot analysis. Strains presented in **Figure S2.2A** in Appendix 1 were grown as above except that the outgrowth medium was supplemented with 0.15% xylose and upon re-dilution in xylose supplemented medium, cultures were grown for 24 h at 30˚C to capture stationary growth phase (OD_{660} > 0.6). Cells from 1 ml of each stationary phase culture were harvested as above and stored at -20˚C until western blot analysis. Strains presented in **Figure S2.2D** in Appendix 1 were grown in PYE overnight. Cells from 1 ml of each overnight culture were collected by centrifugation as described above and the pellets were placed at -20˚C until western blot analysis.

For western blot analysis, cell pellets were thawed and resuspended in 2X SDS loading buffer [100 mM Tris-Cl (pH 6.8), 200 mM dithiothreitol, 4% (w/v) SDS, 0.2% bromophenol blue, 20% (v/v) glycerol] to a concentration of 0.0072 OD_{660} • ml culture / µl loading buffer. After resuspension, genomic DNA is digested by incubation with 1 µl Benzonase per 50 µl sample volume for 20 min at RT. Samples then were denatured at 95˚C for 5 min. 10 µl of each sample was loaded onto a 4-20% mini-PROTEAN precast gel (Bio-Rad) (See **Figure S2.2C** in Appendix 1) or a 7.5% mini-PROTEAN precast gel (BioRad) (See **Figure S2.2A-B&D** in Appendix 1) and resolved at 180 V at RT. Separated proteins were transferred from the acrylamide gel to a PVDF membrane (Millipore) using a semi-dry transfer apparatus (BioRad) at 10 V for 30 min at RT [1X Tris-Glycine, 20% methanol]. The membrane was blocked in 10 ml Blotto [1X Tris-Glycine with 0.1% Tween 20 (TBST) + 5% (w/v) powdered milk] for 1 h to overnight at 4˚C. The membrane was then incubated in 10 ml Blotto + polyclonal rabbit α-NtrC antiserum (1:1,000 dilution) 1 h to overnight at 4˚C. The membrane was washed in TBST three times. The membrane was then incubated in 10 ml Blotto + goat α-rabbit poly-horseradish peroxidase secondary antibody (Invitrogen; 1:10,000 dilution) for 1-2 h at RT. The membrane was then washed three times with TBST and developed with ProSignal Pico ECL Spray (Prometheus Protein Biology Products).

Immediately upon spraying, the membrane was imaged using BioRad ChemiDoc Imaging System (BioRad).

Caulobacter stalk length measurement and analysis

To prepare stationary phase cells, starter cultures were grown in PYE overnight at 30˚C and diluted to OD_{660} 0.1 in fresh PYE or PYE plus 9.3 mM glutamine. After a 2 h outgrowth at 30˚C cultures were re-diluted to OD_{660} 0.1 in fresh medium and grown for 24 h at 30˚C to capture stalk lengths in stationary phase (> OD_{660} 0.6). 2 µl of each stationary phase culture were spotted on an agarose pad [1% agarose dissolved in water] on a glass slide and covered with a glass cover slip. Cells were imaged using a Leica DMI 6000 microscope using phase contrast with an HC PL APO 63x/1.4 numeric aperture oil Ph3 CS2 objective. Images were captured with an Orca-ER digital camera (Hamamatsu) controlled by Leica Application Suite X (Leica). Stalk length was measured using BacStalk [261] with a minimum stalk length threshold of 0.6 microns.

Transcriptional reporter assay

Overnight starter cultures grown in PYE supplemented with chloramphenicol (1.5 µg/ml) to maintain the replicating plasmid were diluted to OD_{660} 0.1 in the same medium and outgrown for 2 h at 30˚C. Outgrown cultures were re-diluted to OD_{660} 0.1 in the same medium and grown at 30˚C for 24 h to capture expression in stationary phase. 200 µl of each culture was transferred to a Costar flat bottom, black, clear bottom 96-well plate (Corning). Cell density assessed by absorbance (660 nm) and mNeonGreen fluorescence (excitation = 497 ± 10 nm; emission = 523 ± 10 nm) were measured in a Tecan Spark 20M plate reader.

Figures

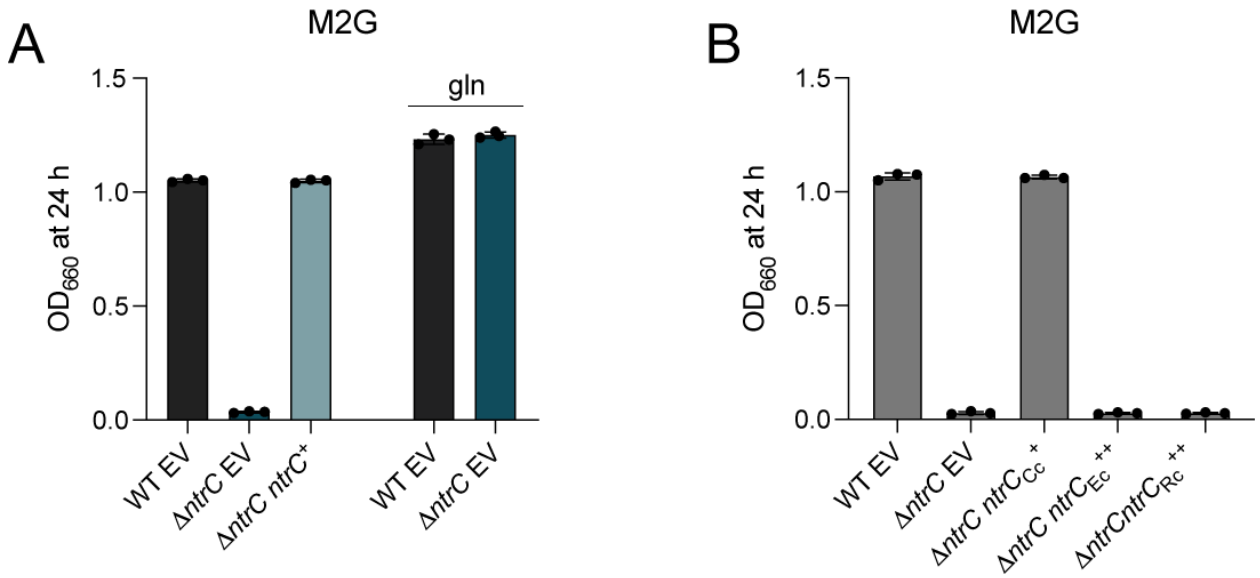

Figure 2.1. *ntrC* is required for growth in defined medium in which NH_4^+ is the sole nitrogen source. (A) Terminal culture densities of WT, Δ*ntrC*, and Δ*ntrC* carrying a complementing copy (*ntrC*$^+$) or empty vector control (EV). Culture growth was measured spectrophotometrically at 660 nm (OD_{660}) after 24 hours (h) of growth in M2G or M2G in which NH_4^+ was replaced with molar-equivalent (9.3 mM) glutamine (gln). Data represent mean ± standard deviation of three replicates. (B) Terminal densities of WT and Δ*ntrC* containing empty vector (EV) or expressing *Caulobacter ntrC* from its native promoter (*ntrC*$_{Cc}^+$) or *E. coli ntrC* or *R. capsulatus ntrC* expressed from P_{xyl} (*ntrC*$_{Ec}^{++}$ or *ntrC*$_{Rc}^{++}$). Culture growth was measured spectrophotometrically at OD_{660} after 24 h of growth in M2G supplemented with 0.15% xylose. Data represent mean ± standard deviation of three independent replicates.

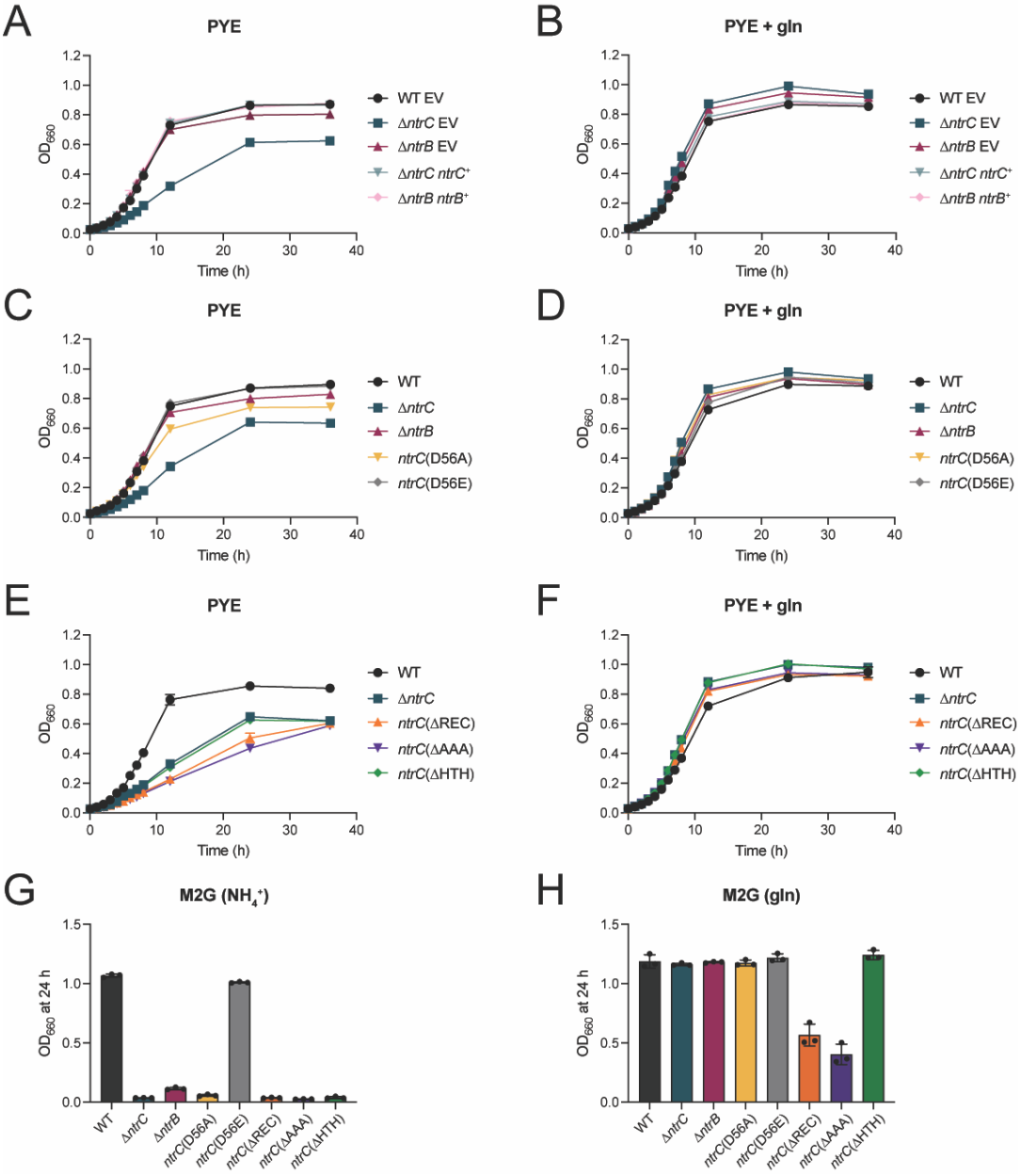

Figure 2.2. Mutants of the *ntrB-ntrC* system have disparate effects on growth in defined versus complex medium. (A) Growth of WT, Δ*ntrC*, and Δ*ntrB* possessing empty vector (EV) or a genetic complementation vector ($^{+}$) in which indicated genes were expressed from their native promoters (ectopically integrated at the *xylX* locus); growth was measured spectrophotometrically at 660 nm (OD_{660}) in PYE complex medium without and (B) with supplemented 9.3 mM glutamine (gln). (C) Growth curves of WT, Δ*ntrC*, Δ*ntrB*, *ntrC*(D56A), and *ntrC*(D56E) in PYE and (D) PYE supplemented with 9.3 mM gln. (E) Growth curves of WT, Δ*ntrC*, *ntrC*(ΔREC) (residues deleted: 17-125), *ntrC*(ΔAAA) (residues deleted: 159-363), *ntrC*(ΔHTH) (residues deleted: 423-462) in PYE and (F) PYE supplemented with 9.3 mM gln. Plotted points for A-F represent average OD_{660} ± standard deviation of three independent replicates. (G) Terminal OD_{660} of WT, Δ*ntrC*, Δ*ntrB*, *ntrC*(D56A), *ntrC*(D56E), *ntrC*(ΔREC), *ntrC*(ΔAAA), and *ntrC*(ΔHTH) after 24 hours (h) of growth in M2G defined medium and (H) M2G in which NH_4^+ was replaced with molar-equivalent (9.3 mM) gln. Data represent mean ± standard deviation of three independent replicates.

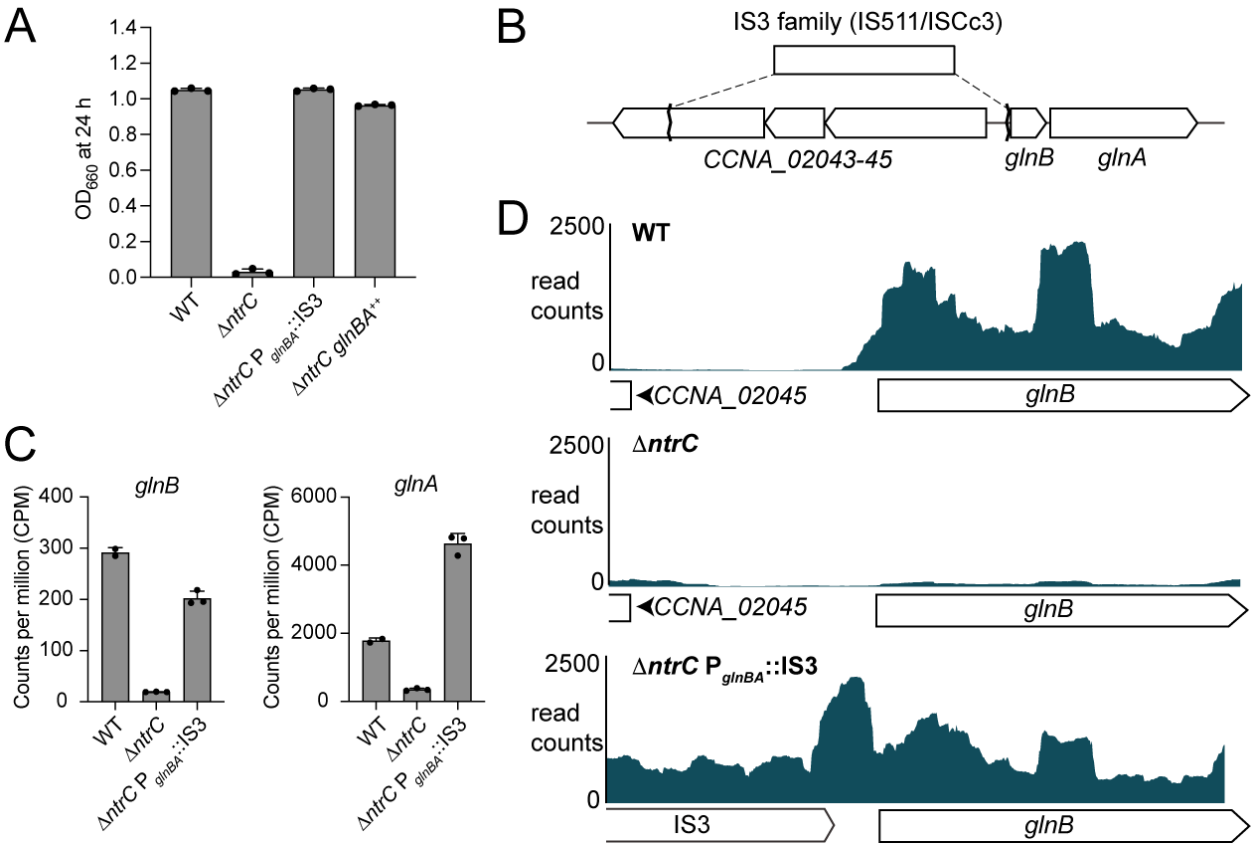

Figure 2.3. Spontaneous transposition of an IS3-family insertion element restores *glnBA* expression in Δ*ntrC* and rescues the Δ*ntrC* growth defect. (A) Terminal optical density (OD_{660}) of WT, Δ*ntrC*, a spontaneous suppressor of Δ*ntrC* (Δ*ntrC* P_{glnBA}::IS3), and Δ*ntrC* expressing *glnBA* from an inducible promoter (Δ*ntrC glnBA*$^{++}$) grown for 24 hours (h) in M2G defined medium. (B) Site of the spontaneous lesion upstream of *glnBA* in the Δ*ntrC* suppressor strain as determined by whole-genome sequencing. The insertion sequence (IS) element in inserted such that the 3' end of the transposase (matching the 3' end of the transposases *CCNA_00660* and *CCNA_02814*) is positioned at nucleotide 2192508, which is 8 nucleotides upstream of the *glnB* start codon. In addition, a 3285 bp deletion eliminated most of *CCNA_02043-45* operon. (C) RNA-seq counts per million (CPM) of *glnB* (left) and *glnA* (right) transcripts in WT, Δ*ntrC*, and Δ*ntrC* P_{glnBA}::IS3 exponential phase cells grown in PYE complex medium. (D) Aligned RNA-seq read counts (blue) corresponding to the 5' end of the *glnBA* operon from WT, Δ*ntrC*, and Δ*ntrC* P_{glnBA}::IS3 cells. Annotated regions are diagramed below the x-axis for each strain.

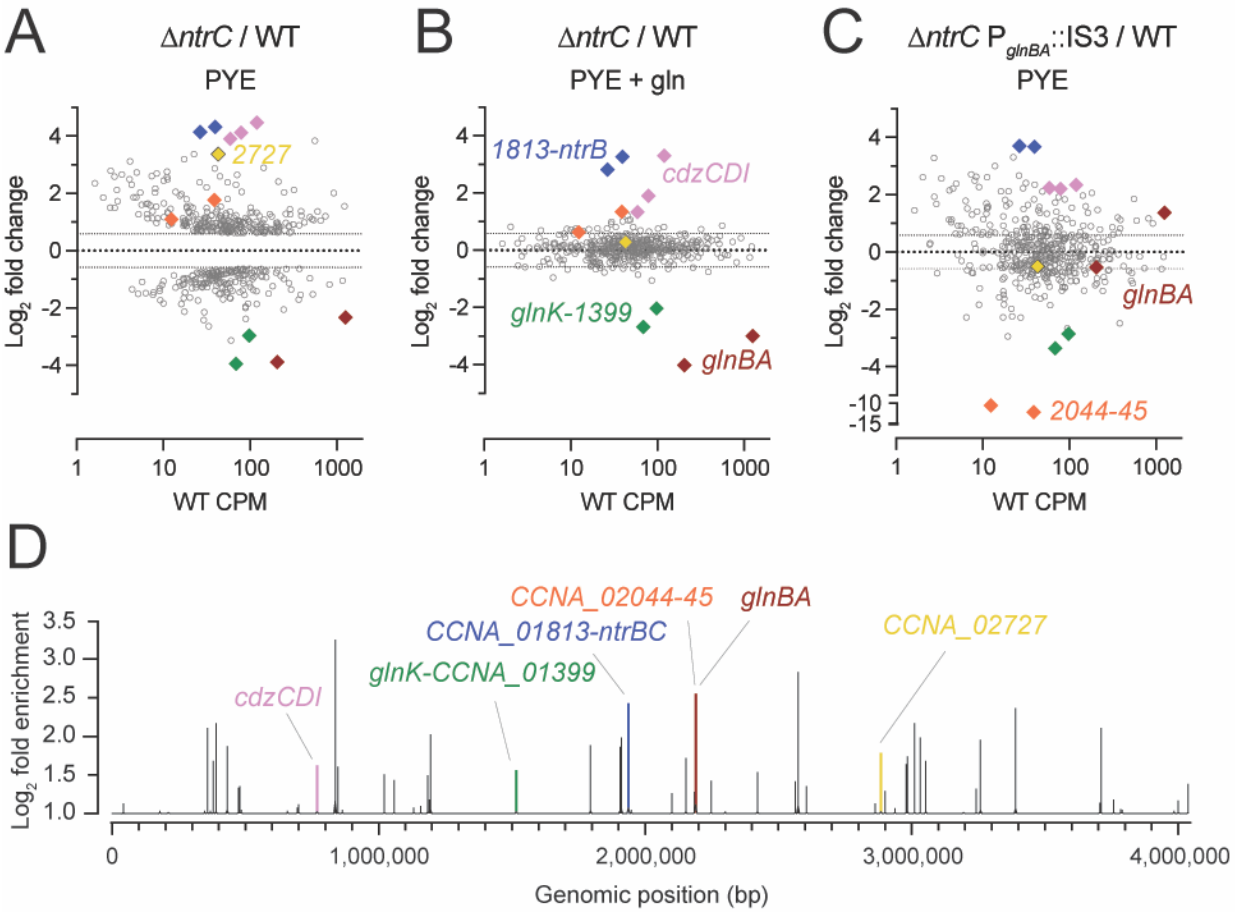

Figure 2.4. NtrC globally regulates gene expression in *Caulobacter*. In PYE complex medium, 473 genes exhibit differential transcript abundance in the Δ*ntrC* mutant compared to WT based on the following criteria: fold change > 1.5, FDR $P < 0.000001$ and maximum group mean RPKM > 10. (A-C) Log_2 fold change in abundance for these 473 transcripts for the following comparisons: (A) Δ*ntrC* vs. WT cultures grown in PYE, (B) Δ*ntrC* vs. WT cultures grown in PYE supplemented with 9.3 mM glutamine (gln). Differentially regulated genes in the Δ*ntrC* mutant are largely restored to WT-like levels upon supplementation with glutamine; exceptions are highlighted in colored diamonds. (C) Δ*ntrC* P_{glnBA}::IS3 vs. WT cultures grown in PYE, where each symbol represents a gene. The x-axis represents WT transcript abundance in PYE (counts per million; CPM) for each gene. (D) NtrC ChIP-seq peaks (q-value < 0.05, area under the curve (AUC) > 20) across the *Caulobacter* genome plotted as log_2 fold enrichment in read counts compared to the input control. Peaks highlighted in color are in the promoter of genes highlighted in (A-C), or, in the case of *cdzCDI*, overlapping the coding region. Colors correspond to the following genes: pink, *cdzCDI*; green, *glnK-CCNA_01399*; blue, *CCNA_01813-ntrB*; orange, *CCNA_02044-45*; red, *glnBA*; yellow, *CCNA_02727*.

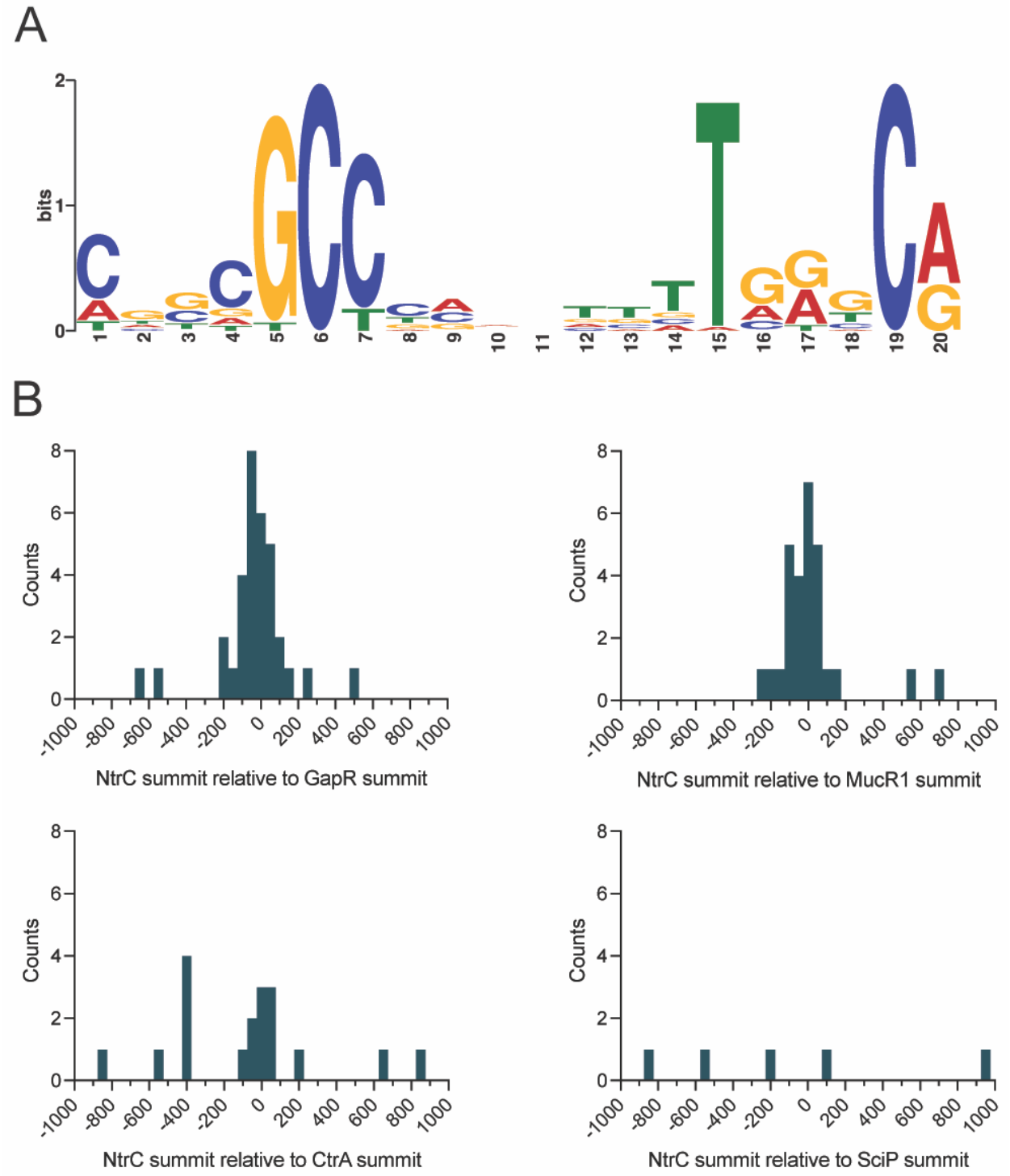

Figure 2.5. NtrC binding sites are often co-located with the binding sites of select chromosome structuring proteins and cell cycle regulators. (A) DNA motif enriched in NtrC ChIP-seq peaks, as identified by MEME [260]. (B) Distribution of the relative position of NtrC ChIP-seq summits to the nearest GapR, MucR1, CtrA, or SciP summit as calculated by ChIPpeakAnno [259]. NtrC summits >1,000 bp away from the nearest cell cycle regulator summits were excluded from the plots. Frequency distributions were plotted as histograms with 50 bp bins.

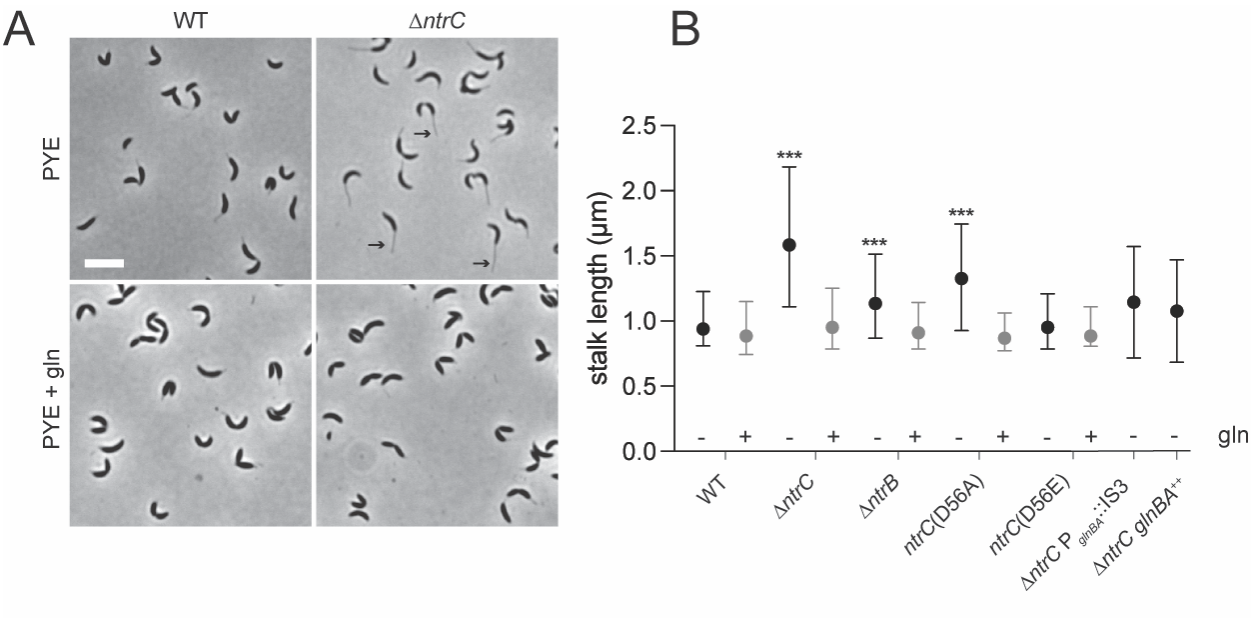

Figure 2.6. Deletion of the *ntrB-ntrC* two-component system results in development of hyper-elongated stalks. (A) Representative phase-contrast images showing the stalk elongation phenotype of a Δ*ntrC* strain compared to WT; strains were cultivated in PYE complex medium (top). The elongated stalk phenotype is chemically complemented by the addition of 9.3 mM glutamine (gln) to the medium (bottom). Scale bar (white; top left) equals 5 μm. Example stalks in the Δ*ntrC* panel are marked with black arrows. (B) Summary of stalk length measurements for WT, Δ*ntrC*, Δ*ntrB*, *ntrC*(D56A), *ntrC*(D56E), Δ*ntrC* P_{glnBA}::IS3, and Δ*ntrC* *glnBA*$^{++}$ cultivated without (-/black) and with (+/gray) gln. Data represent median ± interquartile range. Minimum length for stalk segmentation was 0.6 μm. Statistical significance assessed by Kruskal-Wallis test followed by Dunn's post-test comparison to WT (*** $P < 0.0001$). WT: n=314(- gln) n=207(+ gln); Δ*ntrC*: n=1020(-) n=338(+); Δ*ntrB*: n=440(-) n=75(+); *ntrC*(D56A): n=849(-) n=204(+); *ntrC*(D56E): n=339(-) n=177(+); Δ*ntrC* P_{glnBA}::IS3: n=218(-); Δ*ntrC* *glnBA*$^{++}$: n=503(-).

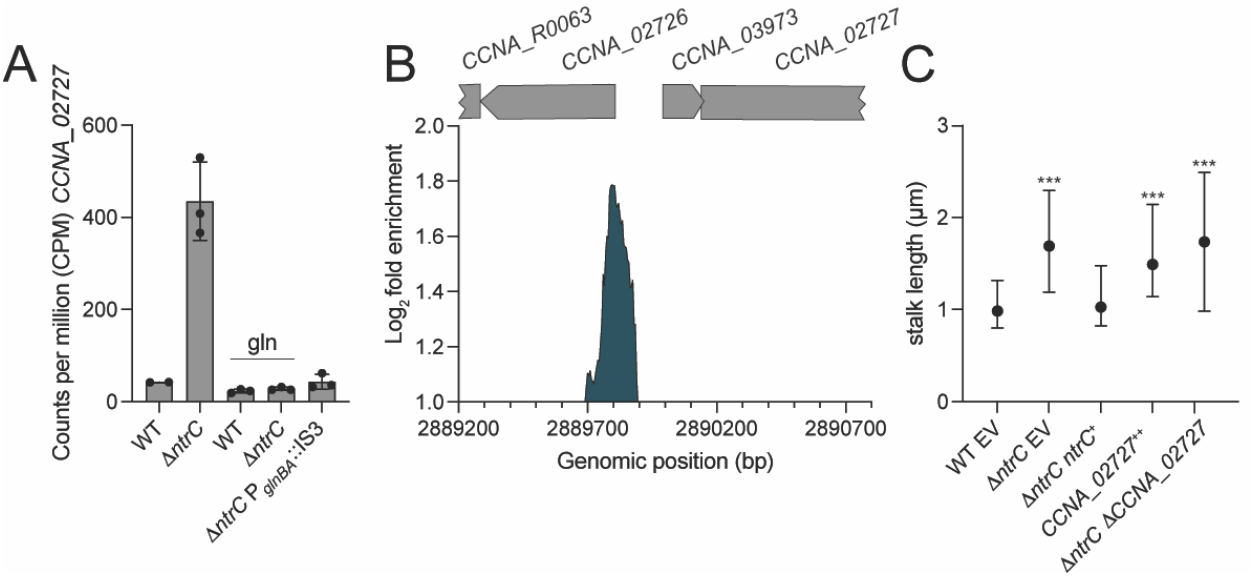

Figure 2.7. Transcriptional regulation and functional impact of the *phoH*-family gene, *CCNA_02727*. (A) Transcript levels of *CCNA_02727* measured by RNA-seq in different genetic backgrounds and conditions: WT and Δ*ntrC* strains grown in PYE complex medium or PYE supplemented with 9.3 mM glutamine (gln), and the Δ*ntrC* P_{glnBA}::IS3 strain grown in PYE. Data represent mean ± standard deviation of three replicate samples. (B) NtrC chromatin immunoprecipitation sequencing (ChIP-seq) revealed a binding peak upstream of an operon containing the small hypothetical gene, *CCNA_03973*, and *CCNA_02727*. Data represent $\log_2$ fold enrichment sequence reads in the NtrC immunoprecipitation samples compared to total input sample. Positions of annotated genes are represented by gray bars above the plot. The genomic positions in the reference genome (Genbank accession CP001340) are indicated. (C) Summary of stalk length data, comparing different strains: WT and Δ*ntrC* strains containing an empty vector (EV), a genetic complementation vector (Δ*ntrC ntrC*$^{+}$), Δ*ntrC* Δ*CCNA_02727*, and *CCNA_02727* overexpressed in WT from a xylose-inducible promoter (*CCNA_02727*$^{++}$). The data represent the median and interquartile range; a minimum length of 0.6 μM was used for stalk segmentation. Statistical significance was assessed using the Kruskal-Wallis test followed by Dunn's test, comparing each condition to WT EV (*** $P < 0.0001$). WT EV: n=330; Δ*ntrC* EV: n=1,481; Δ*ntrC ntrC*$^{+}$: n=366; *CCNA_02727*$^{++}$ n=238; Δ*ntrC* Δ*CCNA_02727*: n=1,261.

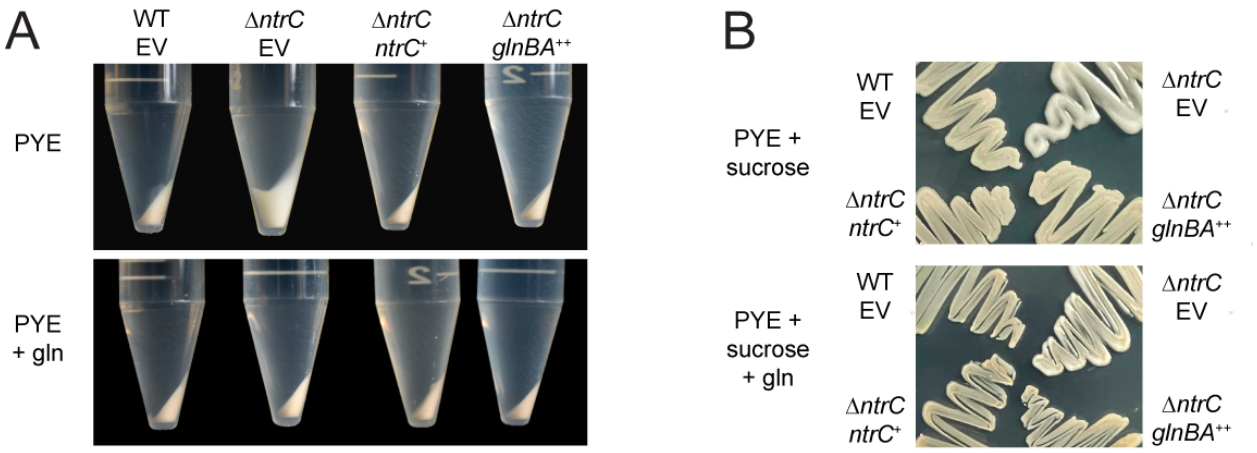

Figure 2.8. The hyper-mucoid phenotype of Δ*ntrC* in PYE complex medium is suppressed by either glutamine supplementation or *glnBA* expression. (A) Cell pellets of WT and Δ*ntrC* carrying an empty vector (EV) or vectors expressing *ntrC* (*ntrC*$^{+}$) or *glnBA* (*glnBA*$^{++}$). Strains were grown overnight in PYE complex medium or PYE supplemented with 9.3 mM glutamine (gln). Overnight cultures were normalized to OD_{660} = 0.5 and cells from 10 ml were centrifuged at 7,197 x g for 3 min at 4°C, and pellets were photographed. (B) Growth of WT EV, Δ*ntrC* EV, Δ*ntrC ntrC*$^{+}$, and Δ*ntrC glnBA*$^{++}$ on PYE agar supplemented with 3% sucrose (PYE + sucrose) or PYE agar supplemented with 3% sucrose and 9.3 mM glutamine (PYE + sucrose + gln). Plates were incubated for 4 days at 30°C and photographed.

Chapter 3: Mutations in *ntrC* restore cell cycle by stabilizing CtrA through increased ppGpp

Preface

The content of this chapter was modified and adapted from its published form: North H, Hydorn M, Dworkin J, Fiebig A, Crosson, S. *mBio* (2025, in revision). Molly Hydorn and Jonathan Dworkin provided the construct for the ppGpp-sensing riboswitch for *in vivo* quantification of ppGpp alarmone in our strains.

Abstract

Bacteria often rely on two-component signaling systems (TCS) to sense environmental cues and coordinate essential cellular functions. In *Caulobacter crescentus*, the sensor histidine kinase CckA and the response regulator CtrA are part of an essential TCS phosphorelay that directs cell cycle progression. Through a forward genetic selection, we identified a diverse set of mutations that bypass the requirement for CckA-CtrA signaling, uncovering multiple genetic routes by which *C. crescentus* can compensate for disruption of an essential cell cycle control system. Among these, we defined structurally distinct classes of mutations in *ntrC*, a conserved regulator of nitrogen assimilation, that differentially suppress the lethal phenotype of a temperature-sensitive (ts) *cckA* mutant. We present evidence that suppression of *cckA*(ts) by mutant *ntrC* involves two mechanisms: 1) increased levels of the alarmone ppGpp resulting from intracellular glutamine limitation, which sustain CtrA protein levels in the cell, and 2) activation of transcription at select σ^{54}-dependent flagellar and cell cycle promoters. Activation of σ^{54}-dependent transcription in mutant *ntrC* backgrounds is associated with increased mutant NtrC protein levels in the cell and occurs despite *C. crescentus* NtrC lacking the conserved GAFTGA motif required for σ^{54}-RNA polymerase activation. We conclude that *cckA*(ts) suppression is not merely a consequence of *ntrC* loss-of-function but, instead, arises from a combination of transcriptional and post-transcriptional changes driven by mutant NtrC expression. These results define a route for genetic bypass of an essential cell cycle signaling system, underscoring the

flexibility of bacterial regulatory networks and the deep connections between nitrogen metabolism, nucleotide signaling, and cell cycle control.

Introduction

Cells use sophisticated molecular mechanisms to monitor both their internal state and the external environment, ensuring the maintenance of homeostasis. In bacteria, a common mechanism of environmental monitoring involves sensor histidine kinase (SHK) proteins, which detect physical and chemical cues and regulate adaptive physiological responses through phosphoryl transfer to their partner response regulator (RR) proteins [46]. SHKs and RRs together form two-component signaling systems (TCSs), one of the most widely conserved gene regulatory mechanisms in bacteria [47]. TCS were initially thought to regulate gene expression and behavioral responses only under specific environmental conditions [48, 49]. However, studies in the years following their discovery uncovered TCS systems and multi-component TCS phosphorelays [50] that regulate core cellular processes including cell envelope biogenesis, cell cycle progression, and cell division. The TCS genes that regulate such core processes are often essential for cell viability under standard cultivation conditions [51-54].

Cell cycle progression in the dimorphic bacterium *Caulobacter crescentus* (hereafter, *Caulobacter*) is governed by the activation and inactivation of the essential RR CtrA, which is under precise spatiotemporal control [55]. Specifically, CtrA is activated by phosphorylation via a multiprotein phosphorelay initiated by the essential SHK CckA [56-58]. Once activated, CtrA directly regulates the transcription of over 90 genes involved in cell cycle progression, cell division, and polar morphogenesis [59] (**Figure 3.1A**) . However, CckA is a bifunctional kinase, capable of switching between kinase and phosphatase states [60]. In its phosphatase mode, CckA dephosphorylates both CtrA and the single-domain RR CpdR (**Figure 3.1A**). Once dephosphorylated, CpdR serves as a proteolytic adapter, directing CtrA for degradation by the ClpXP protease, thereby supporting precise regulation of CtrA protein levels during the cell cycle

[60-62]. The switch in CckA activity from kinase to phosphatase is regulated by changes in levels of cyclic-di-GMP [63] and ADP [64], and its spatial localization within the membrane [65, 66]. In addition to these regulatory inputs, CckA function is influenced by environmental stress cues that are proposed to enhance its phosphatase activity, leading to CtrA degradation and a consequent block in cell division under stress conditions [67]. Additional essential TCS proteins further refine the spatial and temporal control of CckA activity within developmentally distinct *Caulobacter* cell compartments [68].

The essential functions of CckA and CtrA are tightly regulated by a network of supporting TCS regulators, some of which are also considered essential [43, 262]. Given this extensive regulatory control by a consortium of essential regulators, one might expect that *cckA* would be strictly indispensable for *Caulobacter* viability. However, genetic studies have identified specific mutations that can bypass the requirement for CckA function. Specifically, gain-of-function mutations in CtrA allow for growth of *Caulobacter* strains lacking *cckA* [57, 227]. We therefore sought to discover other genetic routes to bypass *cckA* in the hope that such an effort would illuminate new features of the *Caulobacter* cell cycle control system. We utilized a *Caulobacter* mutant bearing a temperature-sensitive (ts) allele of *cckA* [58] (hereafter, *cckA*(ts)), that is not viable at elevated (i.e., restrictive) temperatures. The *cckA*(ts) allele harbors two amino acid substitutions in the ATPase domain region of *cckA* (i.e., I484N, P485A). Notably, these mutations in *cckA* result in dramatically reduced phosphorylation of CtrA *in vivo* [58]. Through a genetic selection for spontaneous mutations that restored growth of the *cckA*(ts) strain at the restrictive temperature, we identified expected gain-of-function mutations in *ctrA*, as well as mutations that enhance proteolytic stability of CtrA. We further identified mutations outside of the known cell cycle regulatory network that restored growth of the *cckA*(ts) mutant at the restrictive temperature, including multiple independent mutations in the β subunit of RNA polymerase (*rpoB*). Additionally, independent mutations in the DNA-binding domain of the nitrogen regulatory protein *ntrC* were

isolated, highlighting potential alternative mechanisms that compensate for the loss of CckA function.

NtrC is a member of a widely conserved class of response regulators known as bacterial enhancer binding proteins (bEBP) and is best known for its role in activating transcription of genes involved in nitrogen assimilation through its interaction with σ^{54}-RNA polymerase (RNAP) [263-265]. However, a recent study has shown that *Caulobacter* NtrC lacks a set of amino acids in its AAA+ domain known as the GAFTGA motif [266], which is necessary for interaction with the σ^{54} N-terminal regulatory domain [233]. Consistent with this result, transcriptomic and ChIP-seq analyses provide evidence that NtrC regulates σ^{70}-dependent promoters in *Caulobacter* both as a transcriptional activator and as a repressor [266]. In addition to its role in promoting the assimilation of ammonium (NH_4^+) into glutamine through its activation of *glnA*, *Caulobacter* NtrC influences polar stalk development, cell envelope polysaccharide biosynthesis, and binds to numerous sites across the *Caulobacter* chromosome, often overlapping with binding sites for the nucleoid-associated protein GapR and the cell cycle regulator MucR1 [266]. These results suggest that NtrC plays a broader role in coordinating nitrogen metabolism with cell cycle and other developmental processes. Our discovery of *ntrC* mutants that rescued growth of a *cckA* loss-of-function mutant is congruent with a model in which NtrC can influence cell cycle and cellular development. Through a detailed analysis of the genetic interactions between *ntrC* and *cckA*, we identified a complex pattern of genetic suppression, in which distinct loss-of-function mutations in *ntrC* variably rescue the temperature-sensitive defects of a *cckA*(ts) mutant. Our data support a tiered genetic suppression mechanism in which specific *ntrC* loss-of-function alleles enhance ppGpp production, thereby sustaining CtrA protein levels in the cell, while also supporting transcriptional rescue of dysregulated cell cycle and cellular development genes from non-native chromosomal sites. These results illuminate the plasticity of an essential *Caulobacter* signaling pathway and underscore the complex interplay between the noncanonical bEBP NtrC,

cell cycle regulation, and cellular development.

Results

A selection to identify mutations that suppress lethality of cckA(ts)

Shifting a culture of a temperature-sensitive (ts) *Caulobacter cckA* mutant (*cckA*(ts)) [58] from a growth-permissive temperature (30°C) to a growth-restrictive temperature (37°C) resulted in expected phenotypes, including cell filamentation and loss of colony formation on peptone yeast extract (PYE) complex solid medium [58] (**Figure 3.1C**; **Figure 3.2D**). However, rare colonies grew at the restrictive temperature. We picked several of these apparent suppressor mutants and confirmed that they grew at the restrictive temperature despite harboring the genetic lesions in the *cckA* ATPase domain region (*cckA*(I484N, P485A)) that cause temperature sensitivity [58]. Through whole genome sequencing we identified mutations that putatively suppress the *cckA*(ts) lesions including a second-site mutation in the *cckA* HisKA dimerization/phosphoacceptor domain (R334S) (**Figure 3.1B**; **Supplemental Table 5**).

Several extragenic mutations in genes associated with the CckA cell cycle signaling pathway were identified through this selection, including multiple strains with mutations in *ctrA* (**Figure 3.1B**; **Supplemental Table 5**), the essential RR [93] and phosphoryl-transfer target of CckA [58]. Among these were four independent isolates harboring a *ctrA*(D8G) mutation and one harboring *ctrA*(T90A). The *ctrA*(D8G) mutation has been previously characterized as a gain-of-function allele that allows *Caulobacter* to grow in the absence of *cckA* [227]. Additionally, we identified putative loss-of-function mutations in *cpdR*, which is also a phosphorylation target of CckA and regulates the proteolytic stability of CtrA [61, 267] (**Figure 3.1A-B**; **Supplemental Table 5**). Loss of CpdR function disrupts its role in targeting CtrA for degradation, thereby enhancing CtrA stability in the cell [61]. To validate *cpdR* as a suppressing target of *cckA*(ts) temperature sensitivity, we constructed a *cpdR* in-frame deletion mutation (Δ*cpdR*) in a *cckA*(ts) genetic background. Deletion of *cpdR* fully suppressed the temperature sensitivity of *cckA*(ts),

restoring growth at the restrictive temperature (37°C) to a level comparable to that observed for the group of *cpdR* point mutant alleles isolated in our genetic selection (**Figure 3.1C**). These results reveal a pattern of suppression whereby loss of CckA function is mitigated by mutations that either enhance CtrA activity or its proteolytic stability.

Suppressing mutations outside of the known CckA regulatory axis

In addition to mutations that were on pathway, we identified mutations in genes that are not known to be a part of the established cell cycle regulatory network, pointing to possible alternative mechanisms that can mitigate loss of CckA function. For example, multiple independent mutations in the β subunit of RNAP (*rpoB*) were associated with rescued growth of *cckA*(ts) strains at the restrictive temperature (**Figure 3.1B**; **Supplemental Table 5**). A prior study demonstrated that a *rpoB* mutation enhances CtrA promoter occupancy, likely via increased (p)ppGpp signaling [268]. The identification of *rpoB* mutations as suppressors of *cckA*(ts) suggests that altered RNAP activity may modulate CtrA function independent of direct phosphorelay input. Mutations in *CCNA_01689*, which encodes inosine-5'-monophosphate dehydrogenase that catalyzes the rate-limiting step in guanine nucleotide synthesis, were also associated with *cckA*(ts) rescue, as were mutations in a LysR-family transcriptional regulator (*CCNA_02227*) and the cell envelope regulator, *cenR* (**Figure 3.1B**; **Supplemental Table 5**). Finally, we identified three independent suppressor isolates carrying mutations in the DNA-binding domain of the bEBP gene, *ntrC* (**Figure 3.1B**; **Supplemental Table 5**). We conclude that a diverse set of mutations can suppress the *cckA*(ts) phenotype, including second-site modifications of *cckA* itself, mutations within the signaling pathway it regulates, and mutations in genes with broader roles in transcription and nucleotide synthesis.

Loss-of-function mutations in the HTH domain of ntrC fully suppress cckA(ts) lethality

Our genetic selection uncovered two distinct point mutations in *ntrC* that were associated with rescued growth of a *cckA*(ts) mutant at the restrictive temperature (**Figure 3.1B**). These mutations, A446P and L424P, are located within the DNA-binding/helix-turn-helix (HTH) domain

of *ntrC* (**Figure 3.2A**). Since a role for *ntrC* in the CckA-ChpT-CtrA phosphorelay had not been previously described, we prioritized *ntrC* for further investigation.

To directly demonstrate that the A446P and L424P alleles of *ntrC* suppress the *cckA*(ts) phenotype, we replaced wild-type *ntrC* with either *ntrC*(L424P) or *ntrC*(A446P) in a *cckA*(ts) genetic background. Both mutant *ntrC* alleles restored the growth of the *cckA*(ts) mutant to wild type (WT) levels on PYE complex solid medium at the restrictive temperature (37°C) without impacting viability at the permissive temperature (30°C) (**Figure 3.2B**). These *ntrC* alleles partially rescued the filamentation and cell division defects of the *cckA*(ts) mutant at the restrictive temperature (**Figure 3.2D**). We postulated that substitution of proline at residues 424 and 446 of the HTH domain resulted in loss of NtrC function since mutations to proline are poorly tolerated [269] and DNA binding is critical for NtrC activity [266].

Deletion of *Caulobacter ntrC* results in several distinct phenotypes, including an inability to grow in defined medium (M2G) with NH_4^+ as the sole nitrogen source, as well as hyper-elongated polar stalks and hyper-mucoid growth on PYE complex medium. These phenotypes are chemically complemented by adding the nitrogen source glutamine to the medium [266]. We introduced the *ntrC*(A446P) and *ntrC*(L424P) alleles into an otherwise wild-type *Caulobacter* background via allele replacement and these mutant strains phenocopied a Δ*ntrC* strain. Specifically, both HTH mutants failed to grow with NH_4^+ as the sole nitrogen source and growth was restored when NH_4^+ was replaced with an equivalent concentration of glutamine (See **Figure S3.1** in Appendix 2). Additionally, both mutants exhibited elongated stalks and a mucoid cell pellet phenotype similar to that of the *ntrC* deletion strain (See **Figure S3.1** in Appendix 2). We confirmed that both mutant proteins were stably expressed in a *cckA*(ts) background (**Figure 3.2C**), indicating that these loss-of-function phenotypes are not due to reduced protein expression or instability. We conclude that the A446P and L424P mutations in the DNA-binding/HTH domain of NtrC result in a loss of protein function.

Distinct contributions of NtrC domains to cckA(ts) suppression: A key role for REC domain

Given the loss-of-function phenotypes observed in *ntrC*(L424P) and *ntrC*(A446P) mutants (See **Figure S3.1** in Appendix 2), we predicted that complete deletion of *ntrC* would similarly suppress the temperature sensitivity of *cckA*(ts) at the restrictive temperature. Contrary to our expectation, *ntrC* deletion (Δ*ntrC*) only partially rescued the growth defect of *cckA*(ts) as shown by serial dilution assays at the restrictive temperature (**Figure 3.2B**). The Δ*ntrC* allele alleviated the filamentation and cell division defects of *cckA*(ts) to a similar extent as the *ntrC*(L424P) and *ntrC*(A446P) point mutants (**Figure 3.2D**). Since these point mutations reside in the HTH domain of NtrC (**Figure 3.2A**), we hypothesized that deleting the entire HTH domain would replicate their suppressive effects. Consistent with this prediction, deletion of the *ntrC* HTH domain (*ntrC*(ΔHTH)) nearly fully restored growth of *cckA*(ts) at the restrictive temperature (**Figure 3.2E**) (See **Figure S3.2** in Appendix 2). These results indicate that disruption of NtrC DNA binding is sufficient to suppress the loss of CckA function.

NtrC, a bEBP [167, 213], consists of three functional domains: 1) a two-component receiver (REC) domain, 2) an ATPase associated with cellular activity (AAA+) domain, and 3) a DNA-binding/HTH domain (**Figure 3.2A**). To assess the specific contributions of the REC and AAA+ domains to *cckA*(ts) suppression, we introduced domain deletions in *ntrC* within the *cckA*(ts) genetic background. The *ntrC*(ΔAAA) allele improved *cckA*(ts) growth but not as effectively as *ntrC*(ΔHTH). In contrast, deleting the REC domain (*ntrC*(ΔREC)) only partially suppressed growth defects, similar to Δ*ntrC* (**Figure 3.2E**). Taken together, these data indicate that suppression is most robust when NtrC retains an intact REC and AAA+ domain, as seen in the *ntrC*(L424P), *ntrC*(A446P), and *ntrC*(ΔHTH) mutants. Notably, we have previously shown that these NtrC domain mutants (ΔHTH, ΔREC, and ΔAAA) are stably expressed in *Caulobacter* at significantly higher levels than wild-type NtrC [266]. The possible impact of increased steady-state levels of these mutant alleles on gene expression is discussed in sections below. These results illuminate a critical role for the REC domain in the *cckA*(ts) suppression mechanism.

Phosphorylation of the NtrC REC domain triggers conformational changes that regulate

its activity [270]. Previously, we demonstrated that phosphorylation of the conserved aspartate residue (D56) in the REC domain is required for *Caulobacter* growth on NH_4^+ as the sole nitrogen source [266]. To test whether REC phosphorylation is necessary for *cckA*(ts) suppression, we introduced the non-phosphorylatable *ntrC*(D56A) allele into the *cckA*(ts) background. Similar to *ntrC*(ΔREC), the *ntrC*(D56A) mutation only partially suppressed *cckA*(ts) temperature sensitivity (**Figure 3.3A**). We further tested whether phosphorylation was required for suppression by *ntrC*(HTH) domain mutants by generating *ntrC*(D56A, L424P) and *ntrC*(D56A, A446P) double mutants. Suppression in these strains was comparable to *ntrC*(D56A), indicating that phosphorylation of the REC domain is required for full suppression by *ntrC*(L424P) and *ntrC*(A446P) (**Figure 3.3A**) (See **Figure S3.2** in Appendix 2).

Given this result, we predicted that deleting *ntrB* (Δ*ntrB*), which encodes the cognate kinase of NtrC [266], would similarly impair suppression of *cckA*(ts) by *ntrC*(L424P) and *ntrC*(A446P). As expected, Δ*ntrB* attenuated suppression by these *ntrC*(HTH) mutant alleles, further supporting a critical role for NtrC phosphorylation in this suppression mechanism (**Figure 3.3B**) (See **Figure S3.2** in Appendix 2). Together, these results show that the essential function of CckA can be robustly bypassed through an NtrC mutant that cannot bind DNA, but that has an intact and phosphorylatable REC domain.

Glutamine reverses cckA(ts) suppression by ntrC mutations

NtrC activates transcription of glutamine synthetase (*glnA*) [266], which is predicted to be the sole route of inorganic nitrogen assimilation in *Caulobacter* [128, 271]. Mutations in the NtrC HTH domain (L424P and A446P), as well as deletions of the HTH, REC, and AAA domains, disrupt NtrC function and suppress the temperature sensitivity of *cckA*(ts) to varying extents (**Figure 3.2**). Given that supplementation with glutamine alleviates the phenotypes associated with loss of *ntrC* function and broadly restores transcriptional balance in a Δ*ntrC* mutant [266], we hypothesized that suppression of *cckA*(ts) by *ntrC* mutations is at least partially mediated by reduced intracellular glutamine levels. Accordingly, we predicted that restoring cellular glutamine

through exogenous supplementation would negate the suppressive effects of *ntrC* mutations. Consistent with this prediction, supplementation with 9.3 mM glutamine had no impact on strain viability at 30°C but significantly impaired the ability of all *ntrC* mutations to rescue the growth defect of *cckA*(ts) at 37°C (**Figure 3.3C**) (See **Figure S3.2** in Appendix 2). We conclude that intracellular glutamine limitation contributes to *ntrC*-mediated suppression of the *cckA*(ts) phenotype.

To further investigate the role of glutamine in *ntrC*-mediated suppression of *cckA*(ts), we isolated spontaneous mutant strains that restored the ability of mutant *ntrC* alleles to suppress the temperature sensitivity of *cckA*(ts) in media containing glutamine (**Figure 3.4A**). Whole genome sequencing of ten "glutamine-blind" mutants revealed that eight harbored frameshift or point mutations in locus *CCNA_01242*, a gene encoding an annotated amino acid permease, and a ninth harbored an 8 kb deletion that included *CCNA_01242* (**Figure 3.4A**; **Supplemental Table 6**). The nature of the mutations in this gene (e.g., nonsense, frameshift, and deletion) strongly suggested they resulted in a loss of function. Supporting this model, an in-frame deletion of *CCNA_01242* (Δ) restored growth at restrictive temperatures of *cckA*(ts) strains carrying *ntrC* mutant alleles (Δ, L424P, or A446P) in the presence of glutamine (**Figure 3.4B**).

As deletion of *CCNA_01242* rendered suppressed strains insensitive to extracellular glutamine, we hypothesized that this gene encodes a glutamine transporter. To test this, we cultivated a *CCNA_01242* in-frame deletion strain in defined medium with either NH_4^+ or glutamine as the sole nitrogen source. As previously demonstrated [266], the Δ*ntrC* strain grew when glutamine was the sole nitrogen source but failed to grow with NH_4^+ (**Figure 3.4C**). However, this ability to utilize glutamine depended on the amino acid permease encoded by *CCNA_01242*, as the Δ*ntrC* Δ*CCNA_01242* double mutant was unable to grow in glutamine-containing medium (**Figure 3.4C**). These results provide evidence that *CCNA_01242* functions as a glutamine transporter and support a model in which glutamine uptake through this permease prevents *ntrC* mutants from rescuing the temperature-sensitive growth defect of *cckA*(ts) when

extracellular glutamine is abundant.

A mechanism to bypass cckA function: Enhancing ppGpp synthesis and CtrA levels

Previous studies in *Caulobacter* have demonstrated that elevated intracellular glutamine suppresses the synthesis of the nucleotide (p)ppGpp [128], a global regulator of cell physiology [98, 272] (**Figure 3.5A**). Building on the established inverse relationship between glutamine and (p)ppGpp levels, along with our previous finding that *Caulobacter* lacking NtrC cannot assimilate NH_4^+ into glutamine [266], we hypothesized that *ntrC* mutations result in elevated (p)ppGpp levels. To test this, we developed an *in vivo* biosensor by placing a *Desulfitobacterium hafniense* ppGpp-regulated riboswitch [273] upstream of *mNeonGreen* [274] following a strategy similar to the RNA aptamer-based (p)ppGpp reporter developed by Sun et al. [275]. Based on the riboswitch mechanism [273], we expected ppGpp to promote transcriptional readthrough, making *mNeonGreen* fluorescence proportional to intracellular ppGpp levels. Consistent with this expectation, fluorescence from the riboswitch-*mNeonGreen* reporter was nearly undetectable in a *spoT* deletion strain, which lacks the sole (p)ppGpp synthetase in *Caulobacter* [118] (**Figure 3.5B**). As predicted, fluorescence intensity from this reporter was significantly higher in a Δ*ntrC* strain compared to WT, and this signal was restored to wild-type levels upon expression of *ntrC* from an ectopic locus (**Figure 3.5B**). Given these results, we predicted that loss of *ntrC* function in the *cckA*(ts) background would similarly result in elevated ppGpp and increased fluorescence from the riboswitch-*mNeonGreen* fusion. Indeed, *cckA*(ts) strains carrying *ntrC* loss-of-function point mutants (L424P or A446P) exhibited fluorescence levels comparable to the Δ*ntrC* mutant (**Figure 3.5B**). Together, these findings support a model in which loss of *ntrC* function in *Caulobacter* leads to elevated intracellular ppGpp levels.

Elevated (p)ppGpp levels have been shown to increase CtrA protein levels through a post-transcriptional mechanism [146] (**Figure 3.5A**). Given that loss-of-function mutations in *cpdR*, which stabilize CtrA [61], rescue the temperature-sensitive growth defect of *cckA*(ts) (**Figure 3.1C),** we hypothesized that elevated (p)ppGpp levels similarly contribute to the suppression of

cckA(ts) in *ntrC* mutants by increasing CtrA levels. To test this, we expressed a truncated version of the *Escherichia coli* RelA enzyme (*relA'*-FLAG), which lacks (p)ppGpp hydrolase activity and constitutively synthesizes (p)ppGpp [276]. This mutant *relA* allele has been previously shown to elevate (p)ppGpp levels and post-transcriptionally enhance CtrA levels in *Caulobacter* [146]. Because (p)ppGpp accumulation slows bacterial growth [272], *relA'*-FLAG expression resulted in smaller colonies at the permissive temperature (30°C) in both WT and *cckA*(ts) strains (**Figure 3.5C**). However, at 37˚C, *relA'*-FLAG expression improved *cckA*(ts) growth by approximately two $\log_{10}$ units, supporting our hypothesis. In contrast, expression of a catalytically inactive *relA* mutant (*relA'*(E335Q)-FLAG) [146], failed to enhance *cckA*(ts) growth at the restrictive temperature (**Figure 3.5C**), directly implicating (p)ppGpp in the suppression mechanism. These findings support a model in which activation of (p)ppGpp synthesis upon loss of *ntrC* function bypasses the requirement for CckA kinase activity, perhaps through increasing CtrA protein levels.

To directly assess CtrA levels in WT, *cckA*(ts), and *cckA*(ts) *ntrC*(L424P) cultures at the restrictive temperature, we inhibited *ctrA* transcription with rifampicin [146, 277] and monitored CtrA protein abundance over time. Consistent with previous reports [57, 61], CtrA levels declined more rapidly in the *cckA*(ts) mutant compared to WT. However, in the *cckA*(ts) *ntrC*(L424P) mutant, CtrA levels were maintained at WT-like levels following transcriptional shutoff (**Figure 3.6A**) (See **Figure S3.3** in Appendix 2). These results provide evidence that suppression of *cckA*(ts) by *ntrC*(L424P) involves mechanisms that either enhance CtrA protein stability or increase *ctrA* mRNA stability, ultimately enhancing CtrA levels in the cell. This conclusion aligns with our observation that loss-of-function mutations in *cpdR*, which stabilize CtrA protein by preventing its degradation [61, 277], can bypass the essential kinase function of CckA (Figure 3.1).

Given the sustained CtrA levels in the suppressing *ntrC* mutant, we next tested whether artificially stabilizing CtrA independent of *ntrC* mutation would similarly rescue *cckA*(ts) growth.

To do this, we expressed *ctrA*DD, a previously characterized stabilized allele [93, 278], in *cckA*(ts) at the restrictive temperature. As predicted, *ctrA*DD expression improved *cckA*(ts) growth by approximately one $\log_{10}$ unit at 37°C (**Figure 3.6B**). These findings support a model in which genetic bypass of *cckA*(ts) is mediated, at least in part, by mechanisms that enhance CtrA protein abundance, either through direct protein stabilization or by increasing *ctrA* transcript stability.

Global transcriptional analysis of a synthetic rescue interaction

Our data reveal a tiered pattern of suppression in *Caulobacter*, where temperature-sensitive loss-of-function mutations in the essential cell cycle regulatory kinase CckA are variably rescued by structurally distinct loss-of-function mutations in *ntrC* (**Figure 3.7A**). Given that NtrC is a transcription factor, we hypothesized several mechanisms through which *ntrC* mutations might rescue *cckA*(ts) conditional lethality by altering transcription: 1) *ntrC* mutations broadly restore gene expression in the *cckA*(ts) background to wild-type levels, 2) *ntrC* mutations create a distinct gene expression profile unrelated to either WT or the primary *cckA*(ts) mutant, or 3) a combination of these effects. To test these models, we performed RNA sequencing (RNA-seq) to evaluate the transcriptional impact of *cckA*(ts) and *ntrC* mutations, both individually and in combination (**Supplemental Table 7**).

Principal component analysis (PCA) of the transcriptomic data revealed that PC1 and PC2 together accounted for 80% of the total variance (**Figure 3.7B**). These principal axes corresponded to transcriptional dysregulation caused by loss of *cckA* function (PC1) and *ntrC* function (PC2). Consistent with their growth, stalk length, and mucoid phenotypes (See **Figure S3.1** in Appendix 2), the transcriptional profiles of the *ntrC*(L424P) and *ntrC*(A446P) mutants in an otherwise wild-type genetic background clustered closely with Δ*ntrC* on the ordination plot (**Figure 3.7B**). When combined, the transcriptional effects of *cckA*(ts) and the *ntrC* mutations were largely independent given the clustering of the double mutant transcriptomes near the diagonal of PC1 and PC2. However, compared to the parental *cckA*(ts) strain, the double mutants are modestly shifted toward WT on PC1. The *ntrC*(HTH) domain point mutants (L424P and

A446P) shifted the transcriptome even closer to WT on PC1 than deletion of *ntrC* (**Figure 3.7B**). This trend aligns with the stronger rescue phenotypes observed for these point mutants compared to Δ*ntrC* (**Figure 3.2B**; **Figure 3.7A**), suggesting their more robust restoration of gene expression patterns disrupted by *cckA*(ts).

Using a conservative statistical cutoff, we identified 247 CckA-regulated genes and 78 NtrC-regulated genes (**Supplemental Table 7**). A combined and clustered dataset containing both CckA and NtrC regulons revealed only one overlapping gene, resulting in a set of 324 genes that are dysregulated by mutation of *cckA* or *ntrC* (**Figure 3.7C**; **Supplemental Table 7**). Genes with significantly decreased transcription upon loss of *cckA* function are consistent with published *cckA*(ts) transcriptomic data [57] and include numerous cell cycle and developmental regulators such as *ccrM*, *sciP*, *tacA*, *staR*, *kidO*, *spmX*, *hvyA*, *divK*, *fliX*, and *flbT*. These genes function in processes including holdfast biosynthesis and attachment, pilus and flagellum biogenesis, cell envelope biogenesis, polysaccharide biosynthesis, cyclic-di-GMP metabolism, and polyamine transport and metabolism [16, 217, 262, 279]. As CckA phosphorylates CtrA, a class I flagellar regulator [280], genes involved in flagellar assembly and chemotaxis also exhibited significantly reduced transcription (**Figure 3.7C-D**; **Supplemental Table 7**) (See **Figure S3.4** in Appendix 2). In contrast, genes significantly upregulated upon loss of CckA function included the nitrogen regulatory IIA protein (*CCNA_03710*) and the cell division genes *ftsL* and *mraZ*. Additionally, the (p)ppGpp-activated cell cycle regulator *mopJ* [281] and the ribosome hibernation factor *hpf* (*CCNA_03711*), which is transcriptionally activated by (p)ppGpp across diverse bacterial taxa [282-284], also showed increased expression. A small set of genes displayed minimal transcriptional changes in either single mutant (*cckA*(ts) or Δ*ntrC*) but had increased transcript levels in the double mutant, including several class II flagellar genes such as *fliP* and the *fliQ-fliR-flhB* operon (**Supplemental Table 7**).

***ntrC* mutation and transcriptional rescue of a subset of the CckA regulon**

Although the transcriptional effects of *cckA* and *ntrC* loss-of-function are largely

independent (**Figure 3.7B-C**), introducing *ntrC* mutations partially or fully restored the expression of a subset of genes that are dysregulated in the *cckA*(ts) mutant (**Figure 3.7C**). To identify the genes whose transcriptional defects were more effectively rescued by *ntrC*(HTH) mutations than by *ntrC* deletion, we compared the fold change in transcript levels between *cckA*(ts) Δ*ntrC* and the two point mutants, *cckA*(ts) *ntrC*(L424P) and *cckA*(ts) *ntrC*(A446P). By averaging these fold-change ratios, we observed a natural cutoff at approximately a 4-fold difference, which defined a set of 24 genes whose expression was most enhanced by the point mutations compared to *ntrC* deletion. This gene set was predominantly composed of σ^{54}-regulated class III and IV flagellar genes [285-288], alongside other critical regulators, including the essential DNA methyltransferase *ccrM*—a known CtrA target [280] — and *sciP*, an inhibitor of CtrA [70, 71] (**Figure 3.7D**; **Supplemental Table 7**) (See **Figure S3.4** in Appendix 2). Transcription of this gene set was modestly activated relative to WT across all three single *ntrC* mutant strains, suggesting that wild-type NtrC exerts a weak repressive effect at these loci [266]. In the *cckA*(ts) strain, transcription of class III and IV flagellar genes was significantly reduced, and this repression was partially alleviated by complete *ntrC* deletion (*cckA*(ts) Δ*ntrC*). However, introducing *ntrC*(HTH) point mutations into the *cckA*(ts) background led to robust activation of these σ^{54}-dependent flagellar genes, which are primarily regulated by the bEBP FlbD [279, 287]. Thus, loss-of-function mutations in the DNA-binding domain of NtrC strongly enhance transcription from select σ^{54}-dependent promoters, effectively rescuing gene expression defects caused by impaired CckA function.

Conclusion

The coordination and timely progression of cell cycle and cellular development in *Caulobacter* is governed by the CckA-ChpT-CtrA TCS phosphorelay. CtrA is spatially and temporally present and activated throughout the cell cycle. The activation and stability of CtrA at different cell cycle phases is determined by its phosphorylation state that is mediated by the

bifunctional SHK CckA. CtrA is phosphorylated and dephosphorylated by CckA in a cell cycle-dependent manner. Dephosphorylation of CpdR and CtrA by CckA phosphatase activity allows for CpdR to recruit CtrA to the cell pole where it is targeted for proteolytic clearance in a cell cycle-dependent manner. In this work, we performed a forward genetic selection using a conditionally-lethal, temperature-sensitive *cckA* allele (i.e., *cckA*(ts)) [58] to identify mutations that bypass the essentiality of this pathway. We discovered multiple types of mutations that suppress lethality, including mutations in the c*ckA-chpT-ctrA* pathway, itself, and genes closely associated with this genetic circuit. Amongst these were characterized hyper-active *ctrA* alleles and loss-of-function mutations in the proteolytic adapter, *cpdR*. These mutations suggested increased CtrA protein levels and increased CtrA activity can bypass the requirement for CckA kinase activity. Additionally, we isolated suppressors that harbored mutations in catalytic β subunit of RNAP, as well as the genes encoding a LysR-family transcription factor (*CCNA_02227*), an inosine-5'-monophosphate dehydrogenase (*CCNA_01689*), and the conserved nitrogen assimilation protein NtrC (*ntrC)*. Mutations in *ntrC* were of great interest due to 1) their full suppression of temperature-sensitive lethality of *cckA*(ts) and 2) the uncharacterized connection between *ntrC* and the *cckA-chpT-ctrA* pathway. In this work, we have established that these *ntrC* mutations (i.e., L424P and A446P) phenocopy loss-of-function (Δ*ntrC*) regarding mucoid growth, stalk length, NH_4^+ assimilation, slow growth in complex medium, etc, which originally suggested loss of *ntrC* function may bypass of the essentiality of the *cckA-chpT-ctrA* pathway. Given the established role of *Caulobacter* NtrC in intracellular glutamine synthesis, we interrogated the role of glutamine in suppression by loss-of-function *ntrC* mutations. Indeed, glutamine supplementation negated rescue of growth by *ntrC* mutations, suggesting decreased intracellular glutamine in *ntrC* mutants play a role in *cckA*(ts) suppression. Given the role of glutamine in activation of nitrogen-mediated stringent response in *Caulobacter* [128], we predicted increased (p)ppGpp levels in these glutamine starved *ntrC* mutants played a role in suppression. Indeed, *ntrC* mutants displayed increased ppGpp levels

and, moreover, artificial induction of (p)ppGpp in *cckA*(ts) suppressed, in part, lethality at the restrictive temperature, independent of *ntrC* mutation. It has been established that increased (p)ppGpp levels in *Caulobacter* stabilizes CtrA levels [86, 117, 146-148]. As mentioned, in our initial screen we identified mutations that stabilize CtrA and increase its activity. Similarly, we were curious if increased levels of CtrA in *ntrC* mutants could be contributing to suppression of *cckA*(ts). Indeed, a *ntrC* suppressor mutant (i.e., *cckA*(ts) *ntrC*(L424P)) had increased levels of CtrA compared to the *cckA*(ts) parental strain and, moreover, introduction of a stable *ctrA* allele (i.e., *ctrA*DD) displayed slight suppression of lethality, independent of *ntrC* mutation. Altogether, these results support a model in which loss of *ntrC* function results in decreased intracellular glutamine synthesis, which, in turn, activates stringent response and subsequent (p)ppGpp synthesis in *Caulobacter* (**Figure 3.8**). Through an unknown mechanism, these increased (p)ppGpp levels increase CtrA stability, which suppresses *cckA*(ts) lethality (**Figure 3.8**).

Notably, full deletion of *ntrC* did not fully suppress lethality of *cckA*(ts) as shown by L424P and A446P alleles. Further interrogation led us to discover that, instead, deletion of the *ntrC* HTH domain fully suppresses *cckA*(ts) lethality. These results suggested presence of the REC domain is required for full suppression of *cckA*(ts) lethality. In support of this, the conserved aspartyl residue for phosphorylation (D56) within the REC domain of L424P and A446P alleles was required for their full rescue of *cckA*(ts). Moreover, deletion of the gene encoding the cognate SHK for NtrC, *ntrB,* negated *cckA*(ts) suppression by L424P and A446P *ntrC* alleles. Altogether, these results suggest that a phosphorylatable REC domain is required for these HTH loss-of-function *ntrC* mutants to fully rescue viability of c*ckA*(ts) at the restrictive temperature (**Figure 3.8**). Transcriptomic data suggests that, unlike a full deletion of *ntrC* (Δ*ntrC*), *ntrC*(HTH) mutants increase the levels of mRNAs transcribed from established FlbD promoters (i.e., class III and IV flagellar genes), which are regulated in a σ^{54}-dependent manner. Given the differential suppression of *cckA*(ts) lethality by *ntrC*(HTH) mutants compared to Δ*ntrC*, we predict a role in the activation of these FlbD-regulated genes in full suppression of *cckA*(ts)

lethality by *ntrC*(HTH) mutants (**Figure 3.8**).

Materials & Methods

Growth conditions

E. coli strains were cultivated in Lysogeny Broth (LB) [10 g tryptone, 5 g yeast extract, 10 g NaCl per L] or LB solidified with 1.5% (w/v) agar at 37˚C. LB was supplemented with appropriate antibiotics when necessary. Antibiotic concentrations for selection of *E. coli* in solid or liquid conditions were as follows: kanamycin 50 μg/ml (solid), 30 μg/ml (liquid), chloramphenicol 20 μg/ml (both), oxytetracycline 12 μg/ml (both). *Caulobacter* strains were cultivated in peptone yeast extract (PYE) [2 g peptone, 1 g yeast extract, 1 mM $MgSO_4$, 0.5 mM $CaCl_2$ per L] medium or PYE solidified with 1.5% (w/v) agar at 30˚C or 37˚C. Antibiotic concentrations for selection of *Caulobacter* in solid and liquid conditions were as follows: kanamycin 25 μg/ml (solid), 5 μg/ml (liquid), chloramphenicol 1.5 μg/ml (both), oxytetracylcine 2 μg/ml (solid), 1 μg/ml (liquid), gentamycin 5 μg/ml (solid), 1 μg/ml (liquid). Nalidixic acid (20 μg/ml) was added to counterselect *E. coli* after conjugations. When noted, PYE was supplemented with an additional 9.3 mM of glutamine. When xylose was used for induction, 0.3% (w/v) xylose was added. For experiments in defined medium, *Caulobacter* strains were grown in M2 mineral salts with glucose (M2G) [6.1 mM Na_2HPO_4, 3.9 mM KH_2PO_4, 9.3 mM NH_4Cl, 0.25 mM $CaCl_2$, 0.5 mM $MgSO_4$, 10 μM ferrous sulfate chelated with EDTA (Sigma), and 0.15% glucose]. When noted, 9.3 mM NH_4Cl was replaced with 9.3 mM glutamine.

Strains and plasmids

Strains, plasmids, and primers used in this study are presented in **Supplemental Table 4**. All *Caulobacter* strains are derivatives of strain NA1000 [14]. To generate plasmid constructs for in-frame deletions and other allele replacements, homologous upstream and downstream fragments (~500 bp/each) were PCR-amplified and joined via overlap extension PCR [249]. PCR products were cloned into plasmid pNPTS138 by restriction enzyme digestion and ligation.

Similarly, to create genetic complementation constructs, target genes were amplified and fused to their upstream promoters (~500 bp fragment immediately upstream of the start of the annotated operon) via overlap extension PCR and these fused PCR products were purified and cloned into pXGFPC-2 (pMT585) [33], which integrates into the *xylX* locus in *Caulobacter*. For complementation, genes with their native promoters were cloned in the opposite orientation of the P_{xylX} promoter. For xylose-inducible expression, target genes were PCR-amplified and ligated into pMT585 in the same orientation as (i.e., downstream of) the P_{xylX} promoter. To build the ppGpp reporter, the ppGpp-sensing riboswitch of *ilvE* from *D. hafniense* [273] was fused to the 5' end of *mNeonGreen* and cloned into pXYFPC-5 (pMT604) [33], a plasmid that also integrates into the *xylX* locus in *Caulobacte*r. The riboswitch-*mNeonGreen* fusion was PCR-amplified and ligated into pXYFPC-5 in the same orientation as (i.e., downstream of) the P_{xylX} promoter for xylose-inducible expression. All ligation products were transformed into *E. coli* TOP10 for propagation, and the constructs were sequence verified prior to use.

Plasmids were transformed into *Caulobacter* via electroporation or triparental mating from TOP10 using FC3 as a helper strain [251]. In-frame deletion and allele replacement strains were generated via two-step recombination using *sacB* counterselection using an approach similar to that described by Fiebig and colleagues [237]. Briefly, primary recombinants bearing pNPTS138-derived allele-replacement plasmids were selected on solidified PYE containing kanamycin. Single colonies were then grown in PYE broth without selection for 6-18 h before secondary recombinants were selected on PYE containing 3% sucrose. The resulting clones were screened to confirm kanamycin sensitivity. Then allele replacement was confirmed by PCR for in-frame deletion alleles or PCR amplification and Sanger sequencing for point mutation alleles.

Selection for mutations that bypass conditional CckA loss of function mutation

A mutant bearing a temperature-sensitive allele of the essential histidine kinase, CckA, was previously isolated [58]. The *cckA*(ts) mutant was plated in a 10-fold dilution series on PYE medium and incubated at the restrictive temperature of 37°C. Colonies that emerged at higher

dilutions (10^{-2} to 10^{-3}) were streak purified. After confirming their ability to grow at 37°C, strains were saved in glycerol stocks. Twenty-six isolates were selected for whole genome sequencing to identify polymorphic sites compared to the parental strain. Briefly, genomic DNA was extracted from 1 ml of saturated PYE culture using guanidinium thiocyanate, chloroform extraction and isopropanol precipitation [253]. Genomic DNA was sequenced (150 bp paired-end reads) at SeqCenter (Pittsburgh, PA) using an Illumina NextSeq 2000. DNA sequencing reads were mapped to the *Caulobacter* NA1000 genome (Genbank accession CP001340) [14] and polymorphisms were identified using breseq [254].

Serial dilution titers

Starter cultures were grown overnight at 30˚C in PYE medium (**Figure 3.1C**; **Figure 3.2E**; **Figure 3.3C; Figure 3.5C**; **Figure 3.6B**) or PYE supplemented with 9.3 mM glutamine (**Figure 3.2B**; **Figure 3.3A-B**; **Figure 3.4A-B**; **Figure S3.2** in Appendix 2). Overnight cultures were diluted to OD_{660} 0.1 in the same medium and grown at 30°C for 2 h. After this initial outgrowth, cultures were again diluted to OD_{660} 0.1 and incubated in the same medium for 24 h. These stationary phase cultures were then normalized to OD_{660} 0.5, 10-fold serially diluted, and 5 µl of each dilution was spotted onto replicate PYE agar plates. As indicated, the agar was supplemented with 9.3 mM glutamine (PYE + gln), or with 0.3% xylose (PYE + xyl). Replicate plates were incubated at 37°C and 30°C for four days before imaging. Dilution plating growth experiments were performed at least three independent times. A representative experiment is shown.

Measurement of growth in M2G defined medium

Starter cultures were shaken overnight in PYE supplemented with 9.3 mM glutamine at 30˚C. Starter cultures were pelleted and washed three times with M2G containing 9.3 mM NH_4Cl or M2G in which NH_4Cl was replaced with molar-equivalent (9.3 mM) glutamine before dilution to OD_{660} 0.025 in the respective medium. These cultures were incubated at 30˚C with shaking for 24 h and culture density was measured optically (OD_{660}).

Light microscopy

To prepare cells for imaging, starter cultures were grown in PYE overnight at 30˚C and diluted to OD_{660} 0.1 in fresh PYE. Cultures were grown for 2 h at 30˚C to allow cells to reach similar logarithmic phase growth. For **Figure 3.2D**, logarithmic phase cultures were diluted to OD_{660} 0.1 in fresh PYE and grown for 3.25 h at 37˚C to capture physiology at the restrictive temperature. For **Figure S3.1C** in Appendix 2, logarithmic phase cultures were diluted to OD_{660} 0.1 in fresh PYE and grown for 24 h at 30˚C to allow cells to reach stationary phase.

2 µl of each culture were spotted on an agarose pad [1% agarose dissolved in water] on a glass slide and covered with a glass cover slip. Cells were imaged using a Leica DMI 6000 microscope using phase contrast with an HC PL APO 63x/1.4 numeric aperture oil Ph3 CS2 objective. Images were captured with an Orca-ER digital camera (Hamamatsu) controlled by Leica Application Suite X (Leica).

RNA extraction, sequencing, and analysis

Starter cultures were grown for 18 h at 30˚C in PYE. Cultures were then diluted to OD_{660} 0.1 in PYE and outgrown for 2 h at 30˚C. Once again, cultures were diluted to OD_{660} 0.1 in their respective medium and grown another 3.25 h (OD_{660} < 0.4) at 37˚C to capture mRNA in logarithmic phase growth at the restrictive temperature. 6 ml of each culture were pelleted via centrifugation (1 min at 17,000 x g). Pellets were immediately resuspended in 1ml TRIzol and stored at -80˚C until RNA extraction. To extract RNA, thawed samples were incubated at 65˚C for 10 min. After addition of 200 µl of chloroform, samples were vortexed for 20 s and incubated at room temperature (RT) for 5 min. Phases were separated by centrifugation (10 min at 17,000 x g). The aqueous phase was transferred to a fresh tube and an equal volume of isopropanol was added to precipitate the nucleic acid. Samples were stored at 80˚C (1 h to overnight), then thawed and centrifuged at 17,000 x g for 30 min at 4˚C to pellet the nucleic acid. Pellets were washed with ice-cold 70% ethanol then centrifuged for at 17,000 x g for 5 min at 4˚C. After discarding the supernatant, pellets were air-dried at RT, resuspended in 100 µl RNAse-free water, and incubated

at 60˚C for 10 min. Samples were treated with TURBO DNAse (Invitrogen) following manufactures protocol for 30 min at RT and then column purified using RNeasy Mini Kit (Qiagen). RNA samples were sequenced at Microbial Genome Sequencing Center (Pittsburgh, PA). Briefly, sequencing libraries were prepared using Illumina's Stranded Total RNA Prep Ligation with Ribo-Zero Plus kit using custom *Caulobacter* specific rRNA depletion probes. 50 bp paired end reads were generated using the Illumina NextSeq 2000 platform (Illumina). RNA sequencing reads used to assess the impact of *ntrC* deletion on transcription have been published [266] and are available at the NCBI GEO database under series accession GSE234097. RNA sequencing reads used to measure the transcriptional impact of shifting *cckA*(ts) to the restrictive temperature and to assess the effect of suppressing *ntrC* mutations are available under NCBI GEO accession GSE285684. RNA sequencing reads were mapped to the *Caulobacter* NA1000 genome (Genbank accession CP001340) [14] using default mapping parameters in CLC Genomics Workbench 22 (Qiagen) and pairwise differential gene expression analysis was performed.

We identified sets of differentially expressed genes between the Δ*ntrC* and wild-type strains, as well as between the *cckA*(ts) mutant and wild-type, using stringent criteria: a maximum RPKM > 10, a fold-change (FC) threshold greater than |3|, and a false discovery rate p-value (FDRP) of less than 10^{-6}. Genes that were differentially regulated in either *cckA*(ts) or *ntrC* loss-of-function mutants were clustered using an uncentered correlation metric with average linkage [255], based on pairwise differential expression patterns relative to wild type. The resulting clusters were visualized using a heatmap. Notably, only a single gene overlapped between the two regulons, underscoring the distinct transcriptional responses triggered by these genetic perturbations.

To further investigate *cckA*(ts)-dysregulated genes that were more effectively restored by *ntrC* point mutations than by *ntrC* deletion, we compared pairwise differences in transcript abundance for each gene differentially expressed in the *cckA*(ts) mutant. Specifically, we evaluated:

(a) $\log_2$(*cckA*(ts)-*ntrC*(L424P)/*cckA*(ts)-Δ*ntrC*)

(b) $\log_2$(*cckA*(ts)-*ntrC*(A446P)/*cckA*(ts)-Δ*ntrC*)

For each gene, we calculated the average of these two comparisons to rank their relative restoration. The top 24 genes, which showed a natural break corresponding to approximately a fourfold higher expression in the presence of a *ntrC* point mutation compared to *ntrC* deletion, were selected for further analysis.

These genes were subsequently clustered based on pairwise expression differences and underwent modest manual reorganization to arrange adjacent genes with similar expression patterns, allowing for clearer visualization of potential regulatory relationships.

Principal Component Analysis of RNA-seq data

RNA-seq count data were imported from a CSV file. Normalization was performed using the counts-per-million (CPM) method to account for differences in sequencing depth across samples. The data were then log transformed ($\log_2$(CPM+1) to stabilize variance and the log-transformed data were standardized to have a mean of zero and unit variance using the `StandardScaler` function. Principal Component Analysis (PCA) was performed to reduce dimensionality and identify major sources of variation in the dataset. The analysis retained three principal components, capturing the most variance in the data. The PCA results were visualized as scatterplots for the first two principal components (PC1, PC2), which accounted for 80% of the variance. Analysis was conducted using Python, leveraging the `pandas`, `numpy`, `scikit-learn`, and `seaborn` libraries for data manipulation, PCA computation, and visualization.

Riboswitch assay

Overnight starter cultures were grown in PYE at 30˚C, diluted to OD_{660} 0.1 in PYE supplemented with 0.3% xylose to induce expression of the riboswitch biosensor, and then outgrown for 2 h at 30˚C. Cultures were diluted again to OD_{660} 0.025 in fresh PYE supplemented with 0.3% xylose and grown for 24 h at 30˚C at which point green fluorescence signal from the

ppGpp riboswitch fusion was measured in a Tecan Spark 20M plate reader. 200 µl of each culture was transferred to a black Costar flat, clear bottom, 96-well plate (Corning). Cell density was measured optically at 660 nm (OD_{660}) and mNeonGreen fluorescence was measured with the following wavelength parameters (excitation = 497 ± 10 nm; emission = 523 ± 10 nm). Fluorescence signal was then normalized by OD_{660}.

CtrA protein purification

Caulobacter ctrA was PCR-amplified and inserted into a pET23b-His6-SUMO expression vector using classical restriction digestion and ligation, such that *ctrA* was inserted 3' of the T7 promoter and the His6-SUMO coding sequence. After sequence confirmation, pET23b-His6-SUMO-*ctrA* was transformed into chemically competent *E. coli* BL21 Rosetta (DE3) / pLysS. This strain was grown in 1 L of LB at 37˚C. When the culture density reached approximately $OD_{600} \approx 0.5$, expression was induced with 0.5 mM isopropyl β-D-1-thiogalactopyranoside (IPTG) overnight at 16˚C. Cells were harvested by centrifugation (10,000 x g for 10 min) and resuspended in 20 ml lysis buffer [20 mM Tris pH 8, 125 mM NaCl, 10 mM imidazole] and stored at -80˚C until purification.

For protein purification, resuspended cell pellets were thawed at RT. 1 mM phenylmethylsulfonyl fluoride (PMSF) was added to inhibit protease activity and DNase I (5 µg/ml) was added to degrade DNA after cell lysis. Cells incubated on ice were lysed by sonication (Branson Instruments) at 20% magnitude for 20 sec on/off pulses until the suspension was clear. The lysate was cleared of cell debris by centrifugation (30,000 x g for 20 min) at 4˚C. The cleared lysate was applied to an affinity chromatography column containing Ni-nitrilotriacetic acid (NTA) superflow resin (Qiagen) pre-equilibrated in lysis buffer. Beads were washed with a high salt wash buffer [20 mM Tris pH 8, 500 mM NaCl, 30 mM imidazole]. Beads were then washed with a low salt wash buffer [20 mM Tris pH 8, 1 M NaCl, 30 mM imidazole]. Protein was eluted with elution buffer [20 mM Tris pH 8, 125 mM NaCl, 300 mM imidazole]. The elution fractions containing His6-SUMO-CtrA were pooled and dialyzed in 2 L dialysis buffer [20 mM Tris pH 8, 150 mM NaCl] for

4 h at 4˚C to dilute the imidazole. Purified ubiquitin-like-specific protease 1 (Ulp1) was added to the eluted His6-SUMO-CtrA containing solution which was then dialyzed overnight at 4˚C in 2 L fresh dialysis buffer to cleave the His6-SUMO tag. Digested protein was mixed with 3 ml of NTA superflow resin (Qiagen) that had been pre-equilibrated in wash buffer. After incubation for 30 min at 4˚C, the solution was placed onto a gravity drip column at 4˚C. Flowthrough containing cleaved CtrA was collected and used to generate α-CtrA polyclonal antibodies (Pacific Immunology).

Expression shut-off

For protein expression shut-off experiments, 25 ml overnight PYE cultures of *Caulobacter* strains were diluted into 100 ml of fresh PYE to OD_{660} 0.1 and outgrown for 2 h at the permissive temperature (30˚C). Cultures were then shifted to the restrictive temperature (37˚C) and grown for 3.25 h before the addition of rifampicin (10 μg/ml final *concentration*) to inhibit transcription and, consequentially, translation. After the addition of rifampicin, aliquots of 1 ml were taken at indicated timepoints (**Figure 3.6A**) and cells were pelleted via centrifugation. Supernatant was discarded and cell pellets were stored at -20˚C until Western blot analysis to monitor CtrA levels, described below.

Western blotting

To evaluate NtrC protein levels in **Figure 3.2C**, overnight PYE starter cultures of *Caulobacter* strains were diluted in fresh PYE to OD_{660} 0.1 and outgrown 2 h at 30˚C, diluted again to OD_{660} 0.1 in fresh PYE, and then grown for 24 h at the restrictive temperature (37˚C). A 1 ml aliquot of each culture was pelleted via centrifugation. After discarding the supernatant, cell pellets were stored at -20˚C until Western blot analysis.

For Western blot analysis, cell pellets were thawed and resuspended in 2X SDS loading buffer [100 mM Tris-Cl (pH 6.8), 200 mM dithiothreitol, 4% (w/v) SDS, 0.2% bromophenol blue, 20% (v/v) glycerol] to a concentration of 0.0072 OD_{660} culture / μl loading buffer. After resuspension, genomic DNA was digested by incubation with 1 μl Benzonase per 50 μl sample

volume for 20 min at RT. Samples then were denatured at 95˚C for 5 min. 10 µl of each sample was loaded onto a 7.5% mini-PROTEAN precast gel (Bio-Rad) (**Figure 3.2C**) or a 4-20% mini-PROTEAN precast gel (Bio-Rad) (**Figure 3.6A**) and resolved at 160-180 V at room temperature (RT). Separated proteins were transferred from the acrylamide gel to a PVDF membrane (Millipore) using a semi-dry transfer apparatus (BioRad) at 10 V for 30 min at RT [1X Tris-Glycine, 20% methanol]. Membranes were blocked in 10 ml Blotto [1X Tris-Glycine, 0.1% Tween 20 (TBST) + 5% (w/v) powdered milk] overnight at 4˚C. The membranes were then incubated in 10 ml Blotto + polyclonal rabbit α-NtrC antiserum (1:1,000 dilution) (**Figure 3.2C**) or polyclonal α-CtrA antiserum (1:1,000 dilution) (**Figure 3.6A**) 1-2 h at RT. Membranes were washed in TBST three times, 5 min per wash before incubation in 10 ml Blotto + goat α-rabbit poly-horseradish peroxidase secondary antibody (Invitrogen; 1:10,000 dilution) for 1-2 h at RT. The membrane was then washed three times with TBST and developed with ProSignal Pico ECL Spray (Prometheus Protein Biology Products). Immediately upon spraying, the membrane was imaged using BioRad ChemiDoc Imaging System (BioRad).

Figures

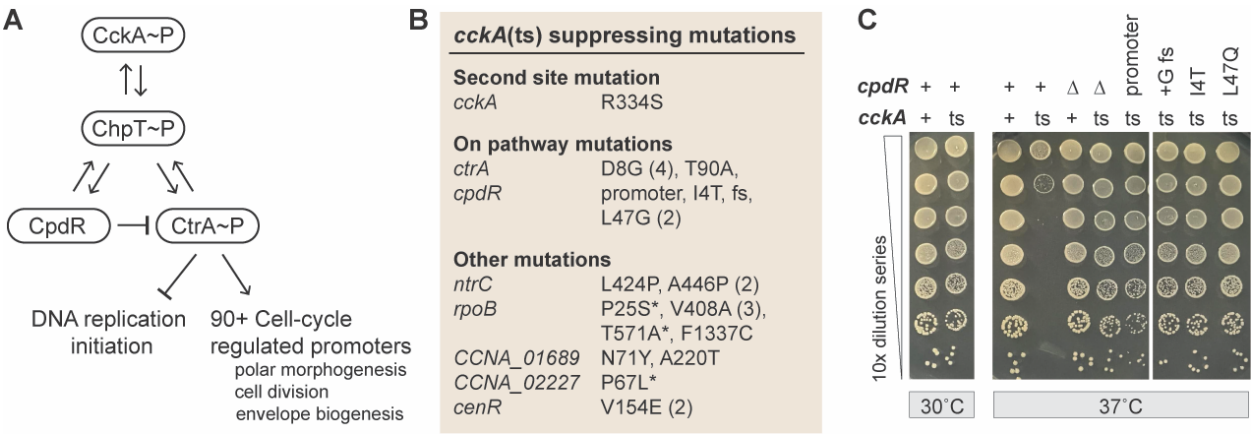

Figure 3.1. A selection for mutations that bypass the essential function of the cell cycle kinase, CckA, reveals multiple routes of suppression. (A) Model of the essential *Caulobacter* cell cycle regulatory phosphorelay. CckA is a bifunctional sensor histidine kinase that regulates CtrA, the master cell cycle and class I flagellar regulator, and its proteolytic adapter CpdR through phosphorylation or dephosphorylation via the histidine phosphotransferase ChpT. When CckA acts as a kinase, it phosphorylates CtrA, enabling it to bind DNA, block chromosome replication initiation, and activate cell cycle-regulated promoters. When CckA acts as a phosphatase, it dephosphorylates CpdR, which then facilitates CtrA degradation. CckA, ChpT, and CtrA are all essential for viability. Strains bearing a *cckA* temperature-sensitive (ts) allele, *cckA*(I484N, P485A), are unable to grow at 37˚C. (B) Spontaneous suppressing mutations identified in 26 *cckA*(ts) strains that grow at the restrictive temperature (37°C). Genes highlighted were mutated in more than one strain or contained the only polymorphic site in a strain. Various alleles for each gene are indicated on the left. Number of occurrences is indicated in parentheses for alleles identified more than once. * denotes cases where no other mutations were detected in the strain. fs = frame-shift. *CCNA_01689* encodes inosine-5'-monophosphate dehydrogenase; *CCNA_02227* encodes a LysR-family transcription factor. **Supplemental Table 5** details all mutations identified in each of the 26 strains. (C) Serial dilution of *Caulobacter* strains encoding wild-type (+) or mutant alleles of *cckA* and *cpdR* grown for four days at the permissive (30˚C) or restrictive (37˚C) temperature. Temperature-sensitive (ts) allele of *cckA*, in-frame deletion of *cpdR* (Δ), and *cpdR* mutants recovered in the *cckA*(ts) suppressor selection are indicated.

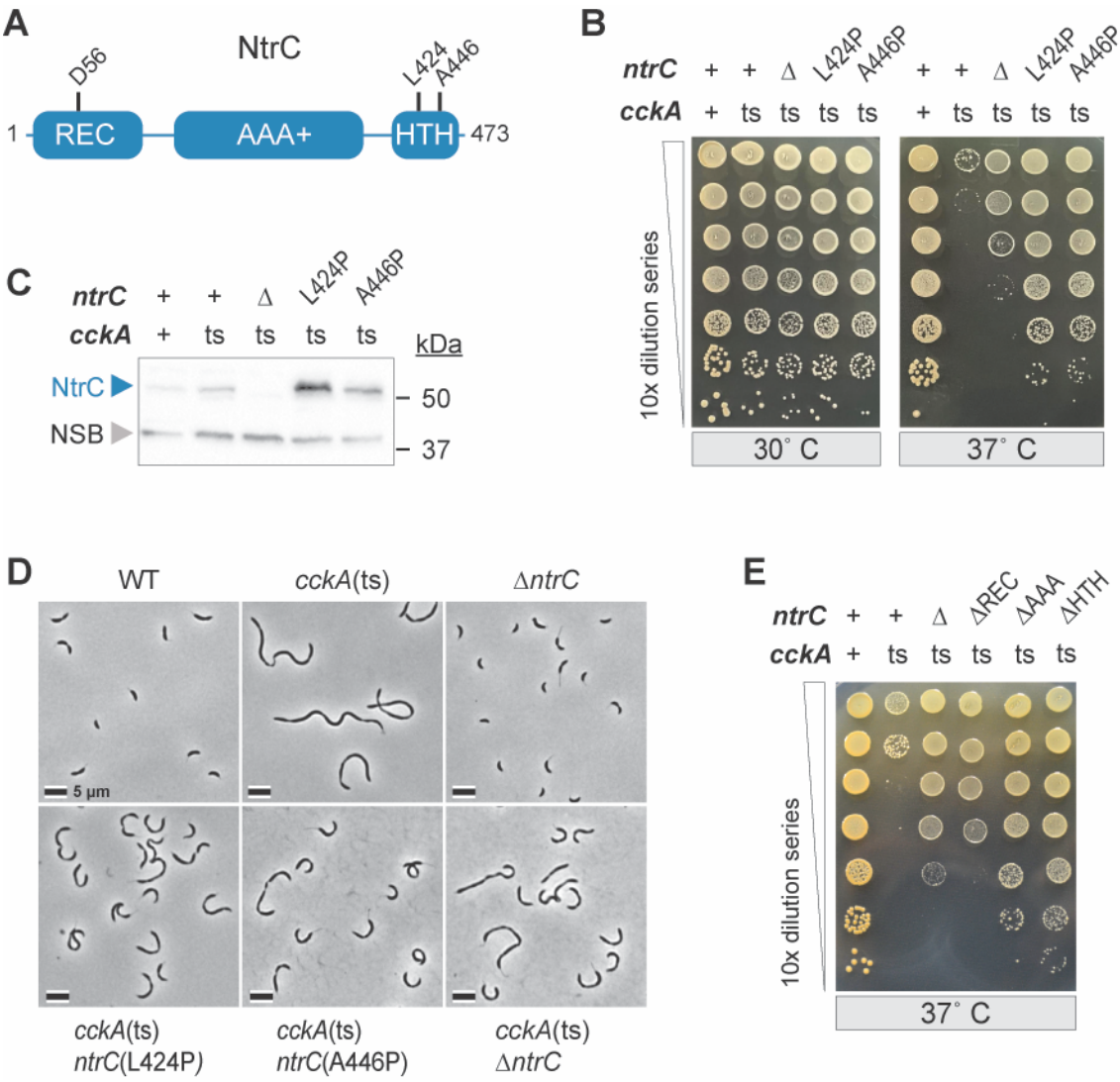

Figure 3.2. A tiered pattern of genetic suppression in *Caulobacter*, where loss of CckA function is variably rescued by structurally distinct *ntrC* loss-of-function mutations. (A) Model of *Caulobacter* NtrC protein showing the receiver (REC) domain and the site of aspartyl phosphorylation on residue D56, the AAA+ ATPase domain, and the DNA-binding/helix-turn-helix (HTH) domain. (B) Serial dilutions of *Caulobacter* strains encoding wild-type (+) or mutant alleles of *cckA* and *ntrC* grown at the indicated temperatures. Temperature-sensitive mutant of *cckA* (ts), in-frame deletion of *ntrC* (Δ), and *ntrC*(HTH) domain point mutants (L424P & A446P) are indicated. (C) Western blot of lysate from wild-type (+) or mutant strains of panel B using NtrC polyclonal antiserum. Non-specific band (NSB) is marked. (D) Phase contrast light micrographs of WT and mutant strains of *Caulobacter* grown at the restrictive temperature for 3.25 hours. Scale bar is 5 μm. (E) Serial dilutions of *Caulobacter* strains encoding wild-type (+) or mutant alleles of *cckA* (as above) and *ntrC* (in-frame deletion (Δ) or lacking individual HTH, AAA+ or REC domains). See **Figure S3.2** in Appendix 2 for paired control titers grown at the permissive temperature (30°C).

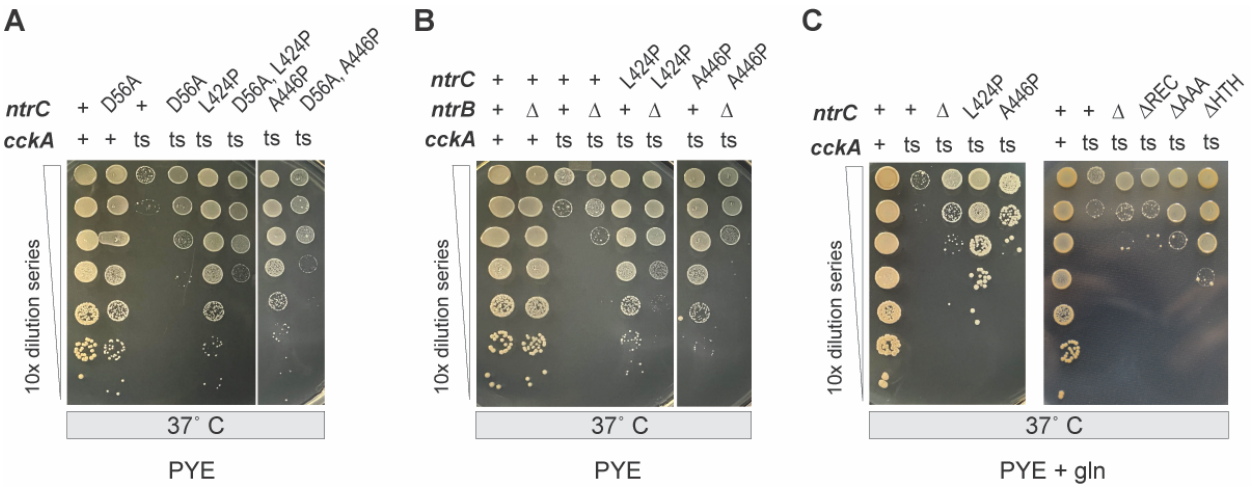

Figure 3.3. Phosphorylation of the NtrC receiver domain by NtrB is required for *cckA*(ts) growth rescue; glutamine supplementation ablates the growth rescue of *ntrC* mutations. Serial dilutions of *Caulobacter* strains encoding wild-type (+) or mutant alleles of *cckA*, *ntrC* and/or *ntrB* cultivated at the restrictive (37°C) temperature. (A) Temperature-sensitive (ts) *cckA* allele and *ntrC* point mutants (D56A, L424P, A446P; single and in combination) are marked. (B) Temperature sensitive (ts) *cckA* allele, in-frame deletion of *ntrB* (Δ), and *ntrC* point mutants (L424P & A446P) are marked. (C) Temperature-sensitive mutant of *cckA* (ts), in-frame deletion of *ntrC* (Δ), *ntrC* point mutants (L424P & A446P), and *ntrC* mutants lacking an HTH, AAA+ or REC domains (as indicated) were titered on agar supplemented with 9.3 mM glutamine (gln). See **Figure S3.2** in Appendix 2 for paired control titers grown at the permissive temperature (30°C).

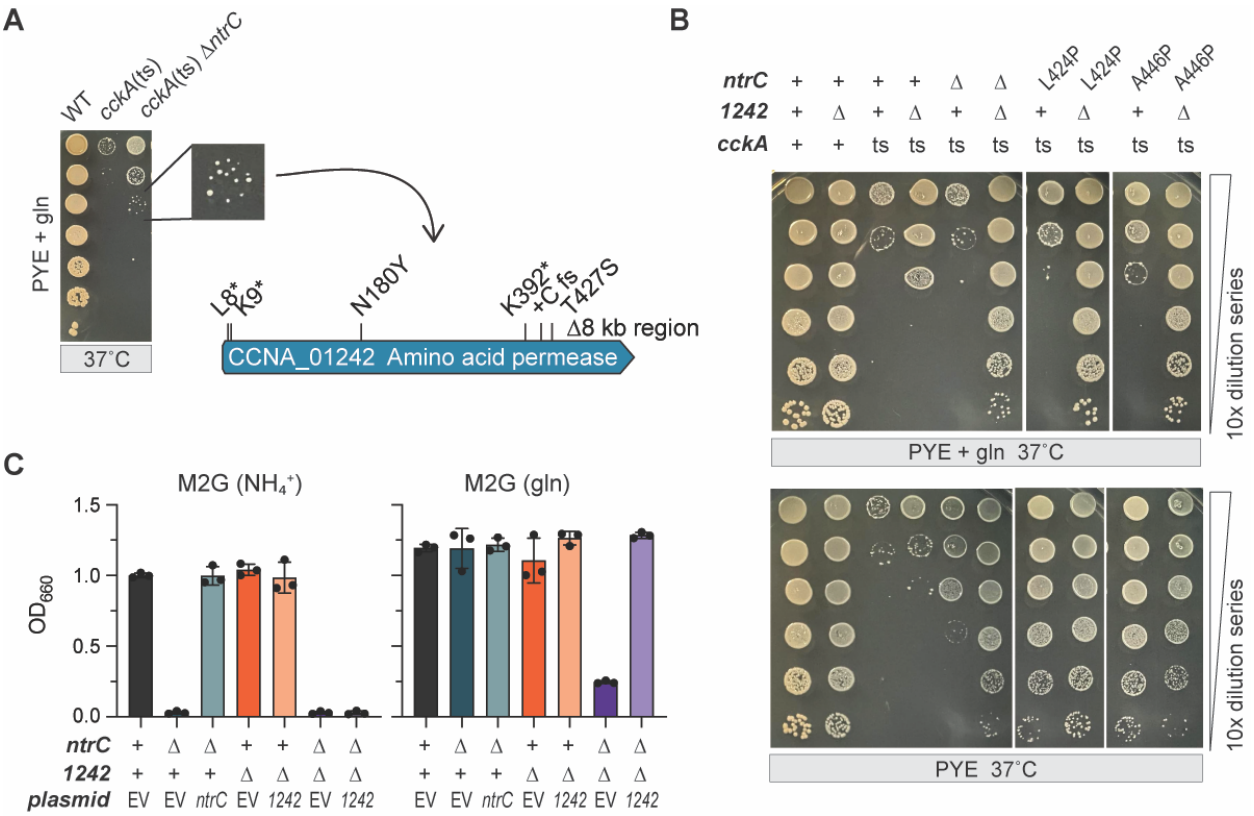

Figure 3.4. A role for the amino acid permease, CCNA_01242, in glutamine transport and its impact on *ntrC*-mediated suppression of *cckA*(ts) temperature sensitivity. (A) Glutamine supplementation abrogates *ntrC*-mediated suppression of *cckA*(ts) temperature sensitivity. The colony inset illustrates the selection approach used to isolate "glutamine-blind" mutants, in which *ntrC*-mediated suppression of *cckA*(ts) was restored despite the presence of glutamine. Whole-genome sequencing of ten such mutants identified deletion, frameshift, nonsense and point mutations in locus *CCNA_01242*, a gene encoding an annotated amino acid permease. (B) Serial dilutions of *Caulobacter* strains encoding wild-type (+) or mutant alleles of *cckA*, *ntrC,* and *CCNA_01242*. Temperature-sensitive mutant of *cckA* (ts), in-frame deletion of CCNA_01242 or *ntrC* (Δ), and *ntrC* point mutants (L424P & A446P) are marked. Strains were cultivated at the restrictive temperature (37°C) in the presence and absence of 9.3 mM glutamine (gln). See **Figure S3.2** in Appendix 2 for paired control titers grown at the permissive temperature (30°C). (C) Culture density of *ntrC* and CCNA_01242 deletion mutants (Δ) after 24 hours of growth in defined M2-glucose (M2G) medium with either ammonium (NH_4^+) or glutamine (gln) as the sole nitrogen source. Genetic complementation of *ntrC* or *CCNA_01242* from a plasmid is indicated. EV = empty vector control plasmid.

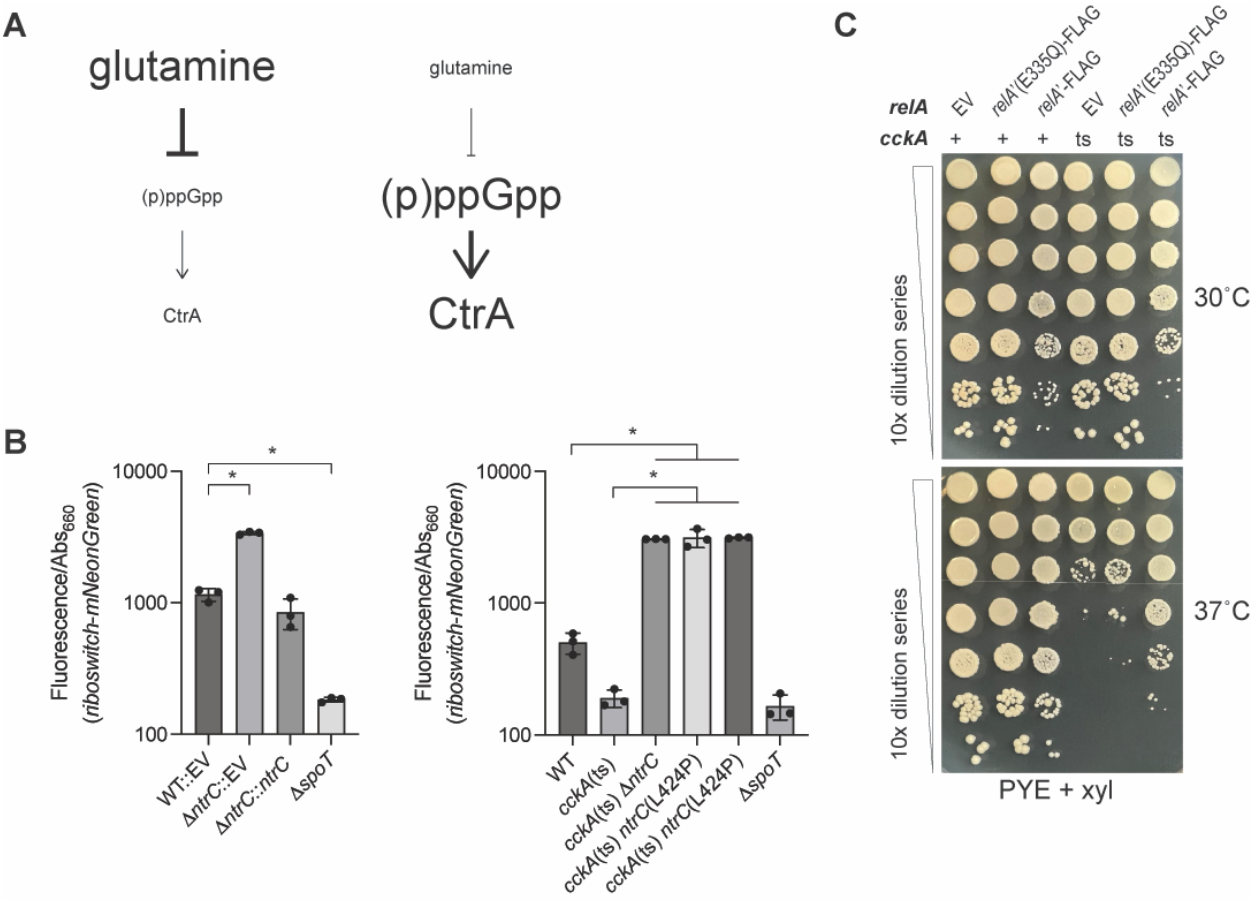

Figure 3.5. Elevated ppGpp levels in *ntrC* mutants stabilize CtrA protein and contribute to bypass of CckA function. (A) Model of the established inverse relationships between intracellular glutamine levels and (p)ppGpp accumulation [128], and (p)ppGpp levels and the rate of CtrA degradation [146]. (B) ppGpp levels were measured using the *D. hafniense ilvE* ppGpp-sensing riboswitch [273] fused to *mNeonGreen* where higher ppGpp leads to increased transcriptional readthrough of *mNeonGreen*. Left: WT and Δ*ntrC* strains carrying an empty vector (EV), the genetically-complemented Δ*ntrC*::*ntrC* strain, and a strain lacking the sole (p)ppGpp synthetase in *Caulobacter* (Δ*spoT)*. Right: WT, *cckA*(ts), *cckA*(ts) harboring mutations in *ntrC*, and the Δ*spoT* negative control strain. Data represent mean ± standard deviation of three replicates. Statistical significance was determined by one-way ANOVA followed by Tukey's multiple comparisons test (* $P \leq 0.0001$). Significant comparisons to WT or *cckA*(ts) strains are shown. (C) Serial dilutions of *Caulobacter* strains harboring wild-type (+) or mutant (ts) *cckA*, and expressing a truncated, constitutively active synthetase version of *E. coli relA* (*relA'*-FLAG), a catalytically inactive mutant (*relA'*(E335Q)-FLAG), or empty vector (EV) grown at the permissive (30°C) and restrictive (37°C) temperatures. Agar was supplemented with 0.3% xylose (xyl) to induce *relA* expression.

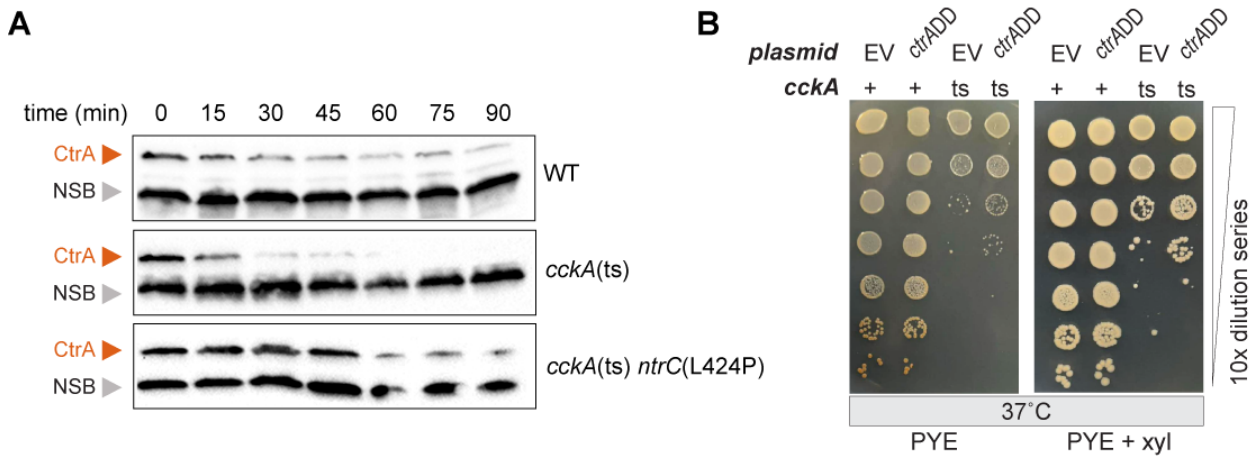

Figure 3.6. Stabilization of CtrA as route to suppress temperature sensitivity of *cckA*(ts). (A) CtrA stability in WT, *cckA*(ts) and *cckA*(ts) *ntrC*(L424P) monitored by immunoblot after addition of rifampin (time 0) to shut off CtrA expression. Cells were shifted to the restrictive temperature (37°C) for 3.25 hours before rifampin treatment. NSB = non-specific band that reacts with polyclonal serum. (B) Serial dilution of *Caulobacter* strains encoding wild-type (+) or mutant (ts) alleles of *cckA* that harbor either empty vector (EV) or the *ctr*ADD [93, 278] overexpression construct. Dilution series were spotted onto PYE and PYE supplemented with inducer (0.3% final concentration xylose (xyl)) and grown at the restrictive temperature (37°C).

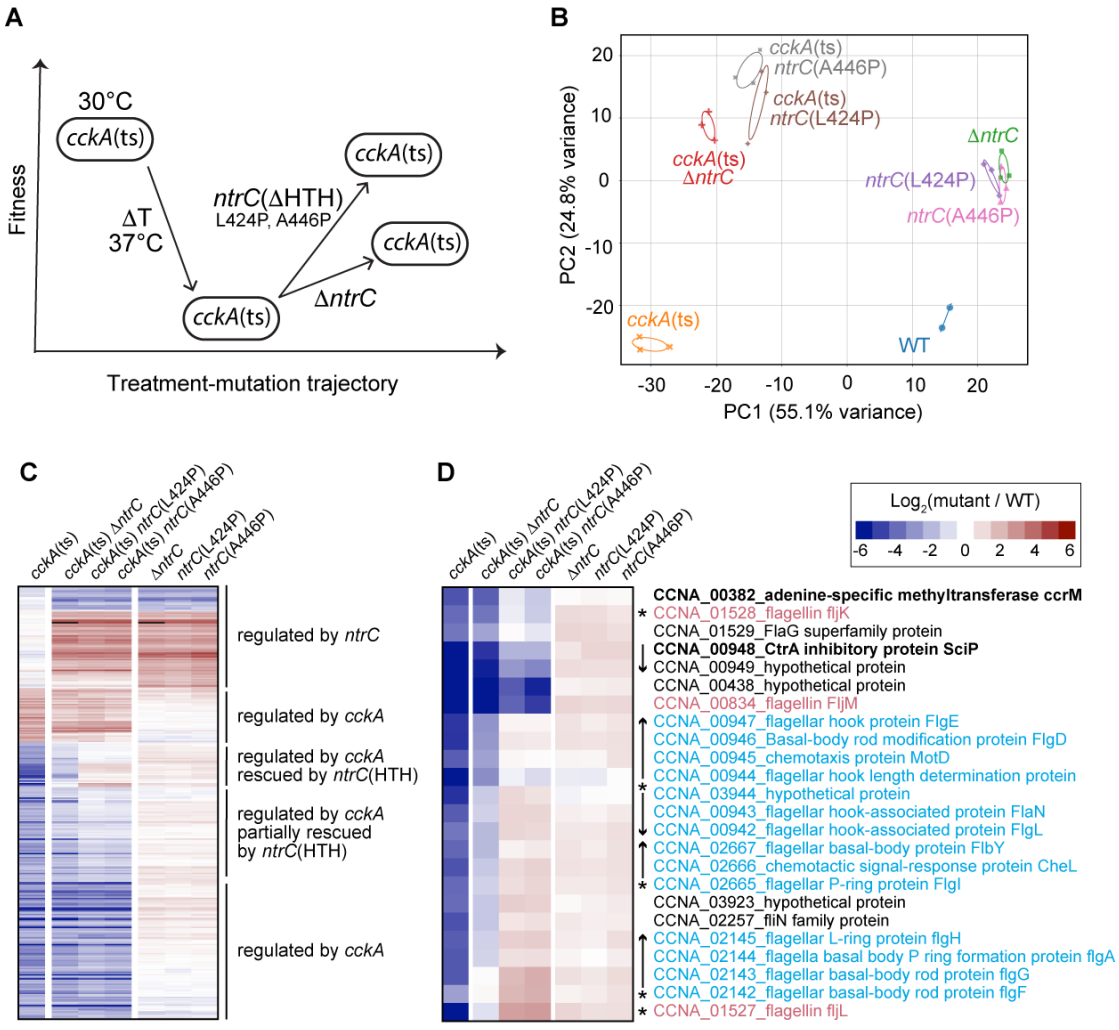

Figure 3.7. Transcriptomic analysis of a synthetic rescue interaction between *ntrC* and the essential sensor kinase *cckA*. (A) Schema of the relationship between *ntrC* loss-of-function mutations and fitness of a *Caulobacter* strain harboring lethal temperature-sensitive mutations in the essential kinase gene, *cckA*. Deletion of *ntrC* (Δ*ntrC*) and point mutations (L424P & A446P) in the NtrC helix-turn-helix (HTH) domain have distinct *cckA*(ts) rescue phenotypes. (B) Principal component analysis (PCA) of transcriptomic datasets of strains harboring *ntrC* mutations (Δ*ntrC*, L424P & A446P) in either a WT or a *cckA*(ts) mutant background. The first two principal axes (PC1 and PC2) are shown. (C) Hierarchically-clustered heatmap displays the 324 genes differentially expressed in either the *cckA*(ts) or Δ*ntrC* backgrounds (see **Supplemental Table 7** for genes in this cluster), highlighting transcriptional differences between *cckA*(ts) and the *cckA*(ts) *ntrC* mutant (i.e., rescued) strains. Genes included in the heatmap met the criteria of |Fold Change| >3 and an FDR-adjusted p-value < 10^{-6} in either *cckA*(ts) or Δ*ntrC* compared to WT. (D) Heatmap highlighting genes with the largest transcriptional differences between *cckA*(ts) strains harboring the *ntrC*(HTH) point mutations (L424P and A446P) and the *cckA*(ts) strain with a Δ*ntrC* deletion. Class III flagellar genes are marked in cyan, and Class IV flagellar genes are marked in salmon. Genes were hierarchically-clustered and then manually arranged to reflect operon arrangements. Arrows indicate operon structures, and asterisks denote genes with FlbD binding sites in their promoter as identified by Fumeaux et al [227]. Heatmap colors represent the $\log_2$(mutant / WT) expression for the mutant strain indicated above the heatmap.

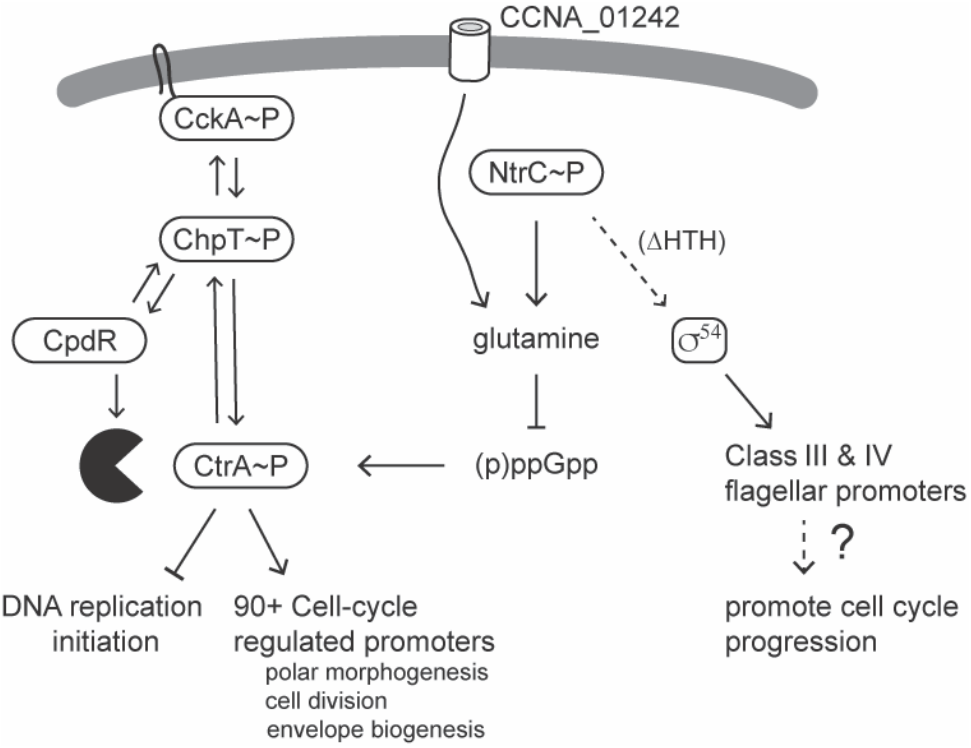

Figure 3.8. Model depicting the mechanism by which *ntrC* mutations bypass the essential function of the sensor kinase CckA. Under normal growth conditions, phosphorylated CtrA (CtrA~P) binds DNA to regulate transcription of cell cycle and cellular development genes. CckA is a membrane-bound, bifunctional sensor histidine kinase that phosphorylates or dephosphorylates CtrA through the histidine phosphotransferase ChpT. CpdR, a proteolytic adaptor, is also phosphorylated and dephosphorylated through ChpT and targets CtrA for degradation. Loss-of-function mutations in *ntrC* lead to reduced intracellular glutamine, which enters the cell through the CCNA_01242 inner membrane permease. Reduced glutamine results in increased cellular ppGpp levels, which stabilizes CtrA by inhibiting its proteolysis (black pacman). Additionally, *ntrC* mutations that disrupt its binding to DNA (ΔHTH) activate transcription at non-native σ^{54}-dependent promoters, contributing to rescue of *cckA*(ts) cell cycle and strain growth at the restrictive temperature. This mechanism reveals a genetic bypass of CckA function through protein stabilization and transcriptional reprogramming.

Chapter 4: Discussion & Future Directions

Preface

The content of this session was modified and adapted from its published forms: 1) North H, McLaughlin M, Fiebig A, Crosson, S. (2023) *J Bacteriol.* 205(10):e0018123 and 2) North H, Hydorn M, Dworkin J, Fiebig A, Crosson, S. *mBio* (2025, in revision).

Discussion

ntrB-ntrC differentially impacts growth in defined and complex medium

Environmental nitrogen is an important cell cycle and developmental regulatory cue in *Caulobacter* [128], which motivated us to explore the function of the NtrB-NtrC two-component system (TCS), a broadly conserved regulator of nitrogen metabolism [153]. We characterized the population-level growth phenotypes of *ntrB* and *ntrC* mutants under media conditions containing distinct nitrogen sources and demonstrated that the sensor histidine kinase (SHK) gene, *ntrB,* and the AAA+-type response regulator (RR) gene, *ntrC,* are essential for growth in a defined medium in which NH_4^+ is the sole nitrogen source (**Figure 2.1**; **Figure 2.2**). Strains expressing a *ntrC* allele harboring a mutated aspartyl phosphorylation site in its receiver domain (*ntrC*(D56A)) also failed to grow in this defined medium (**Figure 2.2G**). These data support an expected model in which phosphorylation of NtrC by NtrB is necessary for NH_4^+ assimilation. An additional SHK/RR pair, *ntrY-ntrX*, is part of the *ntrBC* genetic locus in *Caulobacter* and is postulated to have arisen from gene duplication [234]. The inability of Δ*ntrB* to grow in M2G indicates that NtrB (and not NtrY) is the major SHK for NtrC *in vivo.* Each of the three NtrC domains – 1) Receiver, 2) AAA+ ATPase, and 3) DNA-binding/HTH domain – are required for growth in NH_4^+-defined medium (M2G) (**Figure 2.2G**). Replacement of NH_4^+ with glutamine in M2G fully rescued growth of *ntrC*(ΔHTH) but not *ntrC*(ΔREC) and *ntrC*(ΔAAA) mutants (**Figure 2.2H**). This suggests that some component of the growth defect of *ntrC*(ΔREC) and *ntrC*(ΔAAA) in defined medium is independent of cellular nitrogen status. Considering the overlap of NtrC binding sites with GapR and MucR1, variants of NtrC without the AAA+ or REC domains might exhibit dominant-negative

effects. These truncated alleles could interfere with interactions involving GapR and MucR1, thereby disrupting gene expression at multiple chromosomal loci.

A strain lacking *ntrC* is viable in PYE complex medium but has a reduced growth rate, a phenotype that is complemented by addition of glutamine (**Figure 2.2A-B**) [128]. Surprisingly, Δ*ntrB* and *ntrC*(D56A) had no growth rate defect, but did exhibit a growth yield defect in PYE (i.e., final culture density) (**Figure 2.2C**) that was rescued by the addition of glutamine to the medium (**Figure 2.2D**). From these results, we conclude that NtrC~P is less important in complex medium during log phase growth and becomes more important at higher cell density when organic nitrogen becomes more limited, and waste products accumulate. NtrC domain truncation mutants, *ntrC*(ΔREC), *ntrC*(ΔAAA), and *ntrC*(ΔHTH), grew slower in PYE (**Figure 2.2E**), though the *ntrC*(ΔREC) and *ntrC*(ΔAAA) strains had more severe defects than *ntrC*(ΔHTH), which phenocopied Δ*ntrC*. As discussed above, the *ntrC*(ΔREC) and *ntrC*(ΔAAA) yield phenotypes in PYE may be due to dominant-negative effects of expressing these truncated NtrC polypeptides *in vivo,* though glutamine supplementation to PYE did complement the defects of all NtrC domain truncation mutants in PYE (**Figure 2.2F**).

IS3 transposition repeatedly rescued the growth defect of ntrC mutants

The role of NtrC in activating glutamine synthetase (*glnA*) expression and facilitating NH_4^+ assimilation is well-established in various species [153]. We demonstrated that *Caulobacter ntrC* is essential in NH_4^+-defined medium (M2G) and made the surprising observation that cultures of *Caulobacter* Δ*ntrC* occasionally showed robust growth in M2G; this suggested there was a route for spontaneous genetic rescue of the Δ*ntrC* growth defect. We discovered that these “jackpot”-like cultures [289] were a consequence of random insertion of an IS3-family mobile genetic element at the *glnBA* promoter (P_{glnBA}) of Δ*ntrC* that restored *glnBA* transcription (**Figure 2.3**). IS3 elements are present in multiple copies in the *Caulobacter* NA1000 genome [14], and the IS3-dependent transcriptional rescue phenotype we observe is consistent with a report that IS3

insertion elements can function as mobile promoters [290]. We also identified two independent IS3-family (IS511/ISCc3) insertions upstream of *glnBA* at nucleotide 2192500 (16 bp upstream of the *glnB* start codon) and nucleotide 2192465 (51 bp upstream of the *glnB* start codon) that rescued growth of *ntrC*(ΔHTH) mutants in M2G defined medium (**Supplemental Table 1**), indicating that this is a facile evolutionary route to rescue loss of *ntrC* function under particular conditions.

Caulobacter insertion elements were previously shown to be transcriptionally activated in mutants that accumulate the alarmone (p)ppGpp [118], and Ronneau et al [128] have reported that glutamine limitation results in (p)ppGpp accumulation via activation of the PTS^{Ntr} system in *Caulobacter*. Furthermore, (p)ppGpp accumulates in *Caulobacter* starved for NH_4^+ in defined medium [118]. This work in Chapter 1 of my thesis led us to postulate that in the absence of *ntrC,* decreased levels of intracellular glutamine result in (p)ppGpp accumulation and IS3 activation. Indeed, work in Chapter 2, discussed later, confirms increased ppGpp levels in *ntrC* loss-of-function mutants, which supports the hypothesis that increased (p)ppGpp in *ntrC* mutants results in IS3 activation. It should also be noted that a NtrC binding peak within an IS3-family element (adjacent to *CCNA_02830*), which could contribute to IS3 regulation (**Supplemental Table 3**).

The NtrC regulon in Caulobacter: More than just nitrogen metabolism

NtrC binds to multiple sites on the *Caulobacter* chromosome, playing a role in both activating and repressing gene expression. As expected, NtrC directly activates transcription of nitrogen assimilation genes such as *glnBA*, *glnK*, and the putative NH_4^+ transporter *CCNA_01399*. Conversely, NtrC represses its own operon demonstrating autoregulation, which is well-established for this class of regulators [291]. Our study also identified genes not directly involved in nitrogen assimilation in the NtrC regulon. Nine of the 51 NtrC binding sites are located within a mobile genetic element responsible for biosynthesis of a capsular polysaccharide that is differentially regulated across the cell cycle and confers resistance to a caulophage [17]. The impact of *ntrC* on envelope polysaccharide is discussed below.

Thirty-seven of 51 NtrC binding sites (>70%) directly overlap with one of the 599 reported GapR binding sites [226] across the *Caulobacter* genome (**Figure 2.5B**; **Supplemental Table 3**). GapR is a nucleoid-associated protein that binds positively supercoiled DNA and supports DNA replication [225], suggesting a possible connection between NtrC and chromosome organization/maintenance in *Caulobacter*. In addition, we observed significant overlap in binding sites of NtrC and the cell cycle regulator, MucR1 [227]. Beyond *mucR1*, NtrC directly bound upstream and modulated transcription of other genes that impact cell cycle processes, including *sciP*, *hdaA*, and *socB* [70, 71, 238, 239]. NtrC appears to repress transcription of *sciP* and *mucR1*, which have been implicated in controlling the cell cycle transition from S-to-G1 upon compartmentalization of the nascent swarmer cell and also represses transcription of *socB*, a DNA replication inhibitor toxin. The exact mechanism of repression at these promoters remains undefined. These findings suggest that NtrC directly impacts regulation of the cell cycle in *Caulobacter*.

NtrC also regulates the *cdzCDI* operon that encodes a bacteriocin cell killing system activated in stationary phase [240]. Loss of *ntrC* results in increased expression of the Cdz system; this transcriptional phenotype is not fully complemented by glutamine supplementation to the medium (**Figure 2.4B**; **Supplemental Table 2**). Thus, repression of this locus by NtrC is not solely determined by nitrogen availability.

ntrC is a stalk elongation factor

Caulobacter cell division results in the production of a swarmer cell and a stalked cell. The swarmer cell differentiates into a reproductive stalked cell by shedding its polar flagellum, producing an adhesive holdfast at the same cell pole, and forming and a stalk that extends from that pole. Stalk length is regulated, and phosphate limitation was previously believed to be the only factor that determined *Caulobacter* stalk length [244]. However, recent studies have demonstrated that metabolic imbalances in sugar-phosphate metabolism influence stalk elongation [245].

We have demonstrated that stalk elongation is genetically linked to the *ntrB-ntrC* TCS. The deletion of *ntrC*, *ntrB*, or replacement of wild-type *ntrC* with a non-phosphorylatable allele (D56A) resulted in hyper-elongated stalks in PYE (**Figure 2.6B**). Supplementation of PYE with glutamine or ectopic *glnBA* expression restored stalk lengths of *ntrB* and *ntrC* mutants to WT. We conclude that the stalk lengthening phenotype of *ntrB* and *ntrC* mutants is a consequence of decreased intracellular glutamine and that stalk elongation is linked to loss of *ntrB-ntrC* and possibly nitrogen limitation. Notably, limiting NH_4^+ in defined growth medium does not result in increased stalk length in *Caulobacter* [149, 292]. Furthermore, excess NH_4^+ in combination with high pH restricts stalk elongation even when phosphorus is limited [95]. These findings indicate that, while a connection between nitrogen availability and stalk length exists, not all nitrogen limitation conditions impact stalk development. Links between nitrogen availability, phosphorus availability, starvation signals such as (p)ppGpp [245], and stalk length are clearly complex and require further research.

Stalk elongation was previously postulated to enhance diffusive surface area, allowing for increased uptake of nutrients [293, 294], but subsequent work indicated that this is unlikely due to diffusion barriers within the stalk [292, 295]. A recent model is that stalk lengthening allows *Caulobacter* in surface-attached communities to reach beyond its neighbors to better access available nutrients, thereby outcompeting other attached microbes and assisting in releasing progeny into the environment [95, 295]. We predict that when nitrogen becomes limiting in surface-attached communities, the NtrB-NtrC TCS can cue the cell, perhaps through intracellular glutamine, to lengthen its stalk to better access nitrogen or other nutrients.

NtrC strongly represses transcription of *CCNA_02727*, a gene encoding a PhoH-family protein, and overexpression of *CCNA_02727* in WT cells results in increased stalk length (**Figure 2.7**). However, deletion of *CCNA_02727* in a Δ*ntrC* background did not affect the stalk length of Δ*ntrC*. PhoH-family proteins typically possess ATPase and ribonuclease activity [241, 242, 247] and are often activated by the Pho regulon under phosphate starvation conditions in bacteria [246,

247]. *CCNA_02727* is not regulated by the Pho regulon in *Caulobacter* [296] but is strongly upregulated under other environmental conditions, such as carbon limitation [297] and heavy metal stress [297] in addition to glutamine deprivation via loss of *ntrC* as described here (**Figure 2.7A**). Crosstalk between different sensing systems to balance nutrient levels is well described in bacteria [298] and, therefore, it is possible that regulation of *CCNA_02727* has a general role in controlling nutrient balance or stress response in *Caulobacter*.

ntrC regulates envelope polysaccharide production

Caulobacter Δ*ntrC* displays a hyper-capsulation phenotype (**Figure 2.8**). NtrC orthologs are reported to regulate biofilm formation and EPS production in other bacteria, including *P. aeruginosa*, *V. vulnificus*, and *B. cenocepacia*, where loss of the *ntrB-ntrC* TCS decreases biofilm and EPS production [299-301]. In *V. cholerae*, loss of *ntrC* increases biofilm formation and increases expression of EPS gene regulators [229].

Transcriptomic and ChIP-seq data presented in this study identified a NtrC peak in the promoter of *hvyA*, a gene encoding a transglutaminase homolog that prevents capsulation of swarmer cells [17]. Although deletion of *hvyA* increases *Caulobacter* capsulation, its transcription is increased in Δ*ntrC* by 3-fold. The link between *hvyA* expression and the Δ*ntrC* capsule/mucoid phenotype, if any, remains undefined. We further observed a NtrC peak in the promoter region of the operon containing *CCNA_00471* (*fcl*), encoding a GDP-L-fucose synthase, and *CCNA_00472*, encoding a GDP-mannose 4,6 dehydratase (**Supplemental Table 3**), which reside in the MGE of the *Caulobacter* NA1000 genome. The transcription of these two genes increased 2-fold and 3-fold in Δ*ntrC* relative to WT, respectively. These enzymes function in the two-step synthesis of fucose, which is one of the sugars comprising the tetrasaccharide capsule of *Caulobacter*. It is reported that loss of these genes leads to a significant reduction in EPS production [302]. The upregulation of *CCNA_00471-00472* in Δ*ntrC* may contribute to an increase in EPS production and, consequently, the hyper-mucoid and buoyancy phenotypes of Δ*ntrC*. This is supported by the observation that *Caulobacter* Δ*ntrC* strains lacking the MGE (i.e., NA1000

ΔMGE Δ*ntrC* and CB15 Δ*ntrC*) are not mucoid (See **Figure S2.7** in Appendix 1). However, EPS production is a complex process that involves multiple pathways, and other genetic and physiological factors could also contribute to the envelope polysaccharide phenotype of Δ*ntrC*. Indeed, EPS production is apparently linked to changes in intracellular glutamine levels independent of NtrC, given that adding glutamine to the medium represses EPS gene expression in Δ*ntrC* (**Supplemental Table 2**). The effect of glutamine on EPS gene transcription is congruent with our observation that either addition of glutamine to PYE or the ectopic expression of *glnBA* complements the mucoid phenotype of Δ*ntrC* (**Figure 2.8**).

An unconventional NtrC

Caulobacter NtrC lacks a GAFTGA motif within its primary structure (See **Figure S2.1** in Appendix 1), which is necessary for interaction with σ^{54} [233]. Consistent with previous reports of NtrC orthologs lacking a GAFTGA motif [213, 303], our data indicate that NtrC regulates σ^{70}-dependent promoters. For example, NtrC-repressed genes such as *hvyA* and *sciP* are activated by CtrA, a σ^{70}-dependent transcriptional regulator [17, 70, 71]. The NtrC binding peak summits within P_{hvyA} and P_{sciP} reside 4 bp and 55 bp from the CtrA peak summit at these promoters, respectively (**Supplemental Table 3**), indicating that NtrC may directly compete with CtrA at these sites to repress transcription. We also identified NtrC-activated genes that possess σ^{70} promoters such as *hdaA*, which is also activated by DnaA [238], a σ^{70}-dependent regulator [40, 81]. The mechanism by which *Caulobacter* NtrC functions at σ^{70} promoters remains unclear.

Mutation of the conserved NtrC aspartyl phosphorylation site (D56) results in reduced transcriptional activation of the *glnBA* locus (See **Figure S2.4** in Appendix 1), highlighting the important role of this residue in NtrC-mediated transcriptional activation (at *glnBA*). Similarly, in *R. capsulatus* NtrC, which also lacks GAFTGA, aspartyl phosphorylation is required for transcriptional activation [213, 303]. *V. cholerae* VspR, a bEBP that lacks GAFTGA and regulates σ^{70} promoters, does not require phosphorylation but utilizes the conserved aspartyl

phosphorylation site for phosphate sensing [304]. Whether D56 phosphorylation differentially affects NtrC function at binding sites across the *Caulobacter* chromosome is not known. In *R. capsulatus* NtrC, ATP binding rather than hydrolysis by the AAA+ domain is essential for transcriptional activity [213], while VspR does not require ATP to function [214]. We have shown that conserved residues of the Walker A and Walker B motifs in the *Caulobacter* NtrC AAA+ domain are required for NH_4^+ utilization in defined medium (See **Figure S2.3** in Appendix 1), providing evidence that ATP binding and ATP hydrolysis by NtrC are necessary for controlling the gene expression program that underlies NH_4^+ assimilation. More generally, we predict that ATP binding and hydrolysis by *Caulobacter* NtrC contribute to the regulation of σ^{70}-dependent promoters, distinguishing it from other unconventional σ^{70}-regulating bEBPs. The *Caulobacter* genome [14] encodes four bEBPs: NtrC, NtrX, FlbD, and TacA. Unlike NtrC and NtrX, FlbD and TacA possess the GAFTGA motif. Notably, TacA regulates stalk biogenesis by controlling expression of σ^{54}-dependent genes, including *staR* [305]. Our study establishes a genetic link between the *ntrB-ntrC* TCS and the *Caulobacter* stalk. Thus, development of the polar stalk structure is controlled by at least two distinct bEBPs, NtrC and TacA, which are regulated by different environmental stimuli and have distinct primary structural and regulatory properties.

The CckA-ChpT-CtrA: The conserved "essential" phosphorelay

Francois Jacob famously remarked that the "dream" of a cell is to become two cells [306]. To fulfill this dream, bacteria invest significant resources in precisely coordinating DNA replication, chromosome segregation, and cell division. In *Caulobacter*, decades of research have uncovered a highly regulated network controlling cell cycle progression [16, 307, 308]. Most studies have examined these processes under nutrient-replete conditions, where oscillations of key regulators follow a predictable pattern. However, increasing evidence indicates that *Caulobacter* cell cycle control is highly sensitive to environmental and physiological cues, including nutrient availability, redox balance, and stress responses [128, 146, 309-312]. This raises a fundamental question: to what extent do essential cell cycle regulators respond to physiological signals, and under what

conditions might their function become dispensable?

A striking example of environmental control over the cell cycle is the TCS phosphorelay that governs *Caulobacter* cell cycle progression. Forward genetic screens in the 1990s [58, 280] identified *cckA* and *ctrA*, a SHK and RR, respectively, as essential regulators of the cell cycle. At the time, this finding was unexpected, as TCS proteins were generally considered environmental regulators that were not required under standard laboratory conditions. The discovery that CckA functions as a bifunctional kinase and phosphatase, serving as a master regulator of the *Caulobacter* cell cycle [58] revealed the integration of environmental sensing with cell cycle control in a bacterium.

Identifying genetic routes to bypass CckA function

Motivated by this paradigm, we designed a forward selection strategy to identify genetic routes that bypass the essentiality of *cckA*, reasoning that such mutations might reveal alternative regulatory pathways influencing cell cycle control. We selected for mutations that suppress the temperature-sensitive (ts) lethal phenotype of a *cckA*(ts) mutant and identified multiple classes of suppressors. These included mutations in the *cckA*-*chpT*-*ctrA* phosphorelay, the β subunit of RNAP (*rpoB*), a nucleotide biosynthesis gene (*CCNA_01689*), and—unexpectedly—the nitrogen assimilation regulatory gene *ntrC* (**Figure 1**; **Supplemental Table 5**).

Genetic suppression occurs when the defects caused by a mutation in one gene are mitigated by a second mutation, restoring viability or normal function. Our identification of *ntrC* mutations as *cckA*(ts) suppressors was particularly intriguing, as *ntrC* encodes a bacterial bEBP best known for its conserved role in nitrogen assimilation in bacteria [228]. We previously established *Caulobacter* NtrC as essential for intracellular glutamine synthesis via transcriptional activation of *glnBA* [266]. However, our results support a previously unrecognized connection between NtrC and control of the core cell cycle circuitry and add to the growing understanding of the connection between nitrogen metabolism and cell cycle control [127, 128, 310, 313, 314].

Elevated ppGpp as a mechanism for bypassing CckA

A major consequence of *ntrC* loss-of-function is elevated intracellular ppGpp levels, resulting from impaired glutamine biosynthesis (**Figure 3.5**). Glutamine is a known inhibitor of (p)ppGpp synthesis [128], and our results show that *ntrC* mutants exhibit increased ppGpp levels, as measured using a riboswitch-based reporter (**Figure 3.5B**). Consistent with previous studies [146], we present evidence that CtrA levels are increased in strains with elevated ppGpp, effectively bypassing the requirement for CckA kinase activity. Supporting this model, artificial induction of (p)ppGpp synthesis via expression of a truncated *relA'*-FLAG construct, encoding a constitutively active (p)ppGpp synthetase [146], significantly improved growth of *cckA*(ts) at the restrictive temperature (**Figure 3.5C**). Together, these results, along with our measurements of CtrA levels in WT, *cckA*(ts), and the *cckA*(ts) *ntrC*(L424P) suppressor strain (**Figure 3.6A**), indicate that increased ppGpp enhances CtrA accumulation. This effect may occur through either protein stabilization, by reducing CtrA proteolysis, or mRNA stabilization, by enhancing CtrA production through translation. Our data add to the growing body of evidence supporting the critical role of guanosine nucleotides in controlling *Caulobacter* cell cycle and cellular development [96, 315].

An unexpected connection between Caulobacter NtrC and σ^{54}-regulated gene expression

Caulobacter NtrC is an atypical bEBP that lacks the GAFTGA motif in its AAA+ domain [266], a structural element required for interacting with and activating σ^{54}-RNA polymerase (RNAP) [167, 233]. Our study reveals an unexpected regulatory connection between NtrC point mutants and genes activated by the σ^{54}-dependent bEBP, FlbD [287]. Specifically, we've shown that strains expressing *ntrC* alleles with mutations in the DNA-binding/HTH domain strongly increase the levels of mRNAs transcribed from established FlbD promoters (**Figure 3.7**) (See **Figure S3.4** in Appendix 2). Given that *Caulobacter* NtrC regulates transcription from σ^{70} promoters [266], this result raises the question of how NtrC mutants that are unable to bind their native chromosomal sites influence the levels of σ^{54}-dependent transcripts. One possibility is that

mutant NtrC directly interacts with FlbD-σ^{54} transcriptional complexes to activate transcription. This hypothesis is supported by studies from other systems showing that bEBPs lacking functional DNA-binding domains—whether due to C-terminal truncations or specific mutations—can still activate transcription when present at high concentrations, both *in vitro* and *in vivo* (reviewed in [167]). Additionally, there are examples of naturally occurring bEBPs that lack C-terminal DNA-binding domains yet still activate σ^{54}-dependent transcription (reviewed in [206]).

Our data show that loss-of-function NtrC mutants accumulate at higher intracellular levels compared to wild-type NtrC [266] (**Figure 3.2C**), which invokes a regulatory model proposed by North and Kustu [201]. In this model, DNA binding primarily functions to localize bEBPs near the promoter, facilitating oligomerization and efficient activation of σ^{54}-dependent transcription. However, this localization function can be bypassed when bEBPs reach sufficiently high concentrations, allowing activation to occur directly from solution. Our results suggest that NtrC can promote σ^{54}-dependent gene expression, even without DNA-binding activity or the GAFTGA motif.

NtrC mutations enable cckA(ts) suppression through alternative activation mechanisms

While complete deletion of *ntrC* only partially suppresses *cckA*(ts), point mutations in its DNA-binding/HTH domain more effectively restore both growth and global transcriptional profiles (**Figures 3.7**; **Supplemental Table 7**) (See **Figure S3.4** in Appendix 2). Notably, robust suppression by mutant NtrC requires an intact and phosphorylatable REC domain (**Figure 3.2E**; **Figure 3.3A-B**), indicating that suppression is not simply due to loss of NtrC function but rather a gain of alternative regulatory activity when mutant NtrC accumulates to high concentrations and/or is no longer restricted to its native regulatory sites. This concept aligns with an early model by Magasanik, who proposed that DNA binding was needed to spatially constrain activation by bEBPs [316], preventing spurious transcription activation in bacterial genomes, which lack extensive non-coding DNA. In the case of *cckA*(ts) suppressor mutants, where bEBP expression is elevated but DNA-binding is lost, mutant NtrC may acquire novel regulatory interactions with

transcriptional machinery or other regulatory proteins. Additionally, changes in the levels and localization of mutant NtrC could influence the activity of other bEBPs, such as TacA [305] or FlbD [287] at their respective promoters.

Beyond direct regulatory effects, *ntrC* mutations may also impact gene expression through alterations in chromosomal architecture. NtrC binding sites overlap with those of GapR, a nucleoid-associated protein that affects DNA supercoiling and chromosome organization [226], which can influence cell cycle and cellular development [225]. Additionally, many NtrC binding sites overlap with those of MucR1, a key regulator of *Caulobacter* cell cycle genes [227]. Several flagellar promoters that are strongly activated in *ntrC* suppressor strains are located within chromosomal regions associated with GapR and MucR1 binding (See **Figure S3.4** in Appendix 2). This raises the possibility that loss of NtrC DNA-binding could alter chromatin organization or promote new protein-protein interactions, indirectly facilitating transcription at σ^{54}-regulated sites.

Overall, the ability of *ntrC* mutants to bypass the essential function of *cckA*—through transcriptional reprogramming and activation of (p)ppGpp synthesis—highlights the exceptional plasticity of the *Caulobacter* cell cycle regulatory network. Our results underscore the deep integration of environmental sensing pathways with core cell cycle control systems and suggest that the evolution of novel gene regulatory connections can reshape cellular networks, allowing organisms to circumvent otherwise essential signaling processes.

Future Directions

Caulobacter NtrC: Functional studies

In this work, we have established that *Caulobacter* NtrC displays features that we deem as “unconventional” molecular features of typical σ^{54}-activating bEBPs. To begin, we have provided evidence using transcriptomic and ChIP-seq techniques that *Caulobacter* NtrC regulates σ^{70}-dependent promoters (**Figure 2.4**; **Supplemental Table 3**). As discussed previously, this result is expected due to 1) the absence of the conserved GAFTGA motif which

is required for direct interaction with σ^{54} (See **Figure S2.1** in Appendix 1) [233] and 2) the previously established σ^{70}-dependent action of other bEBPs lacking GAFTGA, such as *R. capsulatus* NtrC and *V. cholerae* VspR [213, 303, 304]. The functional transcriptional mechanism by which these other unconventional bEBPs active σ^{70} promoters has been established. *R. Capsulatus* NtrC requires phosphorylation of its conserved aspartyl residue and, additionally, requires ATP binding but not hydrolysis for σ^{70}-dependent transcription [213]. Conversely, *V. cholerae* VspR does not require phosphorylation but, instead, utilizes the conserved aspartyl phosphorylation site for phosphate sensing and, moreover, does not rely on ATP for transcriptional activation [214, 304]. We have provided genetic evidence that all domains of *Caulobacter* NtrC are required at least for activation of *glnBA* and consequential NH_4^+ assimilation (**Figure 2.2**) (See **Figure S2.4** in Appendix 1) and, moreover, that conserved residues for phosphorylation, ATP binding, and ATP hydrolysis (i.e., D56, K178, and D235, respectively) are also required for this activity (See **Figure S2.3** in Appendix 1). These genetic results suggest that the following are required for transcriptional regulation by *Caulobacter* NtrC: 1) the conserved aspartyl residue for either phosphate sensing or, more likely, for phosphorylation, itself, 2) ATP binding, and 3) ATP hydrolysis. Biochemical studies of *Caulobacter* NtrC are required to 1) confirm binding and transcriptional regulation at these σ^{70}-dependent promoters, 2) determine whether transcriptional activity requires phosphorylation of the conserved aspartyl residue, and 3) assess the role of ATP binding and/or hydrolysis in transcriptional regulation at these promoters. These studies may include electrophoretic mobility shift assays (EMSAs) [317] to confirm binding at target promoters. Additionally, *in vitro* transcription can be used to identify all molecular components needed for transcriptional activation by NtrC (e.g., ATP) and, moreover, can be used to assess the mechanism by which NtrC activates σ^{70}-dependent transcription. If, indeed, GAFTGA-lacking *Caulobacter* NtrC requires ATP binding and hydrolysis at σ^{70} promoters, this would distinguish it from other

unconventional σ^{70}-regulating bEBPs. Altogether, biochemical studies of NtrC-mediated transcription in *Caulobacter* would provide insight into this dynamic class of transcriptional regulators.

***Caulobacter* NtrC: A direct role in cell cycle control and cellular development**

In *E. coli*, it has been established that NtrC indirectly contributes to cell cycle control under nitrogen starvation conditions by modulating stringent response through its role in glutamine synthesis and transcriptional regulation of *relA*. First, under nitrogen starvation, *E. coli* NtrC activates transcription of *glnA*, encoding glutamine synthetase, which synthesizes glutamine — the readout for nitrogen status for Proteobacteria (reviewed in [153]). Notably, GlnA is the sole route of glutamine synthesis in *Caulobacter* [128]. Secondly, *E. coli* NtrC activates expression of *relA* under nitrogen starvation [159]. Our work, as well as work from Ronneau et al [128], established that *Caulobacter* NtrC similarly plays a role *glnA* activation and, consequentially, plays a role in modulation of intracellular glutamine levels in the cell, a signal which directly regulates nitrogen-dependent SpoT activity [128]. In this way, NtrC can indirectly modulate cell cycle progression and cellular development in *Caulobacter* through stringent response. Indeed, cell cycle and developmental defects of Δ*ntrC* in complex medium, including slow growth, mucoid growth, and long stalk development, can all be complemented by glutamine supplementation (**Figure 2.2**; **Figure 2.6**; **Figure 2.8**), suggesting that these Δ*ntrC* phenotypes are mediated through nitrogen starvation in the form of decreased intracellular glutamine. Moreover, ppGpp levels are increased in Δ*ntrC* compared to WT (**Figure 3.5B**). If phenotypes of Δ*ntrC* are simply due to this strain feeling “nitrogen starved,” one might predict these phenotypes are recapitulated when wild-type *Caulobacter* is starved for nitrogen. Indeed, as mentioned previously, NH_4^+ depletion in defined medium slows growth of *Caulobacter*, specifically by delaying the G1-to-S/swarmer-to-stalk transition [86]. On the contrary, *Caulobacter* starved for NH_4^+ in defined medium has not been previously reported to develop long stalks [149]. Given the fact that intracellular glutamine is a direct readout of NH_4^+ and,

therefore, reflective of intracellular NH_4^+ status in *Caulobacter* [128], I would have predicted that *Caulobacter* starved for NH_4^+ would phenocopy a *Caulobacter* Δ*ntrC* mutant that has decreased levels of intracellular glutamine. At least two things should be considered here — First, these glutamine-starved phenotypes of Δ*ntrC* (e.g., long stalks) are manifested when Δ*ntrC* is grown in PYE complex medium, which differs vastly in composition compared to M2G defined medium that is used in previously published NH_4^+ starvation experiments (see Materials & Methods for composition of M2G and PYE media types). Given Δ*ntrC* cannot grow in defined medium with NH_4^+ as the sole nitrogen source (**Figure 2.1**), I cannot probe these phenotypes in that condition. Second, although Δ*ntrC*-mediated glutamine starvation should in theory simulate environmental NH_4^+ starvation, the absence of *ntrC* in the cell may have independent consequences that contribute to these phenotypes. Altogether, these disparate nitrogen starvation phenotypes of Δ*ntrC* suggest that 1) loss of NtrC and subsequent glutamine synthesis in *Caulobacter* is not simply reflective of NH_4^+ starvation and/or 2) media composition or, more broadly, other environmental signals feed into how *Caulobacter* responds to nitrogen starvation. These genetic and environmental questions require further investigation.

ChIP-seq and transcriptomic data provide evidence that NtrC may play direct regulatory roles in *Caulobacter* cell cycle and cellular development through direct transcriptional regulation of cell cycle and cellular development genes. As mentioned, NtrC shows repressive activity at promoters of *hdaA* and *sciP* (**Supplemental Table 2**; **Supplemental Table 3**). HdaA and SciP have direct roles in the regulation of DNA replication, cell cycle progression, and cellular development [70, 238]. As mentioned, orthologous NtrC proteins, such as the copiotroph *E. coli* NtrC, will modulate cell cycle through modulation of stringent response, but, in *Caulobacter*, we see direct regulation of cell cycle genes by NtrC. In further support, NtrC regulates *hvyA* and other capsule biosynthesis genes — genes regulated in a cell cycle-dependent manner. In *Caulobacter*, capsule biosynthesis is cell cycle regulated, associating with the replicative stalked cell [17]. In other bacteria, capsule biosynthesis is often induced upon environmental signals

(reviewed in [318]). It has been shown in other bacteria, such as *V. cholerae*, that loss of *ntrC* has indirect effects on capsule production through modulation of stringent response [319]. Altogether, the cell cycle and developmental effects seen from deletion of *ntrC* in other bacteria are mediated through its role in central nitrogen metabolism and stimulation of stringent response. In *Caulobacter*, NtrC displays direct transcriptional regulation of genes of these cell cycle and development pathways. This raises the question — has *Caulobacter* adapted to use central nitrogen metabolism regulators, like NtrC, to directly modulate cell cycle control through direct transcriptional regulation? In other words, is direct transcriptional regulation of cell cycle and development genes by *Caulobacter* NtrC a tactic to rapidly amplify the nitrogen starvation-induced effects on cell cycle control in addition to activation of stringent response? In the oligotrophic environment of *Caulobacter*, this may be an adapted mechanism to more efficiently respond to these low nitrogen conditions. Given the loss of GAFTGA in NtrC orthologs across multiple species within Alphaproteobacteria (See **Figure S2.1** in Appendix 1), regulation of σ^{70}-dependent cell cycle promoters by NtrC may be a conserved method of cell cycle and developmental control. Further support of a non-canonical role of *Caulobacter* NtrC in cell cycle and developmental control is the frequency of overlap between NtrC binding sites with previously published binding sites of the cell cycle regulators GapR and MucR1 (**Figure 2.5**). Given the conservation of NtrC, GapR, and MucR1 in Alphaproteobacteria [17, 320], these potential functional interactions can be probed in *Caulobacter*, as well as other Alphaproteobacteria species to explore a novel mechanism of cell cycle control by NtrC that is conserved in Alphaproteobacteria.

Molecular mechanisms by which (p)ppGpp alters cell cycle and cellular development

Nitrogen starvation activates stringent response and stimulates (p)ppGpp synthesis, which halts cell cycle progression in *Caulobacter*. This halt typically occurs at the G1-to-S cell cycle transition, resulting in increased time *Caulobacter* will spend in the G1 swarmer cell phase. In this dissertation, I have shown that loss of NtrC function results in increased

intracellular levels of ppGpp (**Figure 3.5B**), most likely due to decreased intracellular glutamine synthesis caused by loss of NtrC-dependent activation of *glnA*. It has been previously established that increased (p)ppGpp levels under starvation conditions corresponds with increased CtrA protein levels in *Caulobacter* [146], which is hypothesized to play a role in the G1 swarmer cell extension phenotype under these starvation conditions. Similarly, in this body of work, I have shown that *ntrC* mutants, which feel nitrogen starved (for glutamine) and synthesize ppGpp accordingly, possess increased CtrA levels (**Figure 3.6A**). The molecular mechanism(s) by which CtrA levels increase upon activation of stringent response and subsequent (p)ppGpp accumulation remain elusive. Famously, (p)ppGpp binds and modulates RNAP activity at certain promoters in Proteobacteria. Although effects on RNAP have been extensively studied in *E. coli*, (p)ppGpp interaction with RNAP in Alphaproteobacteria has not been well established, although, Alphaproteobacterial RNAP contains the conserved binding sites for (p)ppGpp binding [321]. Therefore, it could be hypothesized that increased transcription of *ctrA* by (p)ppGpp-modulated RNAP could contribute to increased CtrA levels. Indeed, *cckA*(ts) strains harboring *ntrC* mutations display increased *ctrA* mRNA transcript levels, although, these increases are modest (i.e., ~1- to 2-fold compared to WT) (**Supplemental Table 7**). These data, along with the fact that CtrA is proteolytically regulated in *Caulobacter*, suggest that mRNA stabilization or increased transcription of *ctrA* is not the sole route by which (p)ppGpp increases CtrA protein levels. In the literature, it is postulated that (p)ppGpp stabilizes CtrA post-transcriptionally [86, 117, 146]. Indeed, in bacteria, (p)ppGpp binds to and modulates activity of proteins other than RNAP, including proteins involved in purine nucleotide metabolism [322, 323], DNA replication [324], ribosome maturation and translation [325], and (p)ppGpp metabolism, itself [323, 326]. Therefore, it is plausible that (p)ppGpp may modulate activity of proteins involved in CtrA stability and degradation, including CpdR, the proteolytic adapter, or ClpXP, itself. However, it is completely plausible that increased CtrA levels in (p)ppGpp accumulated conditions are not due to direct effects on CtrA stability but, instead, (p)ppGpp

alters cellular physiology that results in secondary effects on intracellular CtrA levels. Importantly, it remains to be determined if increased CtrA levels under activation of stringent response is causative of the G1-to-S cell cycle delay or consequential of this delay. Altogether, the molecular mechanisms by which (p)ppGpp alters physiology, as well as cell cycle control and cellular development in *Caulobacter* and other Alphaproteobacteria requires further investigation and characterization.

Overall Conclusion

This dissertation provides new insights into the complex regulatory networks that coordinate nitrogen metabolism, cell cycle progression, and cellular development in *Caulobacter crescentus*. Through detailed genetic, biochemical, and transcriptomic analyses, my work establishes that the NtrB-NtrC two-component signaling system plays a central role in integrating environmental nitrogen availability with cell cycle control and polar morphogenesis. It demonstrates that NtrC is an unconventional bacterial enhancer binding protein (bEBP) that lacks the conserved GAFTGA motif required for σ^{54} activation yet still regulates σ^{70}-dependent transcription of genes involved in nitrogen assimilation, cell envelope biosynthesis, and polar development. Loss of *ntrC* leads to growth defects in NH_4^+-defined medium due to the failure to activate *glnBA* expression, which can be rescued by spontaneous IS3-family transposition events, revealing a potential mechanism of evolutionary adaptation under nitrogen-limited conditions.

The identification of *ntrC* mutations that bypass the essential CckA-ChpT-CtrA phosphorelay provides compelling evidence that NtrC influences core cell cycle regulatory pathways. In loss-of-function *ntrC* mutants, elevated ppGpp levels resulting from impaired glutamine synthesis sustain CtrA protein levels. Furthermore, *ntrC* mutants exhibit increased transcription of FlbD-regulated flagellar and cell cycle genes, despite lacking direct DNA-binding activity at these sites. This suggests that NtrC mutants can promote σ^{54}-dependent transcription

through alternative regulatory mechanisms, potentially involving protein-protein interactions or changes in nucleoid architecture.

This work also defines a direct link between nitrogen status and cellular development, as loss of NtrC leads to hyper-elongated stalks and increased cell envelope polysaccharide production—phenotypes that are rescued by glutamine supplementation. The genetic and biochemical evidence presented here underscores the role of intracellular glutamine as a key signaling molecule that connects nitrogen availability with cell cycle progression and development. Moreover, the overlap between NtrC binding sites and those of GapR and MucR1 suggests that NtrC functions at the interface of chromosome organization and cell cycle control. In summary, this dissertation advances our understanding of the interplay between nitrogen metabolism, nucleotide signaling, and cell cycle regulation in *Caulobacter*. It highlights the plasticity of bacterial regulatory networks and the capacity of alternative signaling pathways to compensate for the loss of essential cell cycle regulators. These findings lay the groundwork for future studies into the molecular mechanisms by which NtrC and other bEBPs coordinate environmental sensing with cell cycle progression and cellular differentiation in bacteria.

REFERENCES

1. Chong, T.N. and L. Shapiro, *Bacterial cell differentiation enables population level survival strategies.* mBio, 2024. **15**(6): p. e0075824.

2. Lopez, D., H. Vlamakis, and R. Kolter, *Generation of multiple cell types in Bacillus subtilis.* FEMS Microbiol Rev, 2009. **33**(1): p. 152-63.

3. Piggot, P.J. and D.W. Hilbert, *Sporulation of Bacillus subtilis.* Curr Opin Microbiol, 2004. **7**(6): p. 579-86.

4. Murphy, P., et al., *Cell behaviors underlying Myxococcus xanthus aggregate dispersal.* mSystems, 2023. **8**(5): p. e0042523.

5. Kaiser, D., M. Robinson, and L. Kroos, *Myxobacteria, polarity, and multicellular morphogenesis.* Cold Spring Harb Perspect Biol, 2010. **2**(8): p. a000380.

6. Justice, S.S., et al., *Bacterial differentiation, development, and disease: mechanisms for survival.* FEMS Microbiol Lett, 2014. **360**(1): p. 1-8.

7. Moller, J., et al., *The race to the pole: how high-aspect ratio shape and heterogeneous environments limit phagocytosis of filamentous Escherichia coli bacteria by macrophages.* Nano Lett, 2012. **12**(6): p. 2901-5.

8. Jones, M., *A peculiar microorganism showing rosette formation.* Zentr Bakteriol Parasitenk Abt II, 1905. **14**: p. 459-463.

9. Omeliansky, V.L., *A new bacillus: Bacillus flagellatus.* Zh Mikrobiol Epidemiol Immunobiol, 1914. **1**: p. 24.

10. Henrici, A.T. and D.E. Johnson, *Studies of Freshwater Bacteria: II. Stalked Bacteria, a New Order of Schizomycetes.* J Bacteriol, 1935. **30**(1): p. 61-93.

11. Houwink, A.L. and I.W. van, *Electron microscopical observations on bacterial cytology; a study on flagellation.* Biochim Biophys Acta, 1950. **5**(1): p. 10-44.

12. Bowers, L.E., et al., *Studies on a strain of Caulobacter from water. I. Isolation and identification as Caulobacter vibrioides Henrici and Johnson with emended description.* J Bacteriol, 1954. **68**(2): p. 194-200.

13. Poindexter, J.S., *Biological Properties and Classification of the Caulobacter Group.* Bacteriol Rev, 1964. **28**(3): p. 231-95.

14. Marks, M.E., et al., *The genetic basis of laboratory adaptation in Caulobacter crescentus.* J Bacteriol, 2010. **192**(14): p. 3678-88.

15. Shapiro, L., N. Agabian-Keshishian, and I. Bendis, *Bacterial differentiation.* Science, 1971. **173**(4000): p. 884-92.

16. Barrows, J.M. and E.D. Goley, *Synchronized Swarmers and Sticky Stalks: Caulobacter crescentus as a Model for Bacterial Cell Biology.* J Bacteriol, 2023. **205**(2): p. e0038422.

17. Ardissone, S., et al., *Cell cycle constraints on capsulation and bacteriophage susceptibility.* Elife, 2014. **3**: p. e03587.

18. Evinger, M. and N. Agabian, *Envelope-associated nucleoid from Caulobacter crescentus stalked and swarmer cells.* J Bacteriol, 1977. **132**(1): p. 294-301.

19. Schrader, J.M. and L. Shapiro, *Synchronization of Caulobacter crescentus for investigation of the bacterial cell cycle.* J Vis Exp, 2015(98).

20. Bodenmiller, D., E. Toh, and Y.V. Brun, *Development of surface adhesion in Caulobacter crescentus.* J Bacteriol, 2004. **186**(5): p. 1438-47.

21. Degnen, S.T. and A. Newton, *Chromosome replication during development in Caulobacter crescentus.* J Mol Biol, 1972. **64**(3): p. 671-80.

22. Shapiro, L. and N. Agabian-Keshishian, *Specific Assay for Differentiation in the Stalked Bacterium Caulobacter crescentus.* Proc Natl Acad Sci U S A, 1970. **67**(1): p. 200-3.

23. Barrett, J.T., et al., *Construction of a genetic map for Caulobacter crescentus.* J Bacteriol, 1982. **149**(3): p. 889-96.

24. Ely, B. and T.W. Ely, *Use of pulsed field gel electrophoresis and transposon mutagenesis to estimate the minimal number of genes required for motility in Caulobacter crescentus.* Genetics, 1989. **123**(4): p. 649-54.

25. Nierman, W.C., et al., *Complete genome sequence of Caulobacter crescentus.* Proc Natl Acad Sci U S A, 2001. **98**(7): p. 4136-41.

26. Ettema, T.J. and S.G. Andersson, *The alpha-proteobacteria: the Darwin finches of the bacterial world.* Biol Lett, 2009. **5**(3): p. 429-32.

27. Wang, S. and H. Luo, *Dating Alphaproteobacteria evolution with eukaryotic fossils.* Nat Commun, 2021. **12**(1): p. 3324.

28. Wilhelm, R.C., *Following the terrestrial tracks of Caulobacter - redefining the ecology of a reputed aquatic oligotroph.* ISME J, 2018. **12**(12): p. 3025-3037.

29. Prischl, M., et al., *Genetically modified Bt maize lines containing cry3Bb1, cry1A105 or cry1Ab2 do not affect the structure and functioning of root-associated endophyte communities.* Applied Soil Ecology, 2012. **54**: p. 39-48.

30. Naveed, M., et al., *The endophyte Enterobacter sp. FD17: a maize growth enhancer selected based on rigorous testing of plant beneficial traits and colonization characteristics.* Biol Fertil Soils, 2014. **50**: p. 249-262.

31. Hottes, A.K., et al., *Transcriptional profiling of Caulobacter crescentus during growth on complex and minimal media.* J Bacteriol, 2004. **186**(5): p. 1448-61.

32. Blanvillain, S., et al., *Plant carbohydrate scavenging through tonB-dependent receptors: a feature shared by phytopathogenic and aquatic bacteria.* PLoS One, 2007. **2**(2): p.

e224.

33. Thanbichler, M., A.A. Iniesta, and L. Shapiro, *A comprehensive set of plasmids for vanillate- and xylose-inducible gene expression in Caulobacter crescentus.* Nucleic Acids Res, 2007. **35**(20): p. e137.

34. Govers, S.K. and C. Jacobs-Wagner, *Caulobacter crescentus: model system extraordinaire.* Curr Biol, 2020. **30**(19): p. R1151-R1158.

35. Flemming, H.C., et al., *Biofilms: an emergent form of bacterial life.* Nat Rev Microbiol, 2016. **14**(9): p. 563-75.

36. Marczynski, G.T., *Chromosome methylation and measurement of faithful, once and only once per cell cycle chromosome replication in Caulobacter crescentus.* J Bacteriol, 1999. **181**(7): p. 1984-93.

37. Ellison, C.K., et al., *A bifunctional ATPase drives tad pilus extension and retraction.* Sci Adv, 2019. **5**(12): p. eaay2591.

38. Sommer, J.M. and A. Newton, *Sequential regulation of developmental events during polar morphogenesis in Caulobacter crescentus: assembly of pili on swarmer cells requires cell separation.* J Bacteriol, 1988. **170**(1): p. 409-15.

39. Holtzendorff, J., et al., *Oscillating global regulators control the genetic circuit driving a bacterial cell cycle.* Science, 2004. **304**(5673): p. 983-7.

40. Zweiger, G. and L. Shapiro, *Expression of Caulobacter dnaA as a function of the cell cycle.* J Bacteriol, 1994. **176**(2): p. 401-8.

41. Collier, J., H.H. McAdams, and L. Shapiro, *A DNA methylation ratchet governs progression through a bacterial cell cycle.* Proc Natl Acad Sci U S A, 2007. **104**(43): p. 17111-6.

42. Brown, P.J., et al., *Complex regulatory pathways coordinate cell-cycle progression and development in Caulobacter crescentus.* Adv Microb Physiol, 2009. **54**: p. 1-101.

43. Kirkpatrick, C.L. and P.H. Viollier, *Decoding Caulobacter development.* FEMS Microbiol Rev, 2012. **36**(1): p. 193-205.

44. Goley, E.D., et al., *Dynamic chromosome organization and protein localization coordinate the regulatory circuitry that drives the bacterial cell cycle.* Cold Spring Harb Symp Quant Biol, 2009. **74**: p. 55-64.

45. Laub, M.T., L. Shapiro, and H.H. McAdams, *Systems biology of Caulobacter.* Annu Rev Genet, 2007. **41**: p. 429-41.

46. Stock, A.M., V.L. Robinson, and P.N. Goudreau, *Two-component signal transduction.* Annu Rev Biochem, 2000. **69**: p. 183-215.

47. Gao, R. and A.M. Stock, *Biological insights from structures of two-component proteins.* Annu Rev Microbiol, 2009. **63**: p. 133-54.

48. Ninfa, A.J. and B. Magasanik, *Covalent modification of the glnG product, NRI, by the glnL product, NRII, regulates the transcription of the glnALG operon in Escherichia coli.* Proc Natl Acad Sci U S A, 1986. **83**(16): p. 5909-13.

49. Nixon, B.T., C.W. Ronson, and F.M. Ausubel, *Two-component regulatory systems responsive to environmental stimuli share strongly conserved domains with the nitrogen assimilation regulatory genes ntrB and ntrC.* Proc Natl Acad Sci U S A, 1986. **83**(20): p. 7850-4.

50. Francis, V.I. and S.L. Porter, *Multikinase Networks: Two-Component Signaling Networks Integrating Multiple Stimuli.* Annu Rev Microbiol, 2019. **73**: p. 199-223.

51. Zahrt, T.C. and V. Deretic, *An essential two-component signal transduction system in Mycobacterium tuberculosis.* J Bacteriol, 2000. **182**(13): p. 3832-8.

52. Martin, P.K., et al., *Role in cell permeability of an essential two-component system in Staphylococcus aureus.* J Bacteriol, 1999. **181**(12): p. 3666-73.

53. Hecht, G.B., et al., *An essential single domain response regulator required for normal cell division and differentiation in Caulobacter crescentus.* EMBO J, 1995. **14**(16): p. 3915-24.

54. Fabret, C. and J.A. Hoch, *A two-component signal transduction system essential for growth of Bacillus subtilis: implications for anti-infective therapy.* J Bacteriol, 1998. **180**(23): p. 6375-83.

55. Bowers, L.M., E.B. Shapland, and K.R. Ryan, *Who's in charge here? Regulating cell cycle regulators.* Curr Opin Microbiol, 2008. **11**(6): p. 547-52.

56. Biondi, E.G., et al., *Regulation of the bacterial cell cycle by an integrated genetic circuit.* Nature, 2006. **444**(7121): p. 899-904.

57. Jacobs, C., et al., *Functions of the CckA histidine kinase in Caulobacter cell cycle control.* Mol Microbiol, 2003. **47**(5): p. 1279-90.

58. Jacobs, C., et al., *Cell cycle-dependent polar localization of an essential bacterial histidine kinase that controls DNA replication and cell division.* Cell, 1999. **97**(1): p. 111-20.

59. Laub, M.T., et al., *Global analysis of the genetic network controlling a bacterial cell cycle.* Science, 2000. **290**(5499): p. 2144-8.

60. Chen, Y.E., et al., *Dynamics of two Phosphorelays controlling cell cycle progression in Caulobacter crescentus.* J Bacteriol, 2009. **191**(24): p. 7417-29.

61. Iniesta, A.A., et al., *A phospho-signaling pathway controls the localization and activity of a protease complex critical for bacterial cell cycle progression.* Proc Natl Acad Sci U S A, 2006. **103**(29): p. 10935-40.

62. Lau, J., et al., *A Phosphosignaling Adaptor Primes the AAA+ Protease ClpXP to Drive Cell Cycle-Regulated Proteolysis.* Mol Cell, 2015. **59**(1): p. 104-16.

63. Lori, C., et al., *Cyclic di-GMP acts as a cell cycle oscillator to drive chromosome replication.* Nature, 2015. **523**(7559): p. 236-9.

64. Dubey, B.N., et al., *Cyclic di-GMP mediates a histidine kinase/phosphatase switch by noncovalent domain cross-linking.* Sci Adv, 2016. **2**(9): p. e1600823.

65. Mann, T.H., et al., *A cell cycle kinase with tandem sensory PAS domains integrates cell fate cues.* Nat Commun, 2016. **7**: p. 11454.

66. Mann, T.H. and L. Shapiro, *Integration of cell cycle signals by multi-PAS domain kinases.* Proc Natl Acad Sci U S A, 2018. **115**(30): p. E7166-E7173.

67. Heinrich, K., P. Sobetzko, and K. Jonas, *A Kinase-Phosphatase Switch Transduces Environmental Information into a Bacterial Cell Cycle Circuit.* PLoS Genet, 2016. **12**(12): p. e1006522.

68. Tsokos, C.G., B.S. Perchuk, and M.T. Laub, *A dynamic complex of signaling proteins uses polar localization to regulate cell-fate asymmetry in Caulobacter crescentus.* Dev Cell, 2011. **20**(3): p. 329-41.

69. Quon, K.C., et al., *Negative control of bacterial DNA replication by a cell cycle regulatory protein that binds at the chromosome origin.* Proc Natl Acad Sci U S A, 1998. **95**(1): p. 120-5.

70. Tan, M.H., et al., *An essential transcription factor, SciP, enhances robustness of Caulobacter cell cycle regulation.* Proc Natl Acad Sci U S A, 2010. **107**(44): p. 18985-90.

71. Gora, K.G., et al., *A cell-type-specific protein-protein interaction modulates transcriptional activity of a master regulator in Caulobacter crescentus.* Mol Cell, 2010. **39**(3): p. 455-67.

72. Skerker, J.M. and L. Shapiro, *Identification and cell cycle control of a novel pilus system in Caulobacter crescentus.* EMBO J, 2000. **19**(13): p. 3223-34.

73. Laub, M.T., et al., *Genes directly controlled by CtrA, a master regulator of the Caulobacter cell cycle.* Proc Natl Acad Sci U S A, 2002. **99**(7): p. 4632-7.

74. Aldridge, P. and U. Jenal, *Cell cycle-dependent degradation of a flagellar motor component requires a novel-type response regulator.* Mol Microbiol, 1999. **32**(2): p. 379-91.

75. Aldridge, P., et al., *Role of the GGDEF regulator PleD in polar development of Caulobacter crescentus.* Mol Microbiol, 2003. **47**(6): p. 1695-708.

76. Hecht, G.B. and A. Newton, *Identification of a novel response regulator required for the swarmer-to-stalked-cell transition in Caulobacter crescentus.* J Bacteriol, 1995. **177**(21): p. 6223-9.

77. McGrath, P.T., et al., *A dynamically localized protease complex and a polar specificity factor control a cell cycle master regulator.* Cell, 2006. **124**(3): p. 535-47.

78. Duerig, A., et al., *Second messenger-mediated spatiotemporal control of protein degradation regulates bacterial cell cycle progression.* Genes Dev, 2009. **23**(1): p. 93-104.

79. Gora, K.G., et al., *Regulated proteolysis of a transcription factor complex is critical to cell cycle progression in Caulobacter crescentus.* Mol Microbiol, 2013. **87**(6): p. 1277-89.

80. Katayama, T., K. Kasho, and H. Kawakami, *The DnaA Cycle in Escherichia coli: Activation, Function and Inactivation of the Initiator Protein.* Front Microbiol, 2017. **8**: p. 2496.

81. Hottes, A.K., L. Shapiro, and H.H. McAdams, *DnaA coordinates replication initiation and cell cycle transcription in Caulobacter crescentus.* Mol Microbiol, 2005. **58**(5): p. 1340-53.

82. Collier, J., S.R. Murray, and L. Shapiro, *DnaA couples DNA replication and the expression of two cell cycle master regulators.* EMBO J, 2006. **25**(2): p. 346-56.

83. Haakonsen, D.L., A.H. Yuan, and M.T. Laub, *The bacterial cell cycle regulator GcrA is a sigma70 cofactor that drives gene expression from a subset of methylated promoters.* Genes Dev, 2015. **29**(21): p. 2272-86.

84. Fioravanti, A., et al., *DNA binding of the cell cycle transcriptional regulator GcrA depends on N6-adenosine methylation in Caulobacter crescentus and other Alphaproteobacteria.* PLoS Genet, 2013. **9**(5): p. e1003541.

85. Ozaki, S., *Regulation of replication initiation: lessons from Caulobacter crescentus.* Genes Genet Syst, 2019. **94**(5): p. 183-196.

86. Gorbatyuk, B. and G.T. Marczynski, *Regulated degradation of chromosome replication proteins DnaA and CtrA in Caulobacter crescentus.* Mol Microbiol, 2005. **55**(4): p. 1233-45.

87. Viollier, P.H., N. Sternheim, and L. Shapiro, *Identification of a localization factor for the polar positioning of bacterial structural and regulatory proteins.* Proc Natl Acad Sci U S A, 2002. **99**(21): p. 13831-6.

88. Sommer, J.M. and A. Newton, *Turning off flagellum rotation requires the pleiotropic gene pleD: pleA, pleC, and pleD define two morphogenic pathways in Caulobacter crescentus.* J Bacteriol, 1989. **171**(1): p. 392-401.

89. Domian, I.J., A. Reisenauer, and L. Shapiro, *Feedback control of a master bacterial cell-cycle regulator.* Proc Natl Acad Sci U S A, 1999. **96**(12): p. 6648-53.

90. Reisenauer, A., K. Quon, and L. Shapiro, *The CtrA response regulator mediates temporal control of gene expression during the Caulobacter cell cycle.* J Bacteriol, 1999. **181**(8): p. 2430-9.

91. Jones, S.E., N.L. Ferguson, and M.R.K. Alley, *New members of the ctrA regulon: the major chemotaxis operon in Caulobacter is CtrA dependent.* Microbiology (Reading),

2001. **147**(Pt 4): p. 949-958.

92. Judd, E.M., et al., *Fluorescence bleaching reveals asymmetric compartment formation prior to cell division in Caulobacter.* Proc Natl Acad Sci U S A, 2003. **100**(14): p. 8235-40.

93. Domian, I.J., K.C. Quon, and L. Shapiro, *Cell type-specific phosphorylation and proteolysis of a transcriptional regulator controls the G1-to-S transition in a bacterial cell cycle.* Cell, 1997. **90**(3): p. 415-24.

94. Wright, R., C. Stephens, and L. Shapiro, *The CcrM DNA methyltransferase is widespread in the alpha subdivision of proteobacteria, and its essential functions are conserved in Rhizobium meliloti and Caulobacter crescentus.* J Bacteriol, 1997. **179**(18): p. 5869-77.

95. Heinrich, K., et al., *Molecular Basis and Ecological Relevance of Caulobacter Cell Filamentation in Freshwater Habitats.* mBio, 2019. **10**(4).

96. Hallez, R., et al., *Hit the right spots: cell cycle control by phosphorylated guanosines in alphaproteobacteria.* Nat Rev Microbiol, 2017. **15**(3): p. 137-148.

97. Potrykus, K. and M. Cashel, *(p)ppGpp: still magical?* Annu Rev Microbiol, 2008. **62**: p. 35-51.

98. Boutte, C.C. and S. Crosson, *Bacterial lifestyle shapes stringent response activation.* Trends Microbiol, 2013. **21**(4): p. 174-80.

99. Dalebroux, Z.D., et al., *ppGpp conjures bacterial virulence.* Microbiol Mol Biol Rev, 2010. **74**(2): p. 171-99.

100. Pacios, O., et al., *(p)ppGpp and Its Role in Bacterial Persistence: New Challenges.* Antimicrob Agents Chemother, 2020. **64**(10).

101. Das, B. and R.K. Bhadra, *(p)ppGpp Metabolism and Antimicrobial Resistance in Bacterial Pathogens.* Front Microbiol, 2020. **11**: p. 563944.

102. Irving, S.E., N.R. Choudhury, and R.M. Corrigan, *The stringent response and physiological roles of (pp)pGpp in bacteria.* Nat Rev Microbiol, 2021. **19**(4): p. 256-271.

103. Cashel, M. and J. Gallant, *Two compounds implicated in the function of the RC gene of Escherichia coli.* Nature, 1969. **221**(5183): p. 838-41.

104. Borek, E., J. Rockenbach, and A. Ryan, *Studies on a mutant of Escherichia coli with unbalanced ribonucleic acid synthesis.* J Bacteriol, 1956. **71**(3): p. 318-23.

105. Borek, E., A. Ryan, and J. Rockenbach, *Nucleic acid metabolism in relation to the lysogenic phenomenon.* J Bacteriol, 1955. **69**(4): p. 460-7.

106. Stent, G.S. and S. Brenner, *A genetic locus for the regulation of ribonucleic acid synthesis.* Proc Natl Acad Sci U S A, 1961. **47**(12): p. 2005-14.

107. Atkinson, G.C., T. Tenson, and V. Hauryliuk, *The RelA/SpoT homolog (RSH) superfamily: distribution and functional evolution of ppGpp synthetases and hydrolases across the tree of life.* PLoS One, 2011. **6**(8): p. e23479.

108. Mittenhuber, G., *Comparative genomics and evolution of genes encoding bacterial (p)ppGpp synthetases/hydrolases (the Rel, RelA and SpoT proteins).* J Mol Microbiol Biotechnol, 2001. **3**(4): p. 585-600.

109. Heinemeyer, E.A. and D. Richter, *Mechanism of the in vitro breakdown of guanosine 5'-diphosphate 3'-diphosphate in Escherichia coli.* Proc Natl Acad Sci U S A, 1978. **75**(9): p. 4180-3.

110. Aravind, L. and E.V. Koonin, *The HD domain defines a new superfamily of metal-dependent phosphohydrolases.* Trends Biochem Sci, 1998. **23**(12): p. 469-72.

111. Sarubbi, E., et al., *Characterization of the spoT gene of Escherichia coli.* J Biol Chem, 1989. **264**(25): p. 15074-82.

112. Metzger, S., et al., *Characterization of the relA1 mutation and a comparison of relA1 with new relA null alleles in Escherichia coli.* J Biol Chem, 1989. **264**(35): p. 21146-52.

113. Xiao, H., et al., *Residual guanosine 3',5'-bispyrophosphate synthetic activity of relA null mutants can be eliminated by spoT null mutations.* J Biol Chem, 1991. **266**(9): p. 5980-90.

114. Laffler, T. and J.A. Gallant, *Stringent control of protein synthesis in E. coli.* Cell, 1974. **3**(1): p. 47-9.

115. Geiger, T., et al., *Role of the (p)ppGpp synthase RSH, a RelA/SpoT homolog, in stringent response and virulence of Staphylococcus aureus.* Infect Immun, 2010. **78**(5): p. 1873-83.

116. Jimmy, S., et al., *A widespread toxin-antitoxin system exploiting growth control via alarmone signaling.* Proc Natl Acad Sci U S A, 2020. **117**(19): p. 10500-10510.

117. Lesley, J.A. and L. Shapiro, *SpoT regulates DnaA stability and initiation of DNA replication in carbon-starved Caulobacter crescentus.* J Bacteriol, 2008. **190**(20): p. 6867-80.

118. Boutte, C.C. and S. Crosson, *The complex logic of stringent response regulation in Caulobacter crescentus: starvation signalling in an oligotrophic environment.* Mol Microbiol, 2011. **80**(3): p. 695-714.

119. Jiang, M., et al., *G-protein control of the ribosome-associated stress response protein SpoT.* J Bacteriol, 2007. **189**(17): p. 6140-7.

120. Raskin, D.M., N. Judson, and J.J. Mekalanos, *Regulation of the stringent response is the essential function of the conserved bacterial G protein CgtA in Vibrio cholerae.* Proc Natl Acad Sci U S A, 2007. **104**(11): p. 4636-41.

121. Seyfzadeh, M., J. Keener, and M. Nomura, *spoT-dependent accumulation of guanosine tetraphosphate in response to fatty acid starvation in Escherichia coli.* Proc Natl Acad

Sci U S A, 1993. **90**(23): p. 11004-8.

122. Battesti, A. and E. Bouveret, *Acyl carrier protein/SpoT interaction, the switch linking SpoT-dependent stress response to fatty acid metabolism.* Mol Microbiol, 2006. **62**(4): p. 1048-63.

123. Battesti, A. and E. Bouveret, *Bacteria possessing two RelA/SpoT-like proteins have evolved a specific stringent response involving the acyl carrier protein-SpoT interaction.* J Bacteriol, 2009. **191**(2): p. 616-24.

124. Germain, E., et al., *YtfK activates the stringent response by triggering the alarmone synthetase SpoT in Escherichia coli.* Nat Commun, 2019. **10**(1): p. 5763.

125. Eccleston, E.D., Jr. and E.D. Gray, *Variations in ppGpp levels in Rhodopseudomonas spheroides during adaptation to decreased light intensity.* Biochem Biophys Res Commun, 1973. **54**(4): p. 1370-6.

126. Belitsky, B. and C. Kari, *Absence of accumulation of ppGpp and RNA during amino acid starvation in Rhizobium meliloti.* J Biol Chem, 1982. **257**(9): p. 4677-9.

127. Chiaverotti, T.A., et al., *Conditions that trigger guanosine tetraphosphate accumulation in Caulobacter crescentus.* J Bacteriol, 1981. **145**(3): p. 1463-5.

128. Ronneau, S., et al., *Phosphotransferase-dependent accumulation of (p)ppGpp in response to glutamine deprivation in Caulobacter crescentus.* Nat Commun, 2016. **7**: p. 11423.

129. Stott, K.V., et al., *(p)ppGpp modulates cell size and the initiation of DNA replication in Caulobacter crescentus in response to a block in lipid biosynthesis.* Microbiology (Reading), 2015. **161**(Pt 3): p. 553-64.

130. Sanselicio, S. and P.H. Viollier, *Convergence of alarmone and cell cycle signaling from trans-encoded sensory domains.* mBio, 2015. **6**(5): p. e01415-15.

131. Deutscher, J., et al., *The bacterial phosphoenolpyruvate:carbohydrate phosphotransferase system: regulation by protein phosphorylation and phosphorylation-dependent protein-protein interactions.* Microbiol Mol Biol Rev, 2014. **78**(2): p. 231-56.

132. Goodwin, R.A. and D.J. Gage, *Biochemical characterization of a nitrogen-type phosphotransferase system reveals that enzyme EI(Ntr) integrates carbon and nitrogen signaling in Sinorhizobium meliloti.* J Bacteriol, 2014. **196**(10): p. 1901-7.

133. Molodtsov, V., et al., *Allosteric Effector ppGpp Potentiates the Inhibition of Transcript Initiation by DksA.* Mol Cell, 2018. **69**(5): p. 828-839 e5.

134. Haugen, S.P., W. Ross, and R.L. Gourse, *Advances in bacterial promoter recognition and its control by factors that do not bind DNA.* Nat Rev Microbiol, 2008. **6**(7): p. 507-19.

135. Sanchez-Vazquez, P., et al., *Genome-wide effects on Escherichia coli transcription from ppGpp binding to its two sites on RNA polymerase.* Proc Natl Acad Sci U S A, 2019. **116**(17): p. 8310-8319.

136. Legault, L., C. Jeantet, and F. Gros, *Inhibition of in vitro protein synthesis by ppGpp.* FEBS Lett, 1972. **27**(1): p. 71-75.

137. Vinogradova, D.S., et al., *How the initiating ribosome copes with ppGpp to translate mRNAs.* PLoS Biol, 2020. **18**(1): p. e3000593.

138. Corrigan, R.M., et al., *ppGpp negatively impacts ribosome assembly affecting growth and antimicrobial tolerance in Gram-positive bacteria.* Proc Natl Acad Sci U S A, 2016. **113**(12): p. E1710-9.

139. Feng, B., et al., *Structural and functional insights into the mode of action of a universally conserved Obg GTPase.* PLoS Biol, 2014. **12**(5): p. e1001866.

140. Wang, J.D., G.M. Sanders, and A.D. Grossman, *Nutritional control of elongation of DNA replication by (p)ppGpp.* Cell, 2007. **128**(5): p. 865-75.

141. Maciag, M., et al., *ppGpp inhibits the activity of Escherichia coli DnaG primase.* Plasmid, 2010. **63**(1): p. 61-7.

142. Chiaramello, A.E. and J.W. Zyskind, *Coupling of DNA replication to growth rate in Escherichia coli: a possible role for guanosine tetraphosphate.* J Bacteriol, 1990. **172**(4): p. 2013-9.

143. Kraemer, J.A., A.G. Sanderlin, and M.T. Laub, *The Stringent Response Inhibits DNA Replication Initiation in E. coli by Modulating Supercoiling of oriC.* mBio, 2019. **10**(4).

144. Harris, B.Z., D. Kaiser, and M. Singer, *The guanosine nucleotide (p)ppGpp initiates development and A-factor production in myxococcus xanthus.* Genes Dev, 1998. **12**(7): p. 1022-35.

145. Singer, M. and D. Kaiser, *Ectopic production of guanosine penta- and tetraphosphate can initiate early developmental gene expression in Myxococcus xanthus.* Genes Dev, 1995. **9**(13): p. 1633-44.

146. Gonzalez, D. and J. Collier, *Effects of (p)ppGpp on the progression of the cell cycle of Caulobacter crescentus.* J Bacteriol, 2014. **196**(14): p. 2514-25.

147. Leslie, D.J., et al., *Nutritional Control of DNA Replication Initiation through the Proteolysis and Regulated Translation of DnaA.* PLoS Genet, 2015. **11**(7): p. e1005342.

148. Felletti, M., et al., *A nascent polypeptide sequence modulates DnaA translation elongation in response to nutrient availability.* Elife, 2021. **10**.

149. Hallgren, J., et al., *Phosphate starvation decouples cell differentiation from DNA replication control in the dimorphic bacterium Caulobacter crescentus.* bioRxiv, 2023.

150. van Heeswijk, W.C., H.V. Westerhoff, and F.C. Boogerd, *Nitrogen assimilation in Escherichia coli: putting molecular data into a systems perspective.* Microbiol Mol Biol Rev, 2013. **77**(4): p. 628-95.

151. Forchhammer, K., *Glutamine signalling in bacteria.* Front Biosci, 2007. **12**: p. 358-70.

152. von Wiren, N., et al., *The molecular physiology of ammonium uptake and retrieval.* Curr Opin Plant Biol, 2000. **3**(3): p. 254-61.

153. Leigh, J.A. and J.A. Dodsworth, *Nitrogen regulation in bacteria and archaea.* Annu Rev Microbiol, 2007. **61**: p. 349-77.

154. Merrick, M.J. and R.A. Edwards, *Nitrogen control in bacteria.* Microbiol Rev, 1995. **59**(4): p. 604-22.

155. Jiang, P., J.A. Peliska, and A.J. Ninfa, *Enzymological characterization of the signal-transducing uridylyltransferase/uridylyl-removing enzyme (EC 2.7.7.59) of Escherichia coli and its interaction with the PII protein.* Biochemistry, 1998. **37**(37): p. 12782-94.

156. Bloom, F.R., et al., *Regulation of glutamine synthetase formation in Escherichia coli: characterization of mutants lacking the uridylyltransferase.* J Bacteriol, 1978. **134**(2): p. 569-77.

157. Zimmer, D.P., et al., *Nitrogen regulatory protein C-controlled genes of Escherichia coli: scavenging as a defense against nitrogen limitation.* Proc Natl Acad Sci U S A, 2000. **97**(26): p. 14674-9.

158. Bender, R.A., *A NAC for regulating metabolism: the nitrogen assimilation control protein (NAC) from Klebsiella pneumoniae.* J Bacteriol, 2010. **192**(19): p. 4801-11.

159. Brown, D.R., et al., *Nitrogen stress response and stringent response are coupled in Escherichia coli.* Nat Commun, 2014. **5**: p. 4115.

160. Nakagawa, A., T. Oshima, and H. Mori, *Identification and characterization of a second, inducible promoter of relA in Escherichia coli.* Genes Genet Syst, 2006. **81**(5): p. 299-310.

161. Buck, M., et al., *The bacterial enhancer-dependent sigma(54) (sigma(N)) transcription factor.* J Bacteriol, 2000. **182**(15): p. 4129-36.

162. Lonetto, M., M. Gribskov, and C.A. Gross, *The sigma 70 family: sequence conservation and evolutionary relationships.* J Bacteriol, 1992. **174**(12): p. 3843-9.

163. Paget, M.S. and J.D. Helmann, *The sigma70 family of sigma factors.* Genome Biol, 2003. **4**(1): p. 203.

164. Grossman, A.D., et al., *Sigma 32 synthesis can regulate the synthesis of heat shock proteins in Escherichia coli.* Genes Dev, 1987. **1**(2): p. 179-84.

165. Merrick, M.J., *In a class of its own--the RNA polymerase sigma factor sigma 54 (sigma N).* Mol Microbiol, 1993. **10**(5): p. 903-9.

166. Guo, Y., C.M. Lew, and J.D. Gralla, *Promoter opening by sigma(54) and sigma(70) RNA polymerases: sigma factor-directed alterations in the mechanism and tightness of control.* Genes Dev, 2000. **14**(17): p. 2242-55.

167. Bush, M. and R. Dixon, *The role of bacterial enhancer binding proteins as specialized activators of sigma54-dependent transcription.* Microbiol Mol Biol Rev, 2012. **76**(3): p. 497-529.

168. Feklistov, A. and S.A. Darst, *Structural basis for promoter-10 element recognition by the bacterial RNA polymerase sigma subunit.* Cell, 2011. **147**(6): p. 1257-69.

169. Cannon, W., M.T. Gallegos, and M. Buck, *DNA melting within a binary sigma(54)-promoter DNA complex.* J Biol Chem, 2001. **276**(1): p. 386-94.

170. Cannon, W.V., M.T. Gallegos, and M. Buck, *Isomerization of a binary sigma-promoter DNA complex by transcription activators.* Nat Struct Biol, 2000. **7**(7): p. 594-601.

171. Neuwald, A.F., et al., *AAA+: A class of chaperone-like ATPases associated with the assembly, operation, and disassembly of protein complexes.* Genome Res, 1999. **9**(1): p. 27-43.

172. Ogura, T. and A.J. Wilkinson, *AAA+ superfamily ATPases: common structure--diverse function.* Genes Cells, 2001. **6**(7): p. 575-97.

173. Hanson, P.I. and S.W. Whiteheart, *AAA+ proteins: have engine, will work.* Nat Rev Mol Cell Biol, 2005. **6**(7): p. 519-29.

174. Erokhin, M., et al., *Eukaryotic enhancers: common features, regulation, and participation in diseases.* Cell Mol Life Sci, 2015. **72**(12): p. 2361-75.

175. Carmona, M. and B. Magasanik, *Activation of transcription at sigma 54-dependent promoters on linear templates requires intrinsic or induced bending of the DNA.* J Mol Biol, 1996. **261**(3): p. 348-56.

176. Hoover, T.R., et al., *The integration host factor stimulates interaction of RNA polymerase with NIFA, the transcriptional activator for nitrogen fixation operons.* Cell, 1990. **63**(1): p. 11-22.

177. Morett, E. and L. Segovia, *The sigma 54 bacterial enhancer-binding protein family: mechanism of action and phylogenetic relationship of their functional domains.* J Bacteriol, 1993. **175**(19): p. 6067-74.

178. Schumacher, J., et al., *Structures and organisation of AAA+ enhancer binding proteins in transcriptional activation.* J Struct Biol, 2006. **156**(1): p. 190-9.

179. Maggiolo, A.O., et al., *Intradimeric Walker A ATPases: Conserved Features of A Functionally Diverse Family.* J Mol Biol, 2023. **435**(11): p. 167965.

180. Rombel, I., et al., *MgATP binding and hydrolysis determinants of NtrC, a bacterial enhancer-binding protein.* J Bacteriol, 1999. **181**(15): p. 4628-38.

181. Schumacher, J., et al., *ATP-dependent transcriptional activation by bacterial PspF AAA+protein.* J Mol Biol, 2004. **338**(5): p. 863-75.

182. Schumacher, J., et al., *Sensor I threonine of the AAA+ ATPase transcriptional activator PspF is involved in coupling nucleotide triphosphate hydrolysis to the restructuring of sigma 54-RNA polymerase.* J Biol Chem, 2007. **282**(13): p. 9825-9833.

183. Zhang, X., et al., *Mechanochemical ATPases and transcriptional activation.* Mol Microbiol, 2002. **45**(4): p. 895-903.

184. Joly, N., P.C. Burrows, and M. Buck, *An intramolecular route for coupling ATPase activity in AAA+ proteins for transcription activation.* J Biol Chem, 2008. **283**(20): p. 13725-35.

185. Rappas, M., D. Bose, and X. Zhang, *Bacterial enhancer-binding proteins: unlocking sigma54-dependent gene transcription.* Curr Opin Struct Biol, 2007. **17**(1): p. 110-6.

186. Bordes, P., et al., *The ATP hydrolyzing transcription activator phage shock protein F of Escherichia coli: identifying a surface that binds sigma 54.* Proc Natl Acad Sci U S A, 2003. **100**(5): p. 2278-83.

187. Jovanovic, G., L. Weiner, and P. Model, *Identification, nucleotide sequence, and characterization of PspF, the transcriptional activator of the Escherichia coli stress-induced psp operon.* J Bacteriol, 1996. **178**(7): p. 1936-45.

188. Brissette, J.L., et al., *Phage shock protein, a stress protein of Escherichia coli.* Proc Natl Acad Sci U S A, 1990. **87**(3): p. 862-6.

189. Park, S., et al., *Two-component signaling in the AAA + ATPase DctD: binding Mg2+ and BeF3- selects between alternate dimeric states of the receiver domain.* FASEB J, 2002. **16**(14): p. 1964-6.

190. Pittard, A.J. and B.E. Davidson, *TyrR protein of Escherichia coli and its role as repressor and activator.* Mol Microbiol, 1991. **5**(7): p. 1585-92.

191. Pittard, J., H. Camakaris, and J. Yang, *The TyrR regulon.* Mol Microbiol, 2005. **55**(1): p. 16-26.

192. Studholme, D.J. and R. Dixon, *Domain architectures of sigma54-dependent transcriptional activators.* J Bacteriol, 2003. **185**(6): p. 1757-67.

193. Ponting, C.P. and L. Aravind, *PAS: a multifunctional domain family comes to light.* Curr Biol, 1997. **7**(11): p. R674-7.

194. Taylor, B.L. and I.B. Zhulin, *PAS domains: internal sensors of oxygen, redox potential, and light.* Microbiol Mol Biol Rev, 1999. **63**(2): p. 479-506.

195. Ho, Y.S., L.M. Burden, and J.H. Hurley, *Structure of the GAF domain, a ubiquitous signaling motif and a new class of cyclic GMP receptor.* EMBO J, 2000. **19**(20): p. 5288-99.

196. Shingler, V., *Signal sensing by sigma 54-dependent regulators: derepression as a control mechanism.* Mol Microbiol, 1996. **19**(3): p. 409-16.

197. Lee, S.Y., et al., *Regulation of the transcriptional activator NtrC1: structural studies of the regulatory and AAA+ ATPase domains.* Genes Dev, 2003. **17**(20): p. 2552-63.

198. Drummond, M.H., A. Contreras, and L.A. Mitchenall, *The function of isolated domains and chimaeric proteins constructed from the transcriptional activators NifA and NtrC of Klebsiella pneumoniae.* Mol Microbiol, 1990. **4**(1): p. 29-37.

199. Weiss, D.S., et al., *The phosphorylated form of the enhancer-binding protein NTRC has an ATPase activity that is essential for activation of transcription.* Cell, 1991. **67**(1): p. 155-67.

200. De Carlo, S., et al., *The structural basis for regulated assembly and function of the transcriptional activator NtrC.* Genes Dev, 2006. **20**(11): p. 1485-95.

201. North, A.K. and S. Kustu, *Mutant forms of the enhancer-binding protein NtrC can activate transcription from solution.* J Mol Biol, 1997. **267**(1): p. 17-36.

202. Jovanovic, G., J. Rakonjac, and P. Model, *In vivo and in vitro activities of the Escherichia coli sigma54 transcription activator, PspF, and its DNA-binding mutant, PspFDeltaHTH.* J Mol Biol, 1999. **285**(2): p. 469-83.

203. Berger, D.K., F. Narberhaus, and S. Kustu, *The isolated catalytic domain of NIFA, a bacterial enhancer-binding protein, activates transcription in vitro: activation is inhibited by NIFL.* Proc Natl Acad Sci U S A, 1994. **91**(1): p. 103-7.

204. Huala, E. and F.M. Ausubel, *The central domain of Rhizobium meliloti NifA is sufficient to activate transcription from the R. meliloti nifH promoter.* J Bacteriol, 1989. **171**(6): p. 3354-65.

205. Morett, E., W. Cannon, and M. Buck, *The DNA-binding domain of the transcriptional activator protein NifA resides in its carboxy terminus, recognises the upstream activator sequences of nif promoters and can be separated from the positive control function of NifA.* Nucleic Acids Res, 1988. **16**(24): p. 11469-88.

206. Beck, L.L., T.G. Smith, and T.R. Hoover, *Look, no hands! Unconventional transcriptional activators in bacteria.* Trends Microbiol, 2007. **15**(12): p. 530-7.

207. Niehus, E., et al., *Genome-wide analysis of transcriptional hierarchy and feedback regulation in the flagellar system of Helicobacter pylori.* Mol Microbiol, 2004. **52**(4): p. 947-61.

208. Koo, I.C. and R.S. Stephens, *A developmentally regulated two-component signal transduction system in Chlamydia.* J Biol Chem, 2003. **278**(19): p. 17314-9.

209. Brahmachary, P., et al., *Helicobacter pylori FlgR is an enhancer-independent activator of sigma54-RNA polymerase holoenzyme.* J Bacteriol, 2004. **186**(14): p. 4535-42.

210. Spohn, G. and V. Scarlato, *Motility of Helicobacter pylori is coordinately regulated by the transcriptional activator FlgR, an NtrC homolog.* J Bacteriol, 1999. **181**(2): p. 593-9.

211. Reitzer, L.J. and B. Magasanik, *Isolation of the nitrogen assimilation regulator NR(I), the*

product of the glnG gene of Escherichia coli. Proc Natl Acad Sci U S A, 1983. **80**(18): p. 5554-8.

212. Poggio, S., et al., *The four different sigma(54) factors of Rhodobacter sphaeroides are not functionally interchangeable.* Mol Microbiol, 2002. **46**(1): p. 75-85.

213. Bowman, W.C. and R.G. Kranz, *A bacterial ATP-dependent, enhancer binding protein that activates the housekeeping RNA polymerase.* Genes Dev, 1998. **12**(12): p. 1884-93.

214. Hsieh, M.L., D.M. Hinton, and C.M. Waters, *VpsR and cyclic di-GMP together drive transcription initiation to activate biofilm formation in Vibrio cholerae.* Nucleic Acids Res, 2018. **46**(17): p. 8876-8887.

215. Studholme, D.J. and M. Buck, *The biology of enhancer-dependent transcriptional regulation in bacteria: insights from genome sequences.* FEMS Microbiol Lett, 2000. **186**(1): p. 1-9.

216. Blattner, F.R., et al., *The complete genome sequence of Escherichia coli K-12.* Science, 1997. **277**(5331): p. 1453-62.

217. Curtis, P.D. and Y.V. Brun, *Getting in the loop: regulation of development in Caulobacter crescentus.* Microbiol Mol Biol Rev, 2010. **74**(1): p. 13-41.

218. Stein, B.J., A. Fiebig, and S. Crosson, *The ChvG-ChvI and NtrY-NtrX Two-Component Systems Coordinately Regulate Growth of Caulobacter crescentus.* J Bacteriol, 2021. **203**(17): p. e0019921.

219. Fiebig, A., et al., *A cell cycle and nutritional checkpoint controlling bacterial surface adhesion.* PLoS Genet, 2014. **10**(1): p. e1004101.

220. Jiang, P. and A.J. Ninfa, *Regulation of autophosphorylation of Escherichia coli nitrogen regulator II by the PII signal transduction protein.* J Bacteriol, 1999. **181**(6): p. 1906-11.

221. Keener, J. and S. Kustu, *Protein kinase and phosphoprotein phosphatase activities of nitrogen regulatory proteins NTRB and NTRC of enteric bacteria: roles of the conserved amino-terminal domain of NTRC.* Proc Natl Acad Sci U S A, 1988. **85**(14): p. 4976-80.

222. Ninfa, A.J. and P. Jiang, *PII signal transduction proteins: sensors of alpha-ketoglutarate that regulate nitrogen metabolism.* Curr Opin Microbiol, 2005. **8**(2): p. 168-73.

223. Schumacher, J., et al., *Nitrogen and carbon status are integrated at the transcriptional level by the nitrogen regulator NtrC in vivo.* mBio, 2013. **4**(6): p. e00881-13.

224. Aquino, P., et al., *Coordinated regulation of acid resistance in Escherichia coli.* BMC Syst Biol, 2017. **11**(1): p. 1.

225. Guo, M.S., et al., *A Bacterial Chromosome Structuring Protein Binds Overtwisted DNA to Stimulate Type II Topoisomerases and Enable DNA Replication.* Cell, 2018. **175**(2): p. 583-597 e23.

226. Ricci, D.P., et al., *Cell cycle progression in Caulobacter requires a nucleoid-associated protein with high AT sequence recognition.* Proc Natl Acad Sci U S A, 2016. **113**(40): p. E5952-E5961.

227. Fumeaux, C., et al., *Cell cycle transition from S-phase to G1 in Caulobacter is mediated by ancestral virulence regulators.* Nat Commun, 2014. **5**: p. 4081.

228. Stewart, V., *Regulation of nitrate and nitrite reductase synthesis in enterobacteria.* Antonie Van Leeuwenhoek, 1994. **66**(1-3): p. 37-45.

229. Cheng, A.T., et al., *NtrC Adds a New Node to the Complex Regulatory Network of Biofilm Formation and vps Expression in Vibrio cholerae.* J Bacteriol, 2018. **200**(15).

230. Hervas, A.B., et al., *NtrC-dependent regulatory network for nitrogen assimilation in Pseudomonas putida.* J Bacteriol, 2009. **191**(19): p. 6123-35.

231. Toukdarian, A. and C. Kennedy, *Regulation of nitrogen metabolism in Azotobacter vinelandii: isolation of ntr and glnA genes and construction of ntr mutants.* EMBO J, 1986. **5**(2): p. 399-407.

232. Wardhan, H., M.J. McPherson, and G.R. Sastry, *Identification, cloning, and sequence analysis of the nitrogen regulation gene ntrC of Agrobacterium tumefaciens C58.* Mol Plant Microbe Interact, 1989. **2**(5): p. 241-8.

233. Dago, A.E., et al., *A role for the conserved GAFTGA motif of AAA+ transcription activators in sensing promoter DNA conformation.* J Biol Chem, 2007. **282**(2): p. 1087-97.

234. Capra, E.J., et al., *Adaptive mutations that prevent crosstalk enable the expansion of paralogous signaling protein families.* Cell, 2012. **150**(1): p. 222-32.

235. Smith, J.G., et al., *A search for amino acid substitutions that universally activate response regulators.* Mol Microbiol, 2004. **51**(3): p. 887-901.

236. van Heeswijk, W.C., et al., *An alternative PII protein in the regulation of glutamine synthetase in Escherichia coli.* Mol Microbiol, 1996. **21**(1): p. 133-46.

237. Fiebig, A., et al., *Interaction specificity, toxicity and regulation of a paralogous set of ParE/RelE-family toxin-antitoxin systems.* Mol Microbiol, 2010. **77**(1): p. 236-51.

238. Collier, J. and L. Shapiro, *Feedback control of DnaA-mediated replication initiation by replisome-associated HdaA protein in Caulobacter.* J Bacteriol, 2009. **191**(18): p. 5706-16.

239. Aakre, C.D., et al., *A bacterial toxin inhibits DNA replication elongation through a direct interaction with the beta sliding clamp.* Mol Cell, 2013. **52**(5): p. 617-28.

240. Garcia-Bayona, L., M.S. Guo, and M.T. Laub, *Contact-dependent killing by Caulobacter crescentus via cell surface-associated, glycine zipper proteins.* Elife, 2017. **6**.

241. Anantharaman, V., E.V. Koonin, and L. Aravind, *Comparative genomics and evolution of*

proteins involved in RNA metabolism. Nucleic Acids Res, 2002. **30**(7): p. 1427-64.

242. Andrews, E.S.V. and V.L. Arcus, *PhoH2 proteins couple RNA helicase and RNAse activities.* Protein Sci, 2020. **29**(4): p. 883-892.

243. da Silva Neto, J.F., et al., *Fur controls iron homeostasis and oxidative stress defense in the oligotrophic alpha-proteobacterium Caulobacter crescentus.* Nucleic Acids Res, 2009. **37**(14): p. 4812-25.

244. Gonin, M., et al., *Regulation of stalk elongation by phosphate in Caulobacter crescentus.* J Bacteriol, 2000. **182**(2): p. 337-47.

245. de Young, K.D., G. Stankeviciute, and E.A. Klein, *Sugar-Phosphate Metabolism Regulates Stationary-Phase Entry and Stalk Elongation in Caulobacter crescentus.* J Bacteriol, 2020. **202**(4).

246. Ishige, T., et al., *The phosphate starvation stimulon of Corynebacterium glutamicum determined by DNA microarray analyses.* J Bacteriol, 2003. **185**(15): p. 4519-29.

247. Kim, S.K., et al., *Molecular analysis of the phoH gene, belonging to the phosphate regulon in Escherichia coli.* J Bacteriol, 1993. **175**(5): p. 1316-24.

248. Ravenscroft, N., et al., *Identification, isolation, and structural studies of extracellular polysaccharides produced by Caulobacter crescentus.* J Bacteriol, 1991. **173**(18): p. 5677-84.

249. Ho, S.N., et al., *Site-directed mutagenesis by overlap extension using the polymerase chain reaction.* Gene, 1989. **77**(1): p. 51-9.

250. McLaughlin, M., et al., *A cryptic transcription factor regulates Caulobacter adhesin development.* PLoS Genet, 2022. **18**(10): p. e1010481.

251. Ely, B., *Genetics of Caulobacter crescentus.* Methods Enzymol, 1991. **204**: p. 372-84.

252. Hmelo, L.R., et al., *Precision-engineering the Pseudomonas aeruginosa genome with two-step allelic exchange.* Nat Protoc, 2015. **10**(11): p. 1820-41.

253. Pitcher, D.G., N.A. Saunders, and R.J. Owen, *Rapid extraction of bacterial genomic DNA with guanidium thiocyanate.* Lett Appl Microbiol, 1989. **8**: p. 151-156.

254. Deatherage, D.E. and J.E. Barrick, *Identification of mutations in laboratory-evolved microbes from next-generation sequencing data using breseq.* Methods Mol Biol, 2014. **1151**: p. 165-88.

255. de Hoon, M.J., et al., *Open source clustering software.* Bioinformatics, 2004. **20**(9): p. 1453-4.

256. Saldanha, A.J., *Java Treeview--extensible visualization of microarray data.* Bioinformatics, 2004. **20**(17): p. 3246-8.

257. Bharmal, M.H., J.R. Aretakis, and J.M. Schrader, *An Improved Caulobacter crescentus*

Operon Annotation Based on Transcriptome Data. Microbiol Resour Announc, 2020. **9**(44).

258. Zhou, B., et al., *The global regulatory architecture of transcription during the Caulobacter cell cycle.* PLoS Genet, 2015. **11**(1): p. e1004831.

259. Zhu, L.J., et al., *ChIPpeakAnno: a Bioconductor package to annotate ChIP-seq and ChIP-chip data.* BMC Bioinformatics, 2010. **11**: p. 237.

260. Bailey, T.L., et al., *The MEME Suite.* Nucleic Acids Res, 2015. **43**(W1): p. W39-49.

261. Hartmann, R., et al., *BacStalk: A comprehensive and interactive image analysis software tool for bacterial cell biology.* Mol Microbiol, 2020. **114**(1): p. 140-150.

262. Lasker, K., T.H. Mann, and L. Shapiro, *An intracellular compass spatially coordinates cell cycle modules in Caulobacter crescentus.* Curr Opin Microbiol, 2016. **33**: p. 131-139.

263. Hirschman, J., et al., *Products of nitrogen regulatory genes ntrA and ntrC of enteric bacteria activate glnA transcription in vitro: evidence that the ntrA product is a sigma factor.* Proc Natl Acad Sci U S A, 1985. **82**(22): p. 7525-9.

264. Hunt, T.P. and B. Magasanik, *Transcription of glnA by purified Escherichia coli components: core RNA polymerase and the products of glnF, glnG, and glnL.* Proc Natl Acad Sci U S A, 1985. **82**(24): p. 8453-7.

265. Wong, P.K., et al., *In vitro transcription of the nitrogen fixation regulatory operon nifLA of Klebsiella pneumoniae.* J Bacteriol, 1987. **169**(6): p. 2876-80.

266. North, H., et al., *The Caulobacter NtrB-NtrC two-component system bridges nitrogen assimilation and cell development.* J Bacteriol, 2023. **205**(10): p. e0018123.

267. Iniesta, A.A. and L. Shapiro, *A bacterial control circuit integrates polar localization and proteolysis of key regulatory proteins with a phospho-signaling cascade.* Proc Natl Acad Sci U S A, 2008. **105**(43): p. 16602-7.

268. Delaby, M., G. Panis, and P.H. Viollier, *Bacterial cell cycle and growth phase switch by the essential transcriptional regulator CtrA.* Nucleic Acids Res, 2019. **47**(20): p. 10628-10644.

269. Gray, V.E., R.J. Hause, and D.M. Fowler, *Analysis of Large-Scale Mutagenesis Data To Assess the Impact of Single Amino Acid Substitutions.* Genetics, 2017. **207**(1): p. 53-61.

270. Hwang, I., et al., *Physical evidence for a phosphorylation-dependent conformational change in the enhancer-binding protein NtrC.* Proc Natl Acad Sci U S A, 1999. **96**(9): p. 4880-5.

271. Poindexter, J.S., *Oligotrophy: Fast and Famine Existence.* Advances in Microbial Ecology, 1981. **5**: p. 63-89.

272. Dworkin, J. and C.S. Harwood, *Metabolic Reprogramming and Longevity in Quiescence.* Annu Rev Microbiol, 2022. **76**: p. 91-111.

273. Sherlock, M.E., N. Sudarsan, and R.R. Breaker, *Riboswitches for the alarmone ppGpp expand the collection of RNA-based signaling systems.* Proc Natl Acad Sci U S A, 2018. **115**(23): p. 6052-6057.

274. Shaner, N.C., et al., *A bright monomeric green fluorescent protein derived from Branchiostoma lanceolatum.* Nat Methods, 2013. **10**(5): p. 407-9.

275. Sun, Z., et al., *Live-Cell Imaging of Guanosine Tetra- and Pentaphosphate (p)ppGpp with RNA-based Fluorescent Sensors*.* Angew Chem Int Ed Engl, 2021. **60**(45): p. 24070-24074.

276. Schreiber, G., et al., *Overexpression of the relA gene in Escherichia coli.* J Biol Chem, 1991. **266**(6): p. 3760-7.

277. Joshi, K.K., et al., *An Adaptor Hierarchy Regulates Proteolysis during a Bacterial Cell Cycle.* Cell, 2015. **163**(2): p. 419-31.

278. Ryan, K.R., E.M. Judd, and L. Shapiro, *The CtrA response regulator essential for Caulobacter crescentus cell-cycle progression requires a bipartite degradation signal for temporally controlled proteolysis.* J Mol Biol, 2002. **324**(3): p. 443-55.

279. Ardissone, S. and P.H. Viollier, *Interplay between flagellation and cell cycle control in Caulobacter.* Curr Opin Microbiol, 2015. **28**: p. 83-92.

280. Quon, K.C., G.T. Marczynski, and L. Shapiro, *Cell cycle control by an essential bacterial two-component signal transduction protein.* Cell, 1996. **84**(1): p. 83-93.

281. Sanselicio, S., et al., *Topological control of the Caulobacter cell cycle circuitry by a polarized single-domain PAS protein.* Nat Commun, 2015. **6**: p. 7005.

282. Hood, R.D., et al., *The stringent response regulates adaptation to darkness in the cyanobacterium Synechococcus elongatus.* Proc Natl Acad Sci U S A, 2016. **113**(33): p. E4867-76.

283. Izutsu, K., A. Wada, and C. Wada, *Expression of ribosome modulation factor (RMF) in Escherichia coli requires ppGpp.* Genes Cells, 2001. **6**(8): p. 665-76.

284. Schafer, H., et al., *The alarmones (p)ppGpp are part of the heat shock response of Bacillus subtilis.* PLoS Genet, 2020. **16**(3): p. e1008275.

285. Benson, A.K., J. Wu, and A. Newton, *The role of FlbD in regulation of flagellar gene transcription in Caulobacter crescentus.* Res Microbiol, 1994. **145**(5-6): p. 420-30.

286. Newton, A., et al., *Genetic switching in the flagellar gene hierarchy of Caulobacter requires negative as well as positive regulation of transcription.* Proc Natl Acad Sci U S A, 1989. **86**(17): p. 6651-5.

287. Wingrove, J.A. and J.W. Gober, *A sigma 54 transcriptional activator also functions as a pole-specific repressor in Caulobacter.* Genes Dev, 1994. **8**(15): p. 1839-52.

288. Xu, H., A. Dingwall, and L. Shapiro, *Negative transcriptional regulation in the Caulobacter flagellar hierarchy.* Proc Natl Acad Sci U S A, 1989. **86**(17): p. 6656-60.

289. Luria, S.E. and M. Delbruck, *Mutations of Bacteria from Virus Sensitivity to Virus Resistance.* Genetics, 1943. **28**(6): p. 491-511.

290. Charlier, D., J. Piette, and N. Glansdorff, *IS3 can function as a mobile promoter in E. coli.* Nucleic Acids Res, 1982. **10**(19): p. 5935-48.

291. Groisman, E.A., *Feedback Control of Two-Component Regulatory Systems.* Annu Rev Microbiol, 2016. **70**: p. 103-24.

292. Schlimpert, S., et al., *General protein diffusion barriers create compartments within bacterial cells.* Cell, 2012. **151**(6): p. 1270-82.

293. Ireland, M.M., et al., *Proteomic analysis of the Caulobacter crescentus stalk indicates competence for nutrient uptake.* Mol Microbiol, 2002. **45**(4): p. 1029-41.

294. Wagner, J.K., et al., *A nutrient uptake role for bacterial cell envelope extensions.* Proc Natl Acad Sci U S A, 2006. **103**(31): p. 11772-7.

295. Klein, E.A., et al., *Physiological role of stalk lengthening in Caulobacter crescentus.* Commun Integr Biol, 2013. **6**(4): p. e24561.

296. Lubin, E.A., et al., *Identification of the PhoB Regulon and Role of PhoU in the Phosphate Starvation Response of Caulobacter crescentus.* J Bacteriol, 2016. **198**(1): p. 187-200.

297. Hu, P., et al., *Whole-genome transcriptional analysis of heavy metal stresses in Caulobacter crescentus.* J Bacteriol, 2005. **187**(24): p. 8437-49.

298. Santos-Beneit, F., *The Pho regulon: a huge regulatory network in bacteria.* Front Microbiol, 2015. **6**: p. 402.

299. Alford, M.A., et al., *NtrBC Regulates Invasiveness and Virulence of Pseudomonas aeruginosa During High-Density Infection.* Front Microbiol, 2020. **11**: p. 773.

300. Kim, H.S., S.J. Park, and K.H. Lee, *Role of NtrC-regulated exopolysaccharides in the biofilm formation and pathogenic interaction of Vibrio vulnificus.* Mol Microbiol, 2009. **74**(2): p. 436-53.

301. Liu, Y., et al., *NtrC-dependent control of exopolysaccharide synthesis and motility in Burkholderia cenocepacia H111.* PLoS One, 2017. **12**(6): p. e0180362.

302. Herr, K.L., et al., *Exopolysaccharide production in Caulobacter crescentus: A resource allocation trade-off between protection and proliferation.* PLoS One, 2018. **13**(1): p. e0190371.

303. Cullen, P.J., W.C. Bowman, and R.G. Kranz, *In vitro reconstitution and characterization of the Rhodobacter capsulatus NtrB and NtrC two-component system.* J Biol Chem, 1996. **271**(11): p. 6530-6.

304. Hsieh, M.L., et al., *The Vibrio cholerae master regulator for the activation of biofilm biogenesis genes, VpsR, senses both cyclic di-GMP and phosphate.* Nucleic Acids Res, 2022. **50**(8): p. 4484-4499.

305. Biondi, E.G., et al., *A phosphorelay system controls stalk biogenesis during cell cycle progression in Caulobacter crescentus.* Mol Microbiol, 2006. **59**(2): p. 386-401.

306. Monod, J., *Chance and necessity; an essay on the natural philosophy of modern biology (English Translation)*. 1972, New York: Vintage Books.

307. Collier, J., *Cell division control in Caulobacter crescentus.* Biochim Biophys Acta Gene Regul Mech, 2019. **1862**(7): p. 685-690.

308. van Teeseling, M.C.F. and M. Thanbichler, *Generating asymmetry in a changing environment: cell cycle regulation in dimorphic alphaproteobacteria.* Biol Chem, 2020. **401**(12): p. 1349-1363.

309. Beaufay, F., et al., *A NAD-dependent glutamate dehydrogenase coordinates metabolism with cell division in Caulobacter crescentus.* EMBO J, 2015. **34**(13): p. 1786-800.

310. Boutte, C.C., J.T. Henry, and S. Crosson, *ppGpp and polyphosphate modulate cell cycle progression in Caulobacter crescentus.* J Bacteriol, 2012. **194**(1): p. 28-35.

311. Hallgren, J., et al., *Phosphate starvation decouples cell differentiation from DNA replication control in the dimorphic bacterium Caulobacter crescentus.* PLoS Genet, 2023. **19**: p. e1010882.

312. Narayanan, S., et al., *A cell cycle-controlled redox switch regulates the topoisomerase IV activity.* Genes Dev, 2015. **29**(11): p. 1175-87.

313. England, J.C., et al., *Global regulation of gene expression and cell differentiation in Caulobacter crescentus in response to nutrient availability.* J Bacteriol, 2010. **192**(3): p. 819-33.

314. Xu, C., et al., *Cell cycle control and environmental response by second messengers in Caulobacter crescentus.* BMC Bioinformatics, 2020. **21**(Suppl 14): p. 408.

315. Glenn, S., et al., *Coupling of cell growth modulation to asymmetric division and cell cycle regulation in Caulobacter crescentus.* Proc Natl Acad Sci U S A, 2024. **121**(41): p. e2406397121.

316. Magasanik, B., *Gene regulation from sites near and far.* New Biol, 1989. **1**(3): p. 247-51.

317. Hellman, L.M. and M.G. Fried, *Electrophoretic mobility shift assay (EMSA) for detecting protein-nucleic acid interactions.* Nat Protoc, 2007. **2**(8): p. 1849-61.

318. Gao, S., et al., *Bacterial capsules: Occurrence, mechanism, and function.* NPJ Biofilms Microbiomes, 2024. **10**(1): p. 21.

319. He, H., et al., *Stringent response regulation of biofilm formation in Vibrio cholerae.* J Bacteriol, 2012. **194**(11): p. 2962-72.

320. Malgieri, G., et al., *The prokaryotic Cys2His2 zinc-finger adopts a novel fold as revealed by the NMR structure of Agrobacterium tumefaciens Ros DNA-binding domain.* Proc Natl Acad Sci U S A, 2007. **104**(44): p. 17341-6.

321. Hauryliuk, V., et al., *Recent functional insights into the role of (p)ppGpp in bacterial physiology.* Nat Rev Microbiol, 2015. **13**(5): p. 298-309.

322. Kriel, A., et al., *Direct regulation of GTP homeostasis by (p)ppGpp: a critical component of viability and stress resistance.* Mol Cell, 2012. **48**(2): p. 231-41.

323. Zhang, Y.E., et al., *(p)ppGpp Regulates a Bacterial Nucleosidase by an Allosteric Two-Domain Switch.* Mol Cell, 2019. **74**(6): p. 1239-1249 e4.

324. Rymer, R.U., et al., *Binding mechanism of metal·NTP substrates and stringent-response alarmones to bacterial DnaG-type primases.* Structure, 2012. **20**(9): p. 1478-89.

325. Ivankovic, A. and M. Jerkovic, *[Iatrogenic factors in periodontal diseases due to inadequate removable construction].* Stomatol Vjesn, 1978. **7**(1-2): p. 41-4.

326. Shyp, V., et al., *Positive allosteric feedback regulation of the stringent response enzyme RelA by its product.* EMBO Rep, 2012. **13**(9): p. 835-9.

327. McWilliam, H., et al., *Analysis Tool Web Services from the EMBL-EBI.* Nucleic Acids Res, 2013. **41**(Web Server issue): p. W597-600.

APPENDIX 1: SUPPLEMENTAL FIGURES FOR CHAPTER 2

Preface

This Appendix is composed of supplemental figures that are referenced to within the body of Chapter 2. Supplemental figures in this Appendix are modified and adapted from their published forms: North H, McLaughlin M, Fiebig A, Crosson, S. (2023) *J Bacteriol.* 205(10):e0018123.

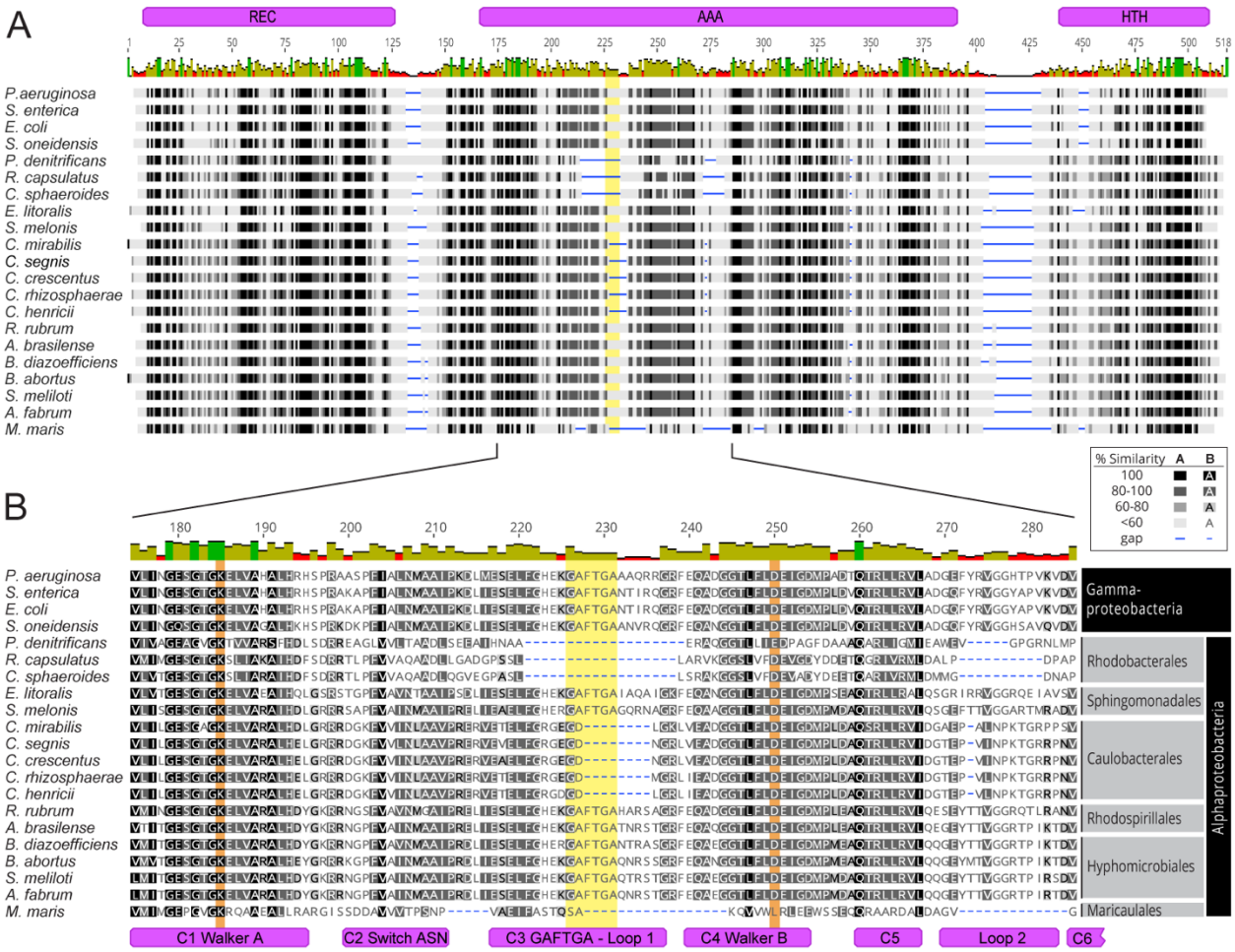

Figure S2.1. Multiple sequence alignment revealing conserved and distinctive characteristics of NtrC/GlnG sequences. (A) Overview of full length NtrC/GlnG protein sequence alignment. Residue numbers indicate alignment positions. (B) Highlight of the sequences surrounding the GAFTGA loop region in the AAA domain. Alignment was performed using Clustal Omega [327], and similarity scores were calculated based on the Blosum62 matrix. In the alignment, gaps are denoted by blue lines, while the L1 loop containing the GAFTGA motif is highlighted in yellow. The domains are described following the nomenclature outlined in Bush and Dixon [167]. Species are indicated at the left of aligned sequences. Full organism names and

Figure S2.1 (cont'd)
genbank accessions for this analysis in the order presented in the alignment are: *Pseudomonas aeruginosa* PAO1 (NZ_CP053028), *Salmonella enterica* subsp. enterica serovar Typhimurium str. 798 (NC_017054), *Escherichia coli* str. K-12 substr. MG1655 (NZ_CP027060), *Shewanella oneidensis* MR-1 (NC_004349), *Paracoccus denitrificans* PD1222 (NC_008686), *Rhodobacter capsulatus* SB 1003 (NC_014035), *Cereibacter sphaeroides* 2.4.1 (formerly *Rhodobacter sphaeroides*; NC_007493), *Erythrobacter litoralis* DSM 8509 (NZ_CP017057), *Sphingomonas melonis* TY (NZ_CP017578), *Caulobacter mirabilis* (NZ_CP024201), *Caulobacter segnis* ATCC 21756 (NC_014100), *Caulobacter crescentus* NA1000 (NC_011916), *Caulobacter rhizosphaerae* (NZ_CP048815), *Caulobacter henricii* (NZ_CP013002), *Rhodospirillum rubrum* ATCC 11170 (NC_007641), *Azospirillum brasilense* (NZ_CP012914), *Bradyrhizobium diazoefficiens* USDA 110 (formerly B. japonicum; NC_004463), *Brucella abortus* 2308 (NC_007618), *Sinorhizobium meliloti* 1021 (NC_003037), *Agrobacterium fabrum* str. C58 (formerly A. tumefaciens; NC_003062), *Maricaulis maris* MCS10 (NC_008347). We note that within the Caulobacterales, we also searched the following complete genomes: *Asticcacaulis excentricus* CB 48 (NC_014816), *Brevundimonas diminuta* (NZ_CP021995), *Brevundimonas nasdae* (NZ_CP080036) and *Brevundimonas subvibrioides* ATCC 15264 (NC_014375). We found that genomes from the genera *Asticcacaulis* and *Brevundimonas* lack *ntrC* and possess only *ntrX* at the *ntr* locus. NtrX appears to be specific to the Alphaproteobacteria and lacks the classical GAFTGA sequence motif; NtrX sequences exhibit a shorter motif (EG**EG---G**xxK/R) where the dashes are gaps compared to the motif found in most enhancer binding proteins (EK**GAFTGA**xxK/R).

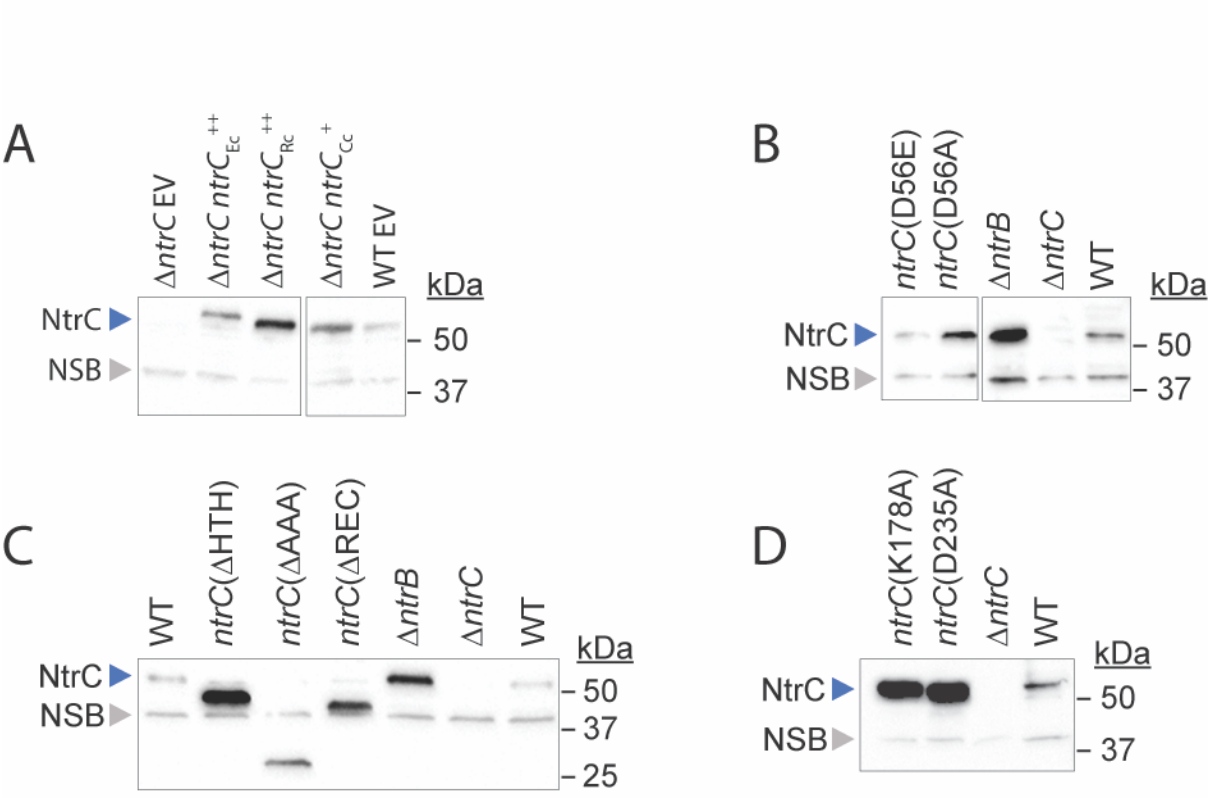

Figure S2.2. Western blot to assess steady state levels of *Caulobacter* NtrC alleles, and *E. coli* and *R. capsulatus* NtrC expressed in *Caulobacter*. In all panels, wild-type *Caulobacter* NtrC is marked by the blue arrow (~52 kDa); the non-specific band (NSB) serving as a loading control is marked with a gray arrow. Panel (A) shows an α-NtrC western blot of lysates from Caulobacter grown to stationary phase in PYE complex medium supplemented with 0.15% xylose. Displayed are WT and Δ*ntrC* carrying either an empty vector (EV) or expression vectors containing *Caulobacter ntrC* under the control of its native promoter ($ntrC_{Cc}^{+}$), or *E. coli* or *R. capsulatus ntrC* under the control of a xylose-inducible promoter ($ntrC_{Ec}^{++}$ or $ntrC_{Rc}^{++}$). Panels (B-C) present an α-NtrC western blot of lysates WT, Δ*ntrC*, Δ*ntrB*, *ntrC*(D56A), *ntrC*(D56E), *ntrC*(ΔREC) (residues deleted: 17-125), *ntrC*(ΔAAA) (residues deleted: 159-363), and *ntrC*(ΔHTH) (residues deleted: 423-462) grown to logarithmic phase in PYE. The predicted molecular weights of NtrC(ΔREC), NtrC(ΔAAA), and NtrC(ΔHTH) are approximately 41 kDa, 30 kDa, and 48 kDa, respectively. Panel (D) shows an α-NtrC western blot of lysates WT, Δ*ntrC*, *ntrC*(K178A) (Walker A mutant), and *ntrC*(D235A) (Walker B mutant) grown to stationary phase in PYE.

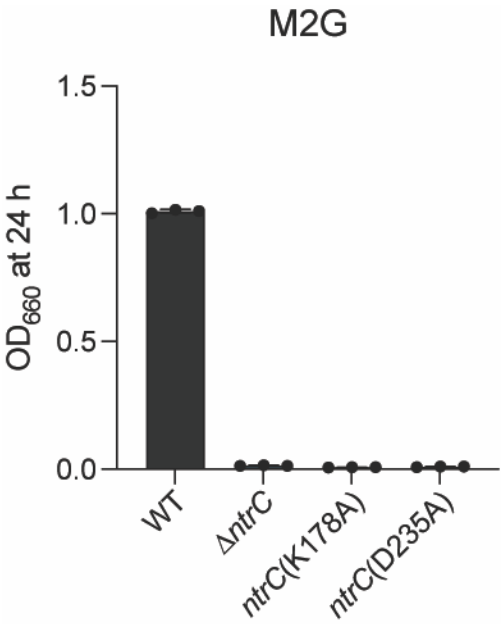

Figure S2.3. Conserved residues of Walker A and Walker B motifs in the NtrC AAA+ domain are required for growth in defined medium. (A) Terminal OD_{660} of WT, Δ*ntrC*, *ntrC*(K178A) (Walker A mutant), and *ntrC*(D235A) (Walker B mutant) after 24 hours (h) of growth in M2G with NH_4^+ as the sole nitrogen source. Data represent mean ± standard deviation of three independent replicates.

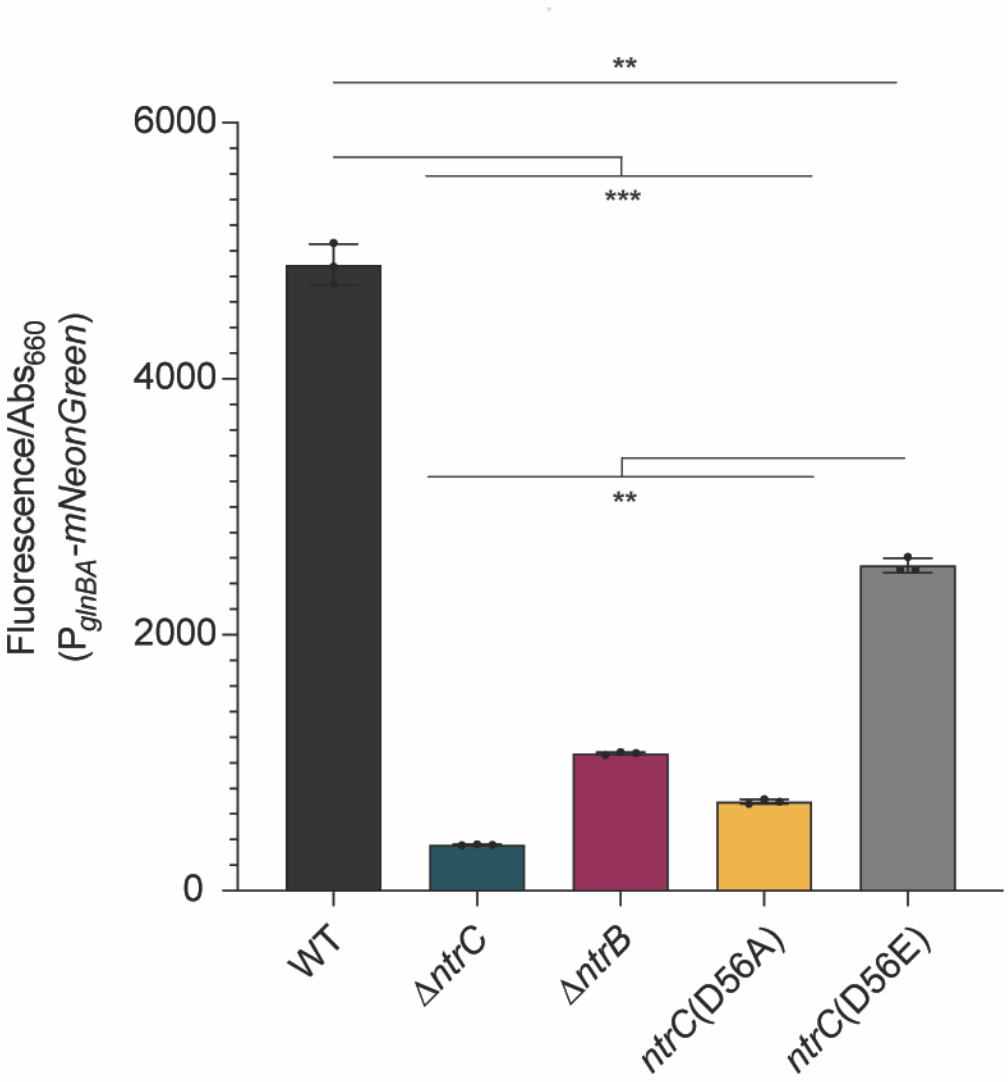

Figure S2.4. P_{glnBA} transcription is diminished in *ntrB* and *ntrC* mutant strains. Transcription from the *glnBA* promoter (P_{glnBA}) was measured in WT, Δ*ntrC*, Δ*ntrB*, ntrC(D56A), *ntrC*(D56E) using a P_{glnBA}-*mNeonGreen* transcriptional fusion reporter. Strains were grown to stationary phase in PYE. Fluorescence signal was measured and normalized to OD_{660}. Data represent mean ± standard deviation of three replicates. Statistical significance was determined by one-way ANOVA followed by Tukey's multiple comparisons test (*** $P < .0001$, ** $P < .0008$).

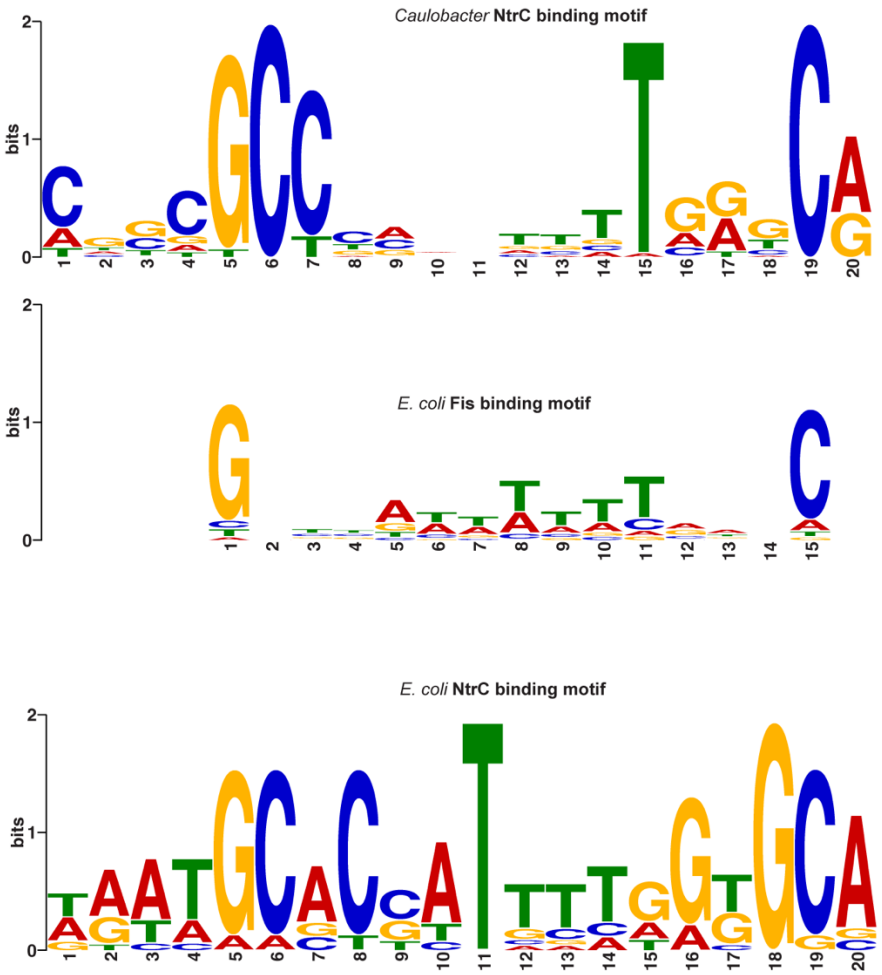

Figure S2.5. *Caulobacter* NtrC binding motif is similar to *E. coli* Fis and NtrC binding motifs. A search of prokaryotic transcription factor binding motifs in SwissRegulon revealed significant similarity between the *Caulobacter* NtrC binding motif and the Fis and NtrC binding motifs of *E. coli* ($P < 0.001$).

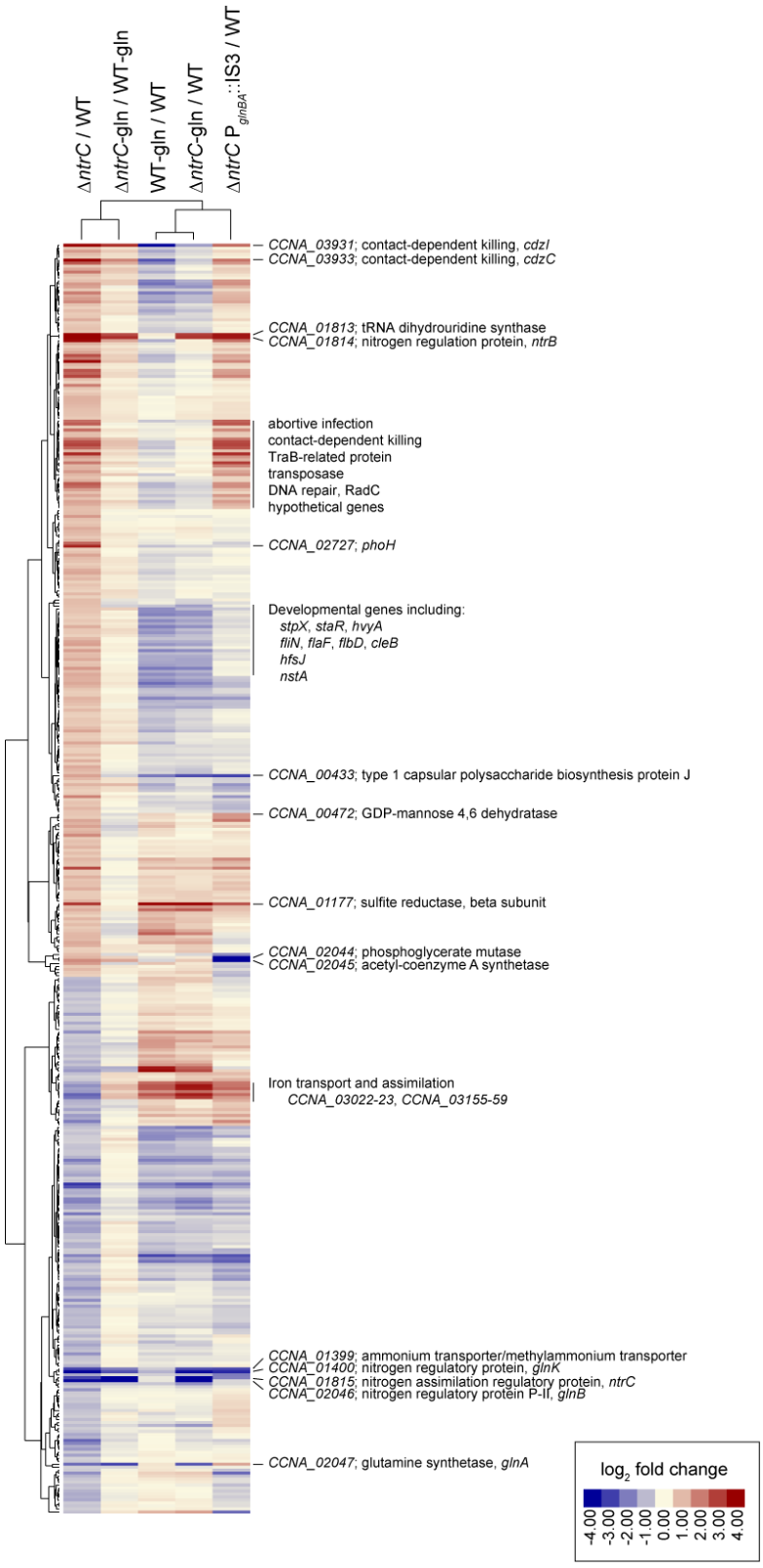

Figure S2.6. Nitrogen-dependent regulation of the NtrC regulon revealed by RNA-seq analysis. The heat map displays the $\log_2$ fold change of 473 genes differentially expressed

Figure S2.6 (cont'd)
between the Δ*ntrC* mutant and WT. Genes with fold change > 1.5, FDR P < 10-6, and WT CPM > 10 are included. Each row represents a gene. Each column represents a comparison between strains and/or different media conditions (PYE complex medium and PYE supplemented with 9.3 mM glutamine (gln)). Hierarchical clustering using Cluster 3.0 was applied, employing an uncentered correlation similarity metric and average linkage for grouping.

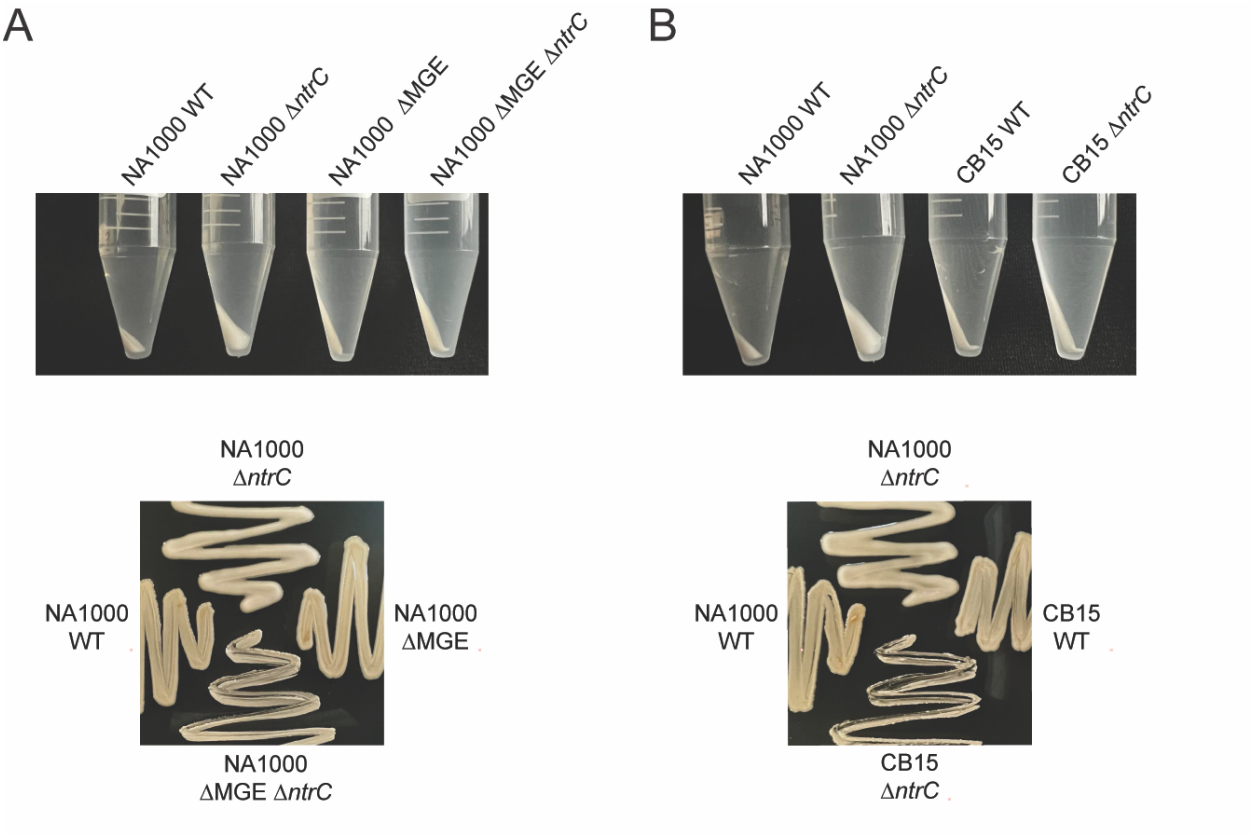

Figure S2.7. Mucoid phenotype of Δ*ntrC* requires the presence of the 26 kb mobile genetic element (MGE). (A) Top panel: Cell pellets of Caulobacter crescentus strain NA1000 WT, NA1000 Δ*ntrC*, NA1000 in which the MGE had spontaneously excised (NA1000 ΔMGE), and NA1000 ΔMGE Δ*ntrC*. Strains were grown overnight in PYE. Overnight cultures were normalized to OD_{660} 0.5 and cells from 10 ml were centrifuged at 7,197 x g for 3 min at 4°C. Bottom panel: Growth of NA1000 WT, NA1000 Δ*ntrC*, NA1000 ΔMGE Δ*ntrC* on PYE agar supplemented with 3% sucrose. Plates were incubated for 4 days at 30°C. (B) Top panel: Cell pellets of NA1000 WT, NA1000 Δ*ntrC*, CB15 WT, and CB15 Δ*ntrC*. Cell pellets were prepared as described in panel A. Bottom panel: Growth of NA1000 WT, NA1000 Δ*ntrC*, CB15 WT, and CB15 Δ*ntrC* in same conditions described in panel A.

APPENDIX 2: SUPPLEMENTAL FIGURES FOR CHAPTER 3

Preface

This Appendix is composed of supplemental figures that are referenced to within the body of Chapter 3. Molly Hydorn and Jonathan Dworkin provided the riboswitch for quantification of ppGpp.

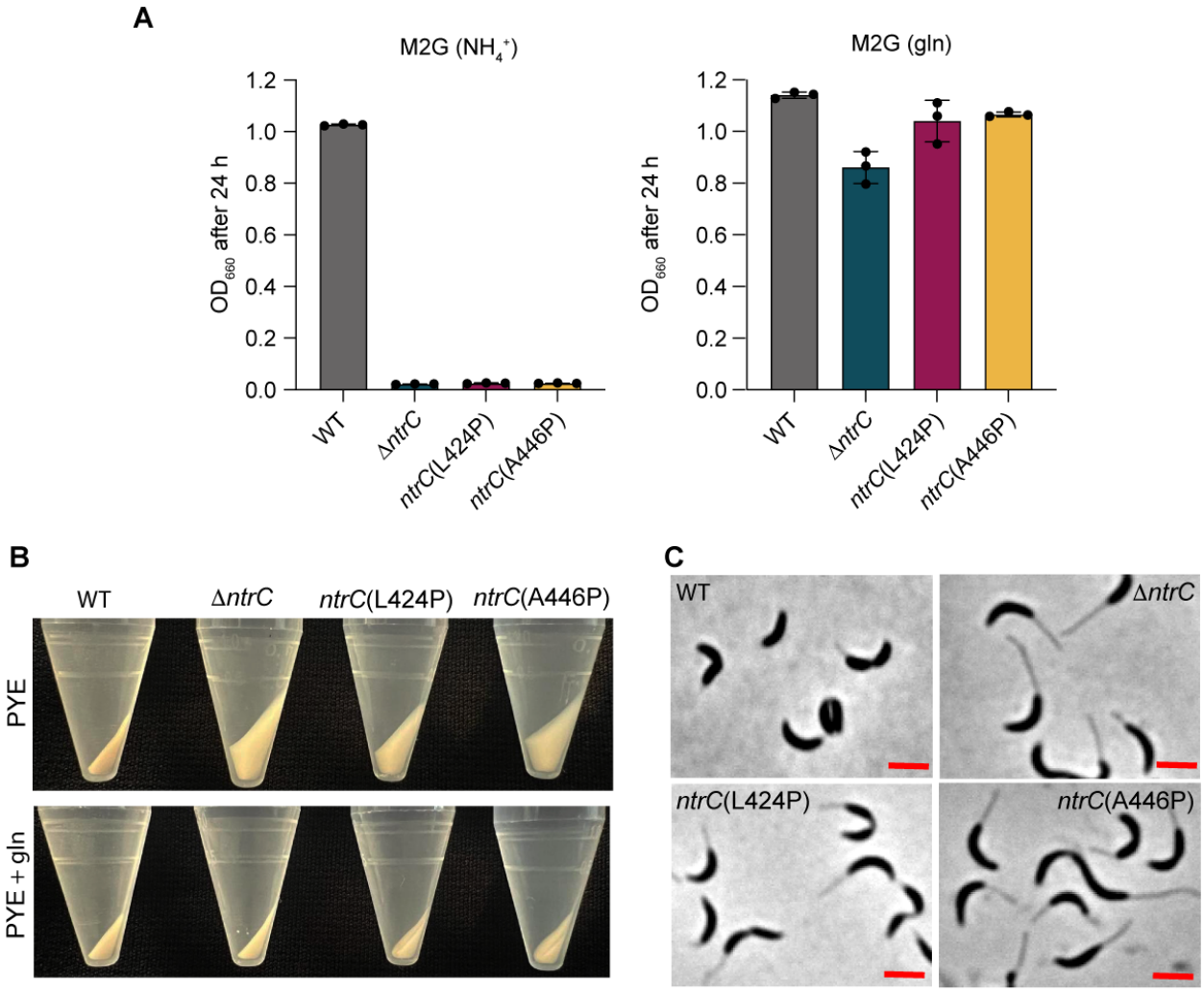

Figure S3.1. NtrC(HTH) point mutants phenocopy Δ*ntrC* in an otherwise wild-type background of *Caulobacter*. (A) Terminal culture densities of WT, Δ*ntrC*, *ntrC*(L424P), and *ntrC*(A446P). Culture growth was measured spectrophotometrically at 660 nm (OD_{660}) after 24 hours (h) of growth in defined M2G or M2G in which NH_4^+ was replaced with molar-equivalent (9.3 mM final concentration) glutamine (gln). Data represent the mean ± standard deviation of three biological replicates. (B) Cell pellets of WT, Δ*ntrC*, *ntrC*(L424P), and *ntrC*(A446P) strains

Figure S3.1 (cont'd)
highlighting differences in pellet density. Strains were grown overnight in PYE complex medium or PYE supplemented with 9.3 mM gln, as indicated. Overnight cultures were normalized to OD_{660} 0.5 and 10 ml of each culture was centrifuged at 7,197 × *g* for 3 min at 4°C to pellet the cells. (C) Representative phase contrast images of cell stalks from WT, Δ*ntrC*, *ntrC*(L424P), and *ntrC*(A446P) strains. Images were taken after 24 h of growth in PYE broth to capture cells in stationary phase. Scale bar (red, bottom right) equals 5 μm.

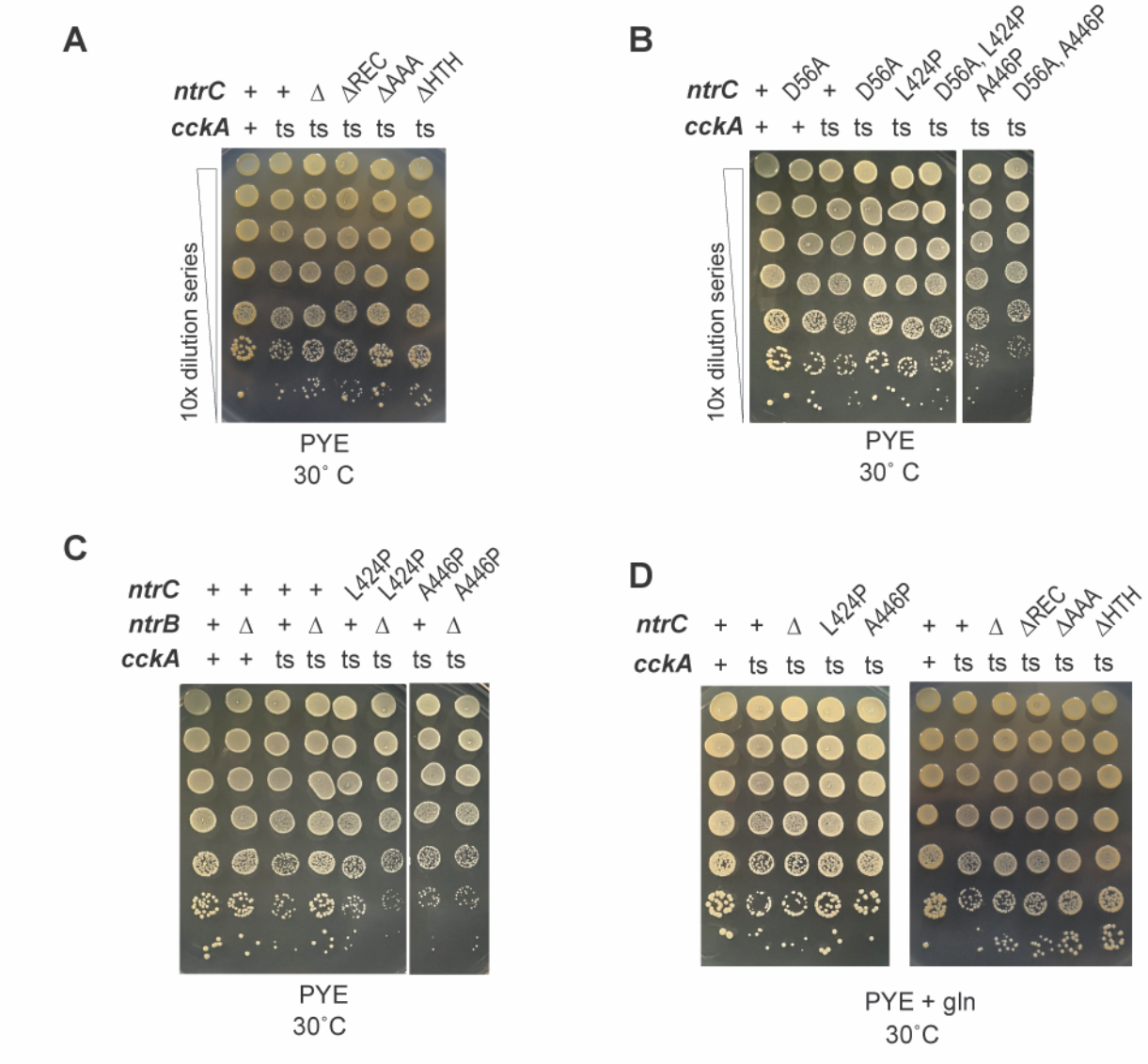

Figure S3.2. Permissive temperature control titers. Control (30˚C) titers corresponding to the following main text figure panels in Chapter 3: (A) **Figure 3.2E**, (B) **Figure 3.3A**, (C) **Figure 3.3B**, and (D) **Figure 3.3C**. All dilution series were spotted onto PYE or PYE supplemented with an additional 9.3 mM glutamine (gln) and incubated for four days at 30°C before imaging.

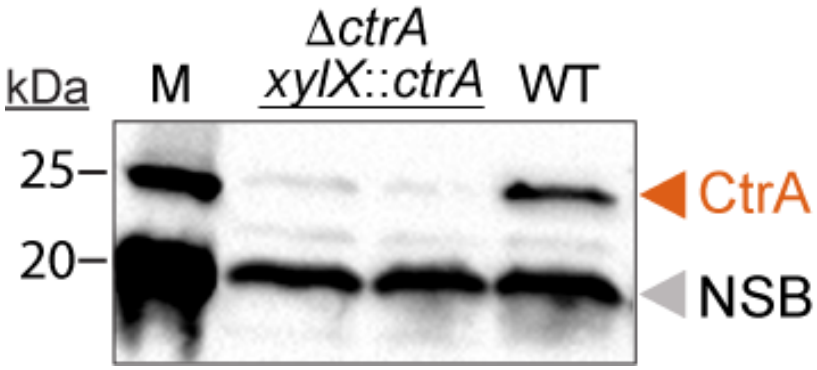

Figure S3.3. Immunoblot of wild type (WT) and replicate cultures of a conditional *ctrA* depletion strain (Δ*ctrA xylX*::*ctrA*) probed with anti-CtrA serum confirms the CtrA band. M = molecular weight standards. NSB = non-specific band that reacts with polyclonal CtrA antiserum.

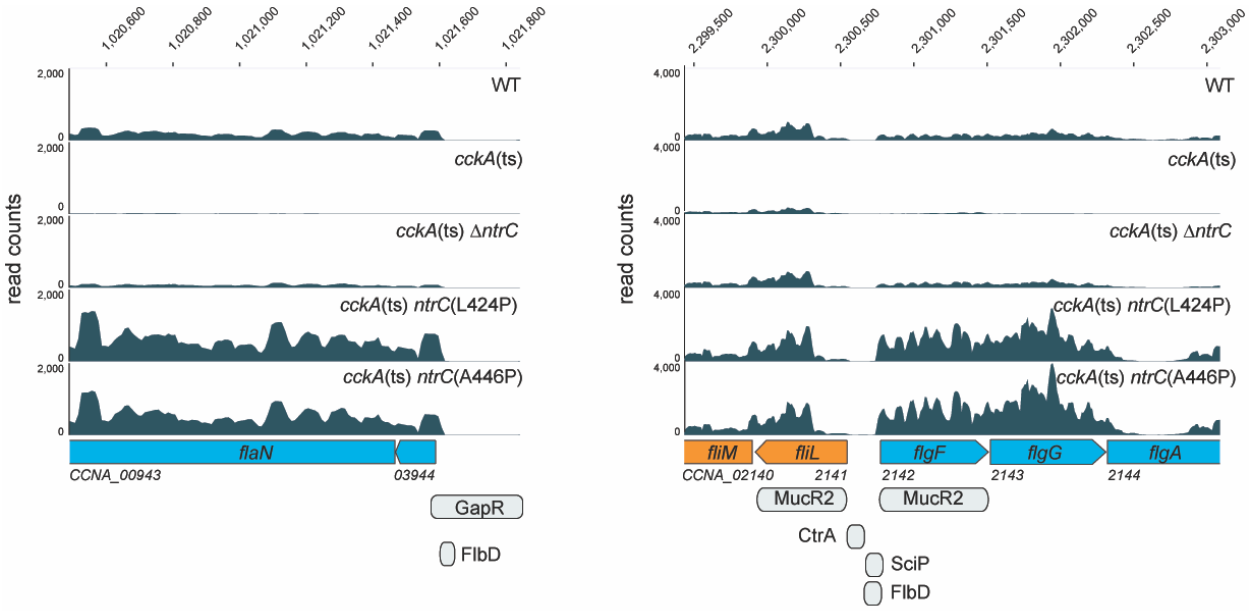

Figure S3.4. Mapped RNA sequencing read depth for select flagellar gene regions in wild type (WT), *cckA*(ts), *cckA*(ts) Δ*ntrC*, *cckA*(ts) *ntrC*(L424P), and *cckA*(ts) *ntrC*(A446P) strains. Class II flagellar genes are indicated in orange, and Class III flagellar genes are indicated in cyan. Locus numbers are indicated below the genes. Chromosome positions in the NA1000 genome (genbank CP001340) are indicated at the top. Binding sites for GapR, MucR, CtrA, SciP, and FlbD are also shown, highlighting their genomic positions relative to transcriptional activity in each strain.